Capillary Electrophoresis – Inductively Coupled Plasma Mass Spectrometry for the Characterization and Quantification of Humic Substances and their Interactions with Metal Species

A Thesis Submitted to the Committee on Graduate Studies

in Partial Fulfillment of the Requirements for the

Degree of Master of Science

in the Faculty of Arts and Science

Trent University

Peterborough, Ontario, Canada

Watershed Ecosystems Graduate Program

June 2001

ABSTRACT

Capillary Electrophoresis – Inductively Coupled Plasma Mass Spectrometry
for the Characterization and Quantification of Humic Substances
and their Interactions with Metal Species

Nancy Anne VanStone

A speciation tool was developed combining capillary electrophoresis (CE) and inductively coupled plasma mass spectrometry (ICP-MS) to elucidate metal binding patterns with commercial humic substances (HS). Two different interfaces were developed and compared for their efficiency and viability: a direct injection high efficiency nebulizer (DIHEN) and a high efficiency nebulizer (HEN) with a cyclonic spray chamber. A thorough analysis of the migration patterns of commercial HS was established using standard CE with UV absorbance detection. Results comparable to published observations were achieved. The results of the CE/ICP-MS analyses of HS inoculated with Pb lacked a high level of confidence for reproducibility. A mass balance approach was used, and the identity of generalized peak areas was hypothesized. The identity of the various peaks could not be determined with confidence, although it appears that both Pb and HS binding to the separation capillary inhibit the characterization of HS interactions with metal species by CE/ICP-MS. Further analyses are warranted using alternative capillaries, and simpler speciation problems.

ACKNOWLEDGMENTS

My thanks and appreciation go out to my supervisory committee, Dr. Doug Evans, Dr. Ewa Dabek-Zlotorzynska, and Dr. Peter Dillon, for their patience and commitment to my work. My special thanks are extended to Dr. Evans for this opportunity to learn. For their technical advice, I thank Dr. Richard Hughes, Janice Villeneuve, Katherine Keppel-Jones, Robert Loney, and Dr. Gord Balch. I offer my appreciation for friendship to these individuals, as well as to Claire Wilson, Brian Dimock, Nelson O'Driscoll, Andrew Bukata, and Dr. Tim Croley.

Special thanks are extended to my brothers and sisters, Susan and Rand Hoenhous, Lynn Finlay and David Slipp, Cynthia Slipp and Steve Katmarian, and Daniel Slipp for their support. I dedicate this thesis to their children: Jacob and Amy Slipp, Elizabeth Hoenhous and Michael Katmarian. I hope they may have the same opportunities to learn and explore as I have been privileged to receive.

I especially want to thank my husband, John, for his patience, support and advice throughout this program of study. In particular, I thank him for the sacrifices he has made to allow me this opportunity, and for his support, understanding and motivation when I most needed it. This work is as much his as it is mine, as I could not and would not have completed it without his encouragement. *Thank you, John.*

TABLE OF CONTENTS

Abstract *i*

Acknowledgments *ii*

Table of Contents *iii*

List of Tables *v*

List of Figures *vi*

List of Acronyms *vii*

1 INTRODUCTION 1

1.1 Metal Speciation 2

1.2 Humic Substances 5

1.2.1 *Definition and Composition* 5

1.2.2 *HS-Metal Ion Interactions* 7

1.3 Capillary Electrophoresis 10

1.3.1 *Introduction to CE* 10

1.3.2 *CE for the Analysis of Humic Substances* 15

1.4 CE/ICP-MS 20

1.4.1 *ICP-MS and Sample Introduction* 20

1.4.2 *CE/ICP-MS for Speciation Studies* 26

1.5 Rationale for Study and Experimental Objectives 31

2 EXPERIMENTAL 34

2.1 CE Separations of Humic Substances (*UV Detection*) 34

2.1.1 *Apparatus* 34

2.1.2 *Reagents* 35

2.1.3 *Samples* 35

2.1.4 *Experimental* 36

2.2 CE/ICP-MS Interfaces: Design and Optimization 38
2.2.1 *Apparatus* 38
2.2.2 *Reagents* 41
2.2.3 *Samples* 42
2.2.4 *Experimental* 42
2.3 Analysis of AHA-Pb by CE/ICP-MS (*ICP-MS Detection*) 44
2.3.1 *Apparatus* 44
2.3.2 *Reagents* 44
2.3.3 *Samples* 44
2.3.4 *Experimental* 45

3 RESULTS AND DISCUSSION 46
3.1 CE Separations of Humic Substances (*UV Detection*) 47
3.1.1 *Method Development: Choice of BGE and Wavelength* 47
3.1.2 *Application to AHA-Pb Samples* 57
3.2 CE/ICP-MS Interfaces: Design and Optimization 67
3.2.1 *Introduction* 67
3.2.2 *The DIHEN Interface* 67
3.2.3 *The HEN/Cyclonic Spray Chamber Interface* 83
3.3 Analysis of AHA-Pb Samples by CE/ICP-MS (*ICP-MS Detection*) 92
3.3.1 *Introduction* 92
3.3.2 *Pb Standard Results, HEN/Cyclonic LOD* 94
3.3.3 *Estimation of Variability* 97
3.3.4 *Mass Balance* 104
3.3.5 *General Trends* 108

4 CONCLUSIONS AND RECOMMENDATIONS FOR FUTURE WORK 126
4.1 Summary and Conclusions 126
4.2 Recommendations for Future Studies 130

5 REFERENCES 132

LIST OF TABLES

Table 3.1	Standard results for CE reproducibility.	58
Table 3.2	AHA-Pb UV analysis: Migration times.	62
Table 3.3	AHA-Pb UV analysis: Peak areas.	63
Table 3.4	Statistics for the migration times of metals.	77
Table 3.5	Statistics for the determination of detection limits for the DIHEN interface.	79
Table 3.6	Regression statistics for limit of detection analysis (DIHEN).	80
Table 3.7	Detection limits for DIHEN interface.	82
Table 3.8	Results of EDTA-Pb analysis.	90
Table 3.9	Pb standard data.	95

LIST OF FIGURES

Figure 1.1:	Schematic diagram of the CE system	12
Figure 1.2	Basic design of the Meinhard® type pneumatic concentric nebulizers.	24
Figure 2.1	Schematic of DIHEN interface.	39
Figure 2.2	Details of the HEN/cyclonic spray chamber interface.	40
Figure 3.1	Comparison of BGE constituents.	50
Figure 3.2	Comparison of BGE constituents: PDA results.	54
Figure 3.3	AHA-Pb UV analysis.	60
Figure 3.4	Peak identification for AHA-Pb UV analysis.	61
Figure 3.5	Optimization parameters for DIHEN interface.	69
Figure 3.6	CE/DIHEN/ICP-MS optimization I.	71
Figure 3.7	CE/DIHEN/ICP-MS optimization II.	74
Figure 3.8	Separation of metal mixture using DIHEN interface.	76
Figure 3.9	Sample electropherograms of metal mixture separation.	78
Figure 3.10	Calibration curves for metal separation analysis using the DIHEN interface.	81
Figure 3.11	CE/HEN/Cyclonic/ICP-MS optimization I.	85
Figure 3.12	CE/HEN/Cyclonic/ICP-MS optimization II.	87
Figure 3.13	EDTA-Pb separation.	89
Figure 3.14	Calibration curve for determination of Pb concentrations.	96
Figure 3.15	Reproducibility of AHA-Pb CE/ICP-MS analysis.	98
Figure 3.16	AHA-Pb CE/ICP-MS analysis: Acidic samples.	101
Figure 3.17	AHA-Pb CE/ICP-MS analysis: Neutral samples.	102
Figure 3.18	AHA-Pb CE/ICP-MS analysis: Alkaline samples.	103
Figure 3.19	Mass balance results.	107
Figure 3.20	Relative concentration of peaks for all samples I.	111
Figure 3.21	Relative concentration of peaks for all samples II.	113
Figure 3.22	Relative concentrations of free and bound Pb.	118
Figure 3.23	Bound Pb concentrations for AHA-Pb as a function of sample pH conditions: Hypothesis 2.	121

AHA	Aldrich® humic acids
BGE	background electrolyte
CE	capillary electrophoresis
CE/ICP-MS	CE-inductively coupled plasma mass spectrometry
CC	complexation capacity
DAD	diode-array detection
ddw	deionized distilled water
DIHEN	direct injection high efficiency nebulizer
DIN	direct injection nebulizer
DOC	dissolved organic carbon
EDA	external detector adapter
EOF	electroosmotic flow
FA	fulvic acid(s)
GC	gas chromatography
HA	humic acid(s)
HEN	high efficiency nebulizer
HS	humic substance(s)
ICP	inductively coupled plasma
ICP-AES	ICP atomic emission spectroscopy
ICP-MS	ICP mass spectrometry
ID	internal diameter
LIF	laser-induced fluorescence
LOD	limit of detection
MT	migration time(s)
PA	peak area(s)
PDA	photodiode array
QMF	quadrupole mass filter
SEC	size exclusion chromatography
Tris	hydroxymethylaminomethane (electrolytic solution)
UV	ultraviolet

1 INTRODUCTION

The past two decades have seen an increasing emphasis on metal speciation for the understanding of metal toxicity in the natural aquatic environment. In short, the paradigm of metal speciation confers the dependence of toxicity upon the biologically available forms in which that metal exists, not upon the total metal concentration. This understanding has grown in part from the development of sensitive and efficient techniques for the separation of metal species, giving the researcher the ability to discern the different species of an element as they exist in nature, and their relative effect on the environment. In particular, the development of highly sensitive and selective speciation methods has supported such work. This thesis is dedicated to such a task: the development of a state-of-the-art speciation technique, combining capillary electrophoresis (CE) and inductively coupled plasma mass spectrometry (ICP-MS) (henceforth, the coupled instruments will be referred to as CE/ICP-MS). Accordingly, an application is identified for which inadequate analytical techniques to elucidate important speciation properties exists, and the new method is applied to this problem. The relationship between humic substances (HS) and metal species is such an application. HS have been studied since the nineteenth century, yet their structural characteristics and related metal species interactions are still largely misunderstood.

The role of HS in metal speciation has been shown to be of utmost importance by many studies (e.g. Piccolo 1989; Zhang *et al* 1996; Spark *et al.* 1997; Pinheiro *et al.* 1999), although a simple and reliable method for characterizing these

relationships has not been established. The goal of this work, therefore, is to develop such a method and apply it to the analysis of HS-metal ion interactions.

To place this work in the context of existing literature and to understand the logical progression of this work, several topics must be explored. These topics include the development of speciation paradigms, the role of HS studies in metal speciation with emphasis upon their composition and structure, the development of CE as an analytical tool, the use of CE for the characterization of HS, and the recent work done towards production of a viable CE/ICP-MS hyphenation. Finally, the rationale for the current study will be described including the objectives of the study.

1.1 Metal Speciation

The understanding that the distribution, fate and biological availability of metals is not solely dependent upon their total concentrations is the driving force of metal speciation studies (Allen *et al.* 1980; Campbell 1995; Dabek-Zlotorzynska *et al.* 1998). The most critical factor in determining these parameters is the chemical and physical associations metals undergo in natural systems. These chemical and physical factors include the pH and redox potential of natural systems, and the availability of reactive species such as complexing ligands (Ure and Davidson 1995). Of course, it would be impossible to fully describe all the chemical forms of a given element in a natural open system due to the range of possible conditions and the complexity of such systems. It is

possible, however, to characterize some of the most important forms of an element in a system to provide a general idea of the behaviour of these species.

The term speciation has taken several meanings. It is typically defined as either the "process of identifying and quantifying the different, defined species, forms or phases present in a material" or "the description of the amounts and kinds of these species, forms or phases present in a material" (Ure and Davidson 1995). Chemical species can be defined in functional terms (e.g. biologically available), operational terms (e.g. lipid soluble), or as a special chemical compound or oxidation state [e.g. arsenobetaine vs. As(III) and As(V); Cr(III) vs. Cr(VI)] (Bunce 1994; Ure and Davidson 1995; Olesik *et al.* 1998; Allen *et al.* 1998). These definitions are dependent upon the methods used by the analyst to detect the species.

The determination of specific species within an environmental sample is more difficult than the measurement of the total concentration of an element for several reasons. Firstly, it is often difficult to isolate the compound(s) of interest from sample matrices. Secondly, the act of measuring species often disturbs the equilibria existing in the sample initially (Pickering 1995). This concern is present throughout the process a speciation study, from the sampling stage through to actual analytical analysis. For example, species exist in equilibria defined by the myriad of physical and chemical parameters existing within its original system. By removing a small amount of sample, the conditions may be changed within that sample. A third difficulty in speciation measurements is that the species of interest is often present at ultra-trace levels (sub-ng L^{-1} to $\mu g\ L^{-1}$) (Zoorob *et al.* 1998), and even the most sensitive speciation techniques

may not be able to measure such low concentrations. Finally, there are rarely standards available for method verification of validation of analyses (Olesik *et al.* 1998).

The ideal speciation technique would take into account these problems. It would therefore need to be extremely sensitive (i.e. sub-μg L^{-1} range), and provide separation and quantification of the various species present in a sample with minimal disturbance to the equilibria between these species. The act of separating species must disturb the equilibrium between chemical forms to a certain extent, as the kinetic and thermodynamic nature of the system is modified. Thus, methods that allow minimal disturbance to the initial system must be found. For example, one may add a chelating agent to a sample to bind with the free metal and precipitate out of solution. As the metal binds and precipitates, the equilibrium of the system will be affected such that more metal may become free, and in turn be bound to the chelator and precipitated out of solution. Hence, the estimation of free metal based on the amount of precipitation will be erroneously high. As most equilibria are limited by reaction kinetics (Ebbing 1990), a method that allows for rapid separation of components may allow for the most accurate measures of speciation.

Several analytical methods are used routinely for metal speciation studies. These include methods similar to the example given in the previous paragraph, such as using a chelating agent to bind with the species of interest (Pickering 1995). Generally, chromatographic methods are used to first separate the species of interest, followed by an elemental detection step. For example, gas chromatography (Chau and Wong 1989) and high performance liquid chromatography (Batley and Low 1989) have been used for

speciation studies. Kinetic effects on the species' state limit these methods after separation and before detection. These methods must be coupled to a sensitive detector in order to achieve the measurement of the concentration of analytes necessary for many speciation studies. ICP-MS is considered the state-of-the-art for many such techniques, considering its elemental selectivity and sensitivity (Zoorob *et al.* 1998) (see also section 1.4.1).

1.2 Humic Substances

1.2.1 *Definition and Composition*

HS are a group of naturally occurring, heterogeneous and polyfunctional organic molecules (Aiken *et al.* 1985). HS are ubiquitous in the sense that they are found everywhere that there is decomposing organic matter. For example, it has been estimated that HS comprise approximately 50% of the organic matter of soil (Hayes *et al.* 1989). As well, they are the main constituents of the dissolved organic carbon (DOC) pool in surface and ground waters, and soil pore waters. HS are formed by the decomposition of microbial, vegetative and animal matter; a characteristic yellow to black colour indicates their presence.

Although the structure of the precursors for HS genesis is known (e.g. polysaccharides, lignin, peptides, lipids), the composition and structural chemistry of humic substances are not clear (Hayes *et al.* 1989). A variety of chemical reactions and biological transformation reactions are involved in their formation, and as there is no

genetic control of their synthesis, their formation is likely random (Hayes 1997). It is understood that HS are groups of molecules with hydrophobic organic backbones interspersed by hydrophilic functional groups. The interaction of the backbone and functional groups leads to structures analogous to the tertiary and quaternary structures of proteins (Hayes *et al.* 1989). The composition of HS is site-specific due to their dependence upon geography, climate, and physical and biological circumstances (Perdue 1998a). A representative structure is therefore difficult to define due to the site- and temporal- specificity of the substances. Limited information has been gained on the structure of these molecules: elemental analysis can estimate the relative proportion of elements in samples, titrations can be performed allowing estimations of the number of functional groups (e.g. carboxylic, phenolic), and various spectrometric and electrochemical methods have been employed for further elucidation of structure (Perdue 1998a). Nevertheless, because of the inherent difficulties in determining structure, little progress has been made thus far.

As they do not belong to any unique chemical category, HS cannot be defined in unambiguous structural terms; as they do not perform any specific biochemical function, they cannot be defined in any unique functional terms. For these reasons, HS have historically been defined in operational terms in reference to their solubility in aqueous acid and base solutions. HS consist of humic acids (HA), which precipitate out of solution when the pH is decreased below 2, and fulvic acids (FA), which are soluble under all conditions of pH. A less studied component is humin, or that fraction of HS that is insoluble in water at any pH value (Hayes *et al.* 1989). This classification into

operationally defined fractions has allowed for specific analysis of each component, although these fractions are still highly variable and complex in terms of elemental composition and structure.

Many researchers are interested in developing a concise structure of HS, or at least a group of model structures. As nuclear magnetic resonance (NMR) appears to be the most useful method for HS compositional information (Hayes 1997), various groups have used the results of such analyses for the development of model structures (e.g. Grassi *et al.* 1996). As well, chemical degradation studies are used to determine the building blocks of HS. The utility of structural models, however, is limited by the heterogeneity of the substances, although less ambiguous structural information such as its basic elemental composition, carboxyl content and number-average molecular weight can be used to obtain a probabilistic description of the major structural features (Perdue 1998a). While some authors discuss the futility of determining HS structure due to the complexity and uniqueness of the substances (e.g. Ziechmann 1988; Hayes *et al.* 1989), others continue to attempt to establish some representative characteristic structural pattern (e.g. Schulten 1996).

1.2.2 *HS-Metal Ion Interactions*

HS are important metal chelators in the environment; their many non-identical functional groups act as binding sites for charged elemental species (Perdue 1998b). The ubiquity of HS combined with their inherent complexation capacity (CC) for metal binding makes them important for the mobility and fate of metals in the

environment. Metals bound to HS have been considered refractory to biotic uptake, although recent evidence suggests that HS are an important carbon source to microbial colonies in some ecosystems (Tranvik 1998). Nonetheless, HS is considered one of the most important sinks for metals in natural waters (Decho and Luoma 1994). Understanding the structure of HS could lead to a better comprehension of this metal reservoir, allowing a greater ability to effectively recover polluted sites.

Metal binding with HS is a highly complex and variable phenomenon. It depends on the pH and ionic strength of the medium, the concentration ratio between the metal ion and the humic ligand, competitive binding among all metal ions present, the intermolecular and intramolecular heterogeneity of metal binding functional group distributions in HS, and size, shape, and phase differences between different humic molecules (Weber 1988; Leenheer *et al.* 1998; Perdue 1998a; Perdue 1998b). Metals are present in all natural waters at varying concentrations dependent upon the intrinsic geochemistry of the locale or anthropogenic sources. Many metals in natural waters, however, have higher than expected solubilities based on calculations derived from the inorganic ions present in the waters (Weber 1988). This enhanced solubility is most probably due to their complexation with HS. The CC, or the amount of metal that can bind with a given amount of HS, of HA for metal ions is approximately 200 to 600 $\mu mol\ g^{-1}$ (Rashid 1985), or 40 to 125 $mg\ g^{-1}$ for Pb^{2+}. The most important binding sites found within HS have been found to be either carboxyl or phenol groups, or a combination of these two functional groups as a bidentate ligand (Weber 1988, Lund 1989). It has been estimated that approximately one-third of these complexes is due to

simple cation exchange associations, and the remainder being binding sites such as the carboxyl and phenolic functionalities (Weber 1988).

Generally, HS are considered a mixture of organic acids that can bind a metal ion with a 1:1 stoichiometry. Under such constraints, the CC can be defined. If the assumption of stoichiometry were true, that would mean that the CC should be independent of conditions (i.e. pH, ionic strength, nature of metal, etc.) (Lund 1989). This is certainly not what most research shows. The dependence of CC upon conditions, however, is intuitive if one realizes that the structure of HS, although complex, is comparable to the structures of other large biomolecules. At various pH values, for example, a large biomolecule will display different conformational characteristics (Hayes *et al.* 1989; Lehninger *et al.* 1993). By applying this understanding to HS, an assumption of the importance of conformation upon metal binding can be inferred, and thus its dependence upon environmental conditions.

When determining the metal concentrations of natural water samples, historically the total concentration was measured as opposed to the different species of that metal. Thus, in a sample of HS, it was difficult to interpret what portion of that concentration is complexed with HS, or with what general fractions it is associated. Analytical methods are available to determine the concentration of the free ion or other specific species, such as various electrochemical methods [e.g. anodic or cathodic stripping voltammetry (van den Hoop and Leeuwen 1997; van den Berg 1998)], but these methods are more time-consuming than methods for the determination of total metal in a sample. There is some criticism that these techniques cannot show accurate results due to

changes in equilibria during analysis. As well, there is no allowance for simultaneous structural analysis of HS.

To determine the structure of HS and their interaction with metals, some possible methods are available. Usually this would include a separation step [e.g. ultrafiltration, electrophoresis, chromatography] to reduce the complexity of the HS mixture, followed by a sensitive elemental detection technique (e.g. ICP-MS).
CE has recently been added to this arsenal of analytical techniques for analyzing the structural features of HS, although the application of a sensitive detection system for simultaneous speciation studies has not been effectively applied.

1.3 Capillary Electrophoresis

1.3.1 *Introduction to CE*

CE has seen an exponential growth in all analytical fields in recent years, in particular biochemistry and pharmacology. This analytical technique has its roots in more conventional electrophoretic processes, such as paper, agarose gel and polyacrylamide gel electrophoresis. Initial work with CE was done with wide-bore capillary columns with an internal diameter (ID) of 3 mm (Hjerten 1967). The development of modern CE technologies began in 1981 when Jorgenson and Luckas used zone electrophoresis in open-tubular glass capillaries to separate amino acids, dipeptides and amines (Jorgenson and Luckas 1981). Indeed, the growth of this technique can be

described by the vast number of publications regarding its use, with over 7000 journal publications in 1996 alone (Oda and Landers 1997).

The schematic shown in Figure 1.1 illustrates the basic principle of CE. A narrow (typically 20 to 100 μm ID), fused silica capillary is filled with an appropriate electrolytic solution, a small amount (1 to 30 nL) of sample injected in one end, and both ends placed in reservoirs of the same electrolytic solution used for filling the capillary. A voltage is applied across the capillary, and separation occurs according to charge to size ratio differences of ionized sample molecules and due to an electroosmotic flow (EOF) within the capillary. Detection is typically via UV absorbance or fluorescence.

The role of EOF in CE is very important. This phenomenon is the result of surface charge on the inside wall of the capillary; the degree of ionization of the silanol groups of the capillary is controlled by the pH of the electrolytic solution, or background electrolyte (BGE). When the silanol groups are negatively charged, they attract positively charged ions from the BGE solution, creating an electrical double layer near the inner wall of the capillary. When a voltage is applied across the capillary, cations near the capillary wall migrate in the direction of the opposite charge (the cathode) resulting in the bulk movement of BGE towards the negative electrode. This flow transports all components of the capillary contents at the same velocity, but does affect the speed of analysis, separation efficiency, selectivity and resolution of the analysis.

Although CE is theoretically simple, in practical use several areas are of concern for day-to-day reproducibility and overall technique reliability. For example, BGE composition is very important for the successful separation of analytes and small

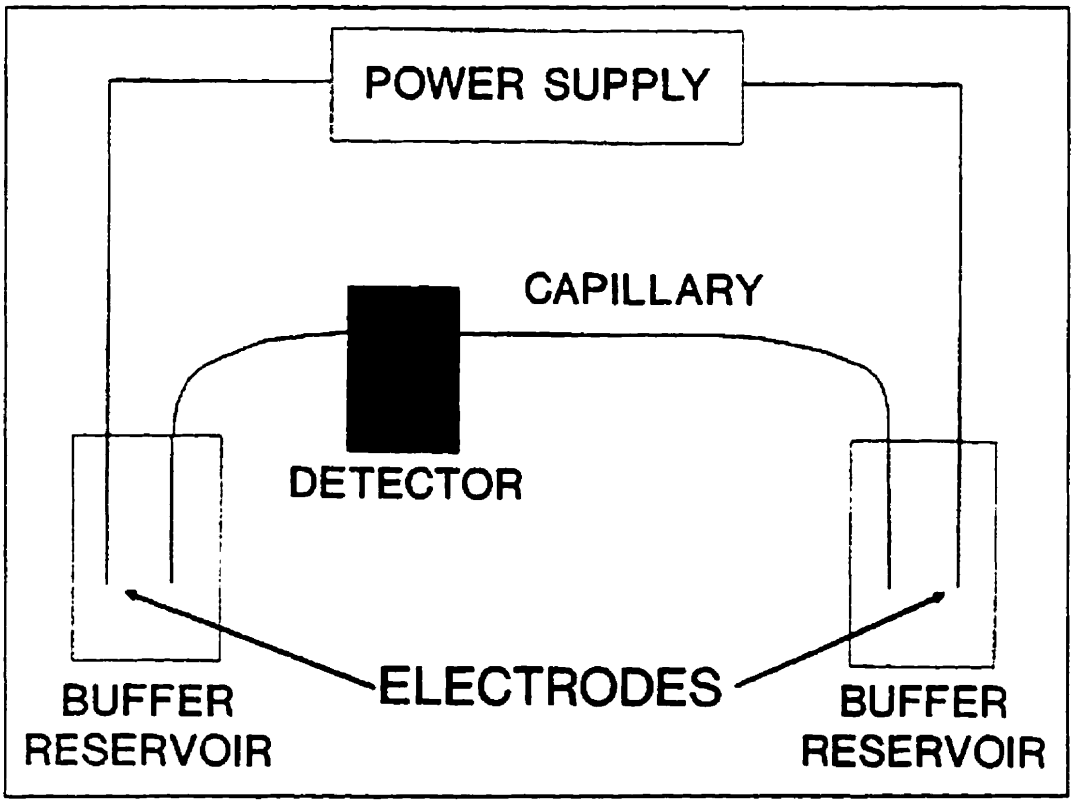

Figure 1.1: **Schematic diagram of the CE system.** BGE is placed in the buffer reservoirs, and the capillary is filled with the same solution. A small volume of sample is injected at one end of the capillary, and a voltage applied. The separation of the sample components can be monitored with on-line detection, as indicated in the above diagram.

changes can cause dramatic changes in performance. The EOF is also another parameter of concern: both BGE composition and applied voltage can affect its relative speed. Finally, the sample injection itself can affect CE performance. Several different modes of injection have been developed each with its unique considerations. As well, the amount and composition of the sample injected can have considerable effects in separation. Each of these factors will be discussed in turn in the following paragraphs.

The BGE used in CE is important for many reasons, the first and foremost of these is to maintain the pH of the solution such that the ionization of the sample is maintained throughout the separatory process, as well as maintaining the silanol groups of the capillary as charged moieties allowing the EOF. Untreated fused silica is comprised of a number of different acidic surface silanol groups with a total density of about 8.3×10^{-6} M m^{-2} (Chiari *et al.* 1996). The pK_a of these silanol groups range from 5.3 to 6.3, meaning that appreciable ionization of these groups will be seen at pH values above 2 (Chiari *et al.* 1996). When the silanol groups are bathed in a solution of pH greater than 2, a thin sheath of charged fluid will form adjacent to these groups. In an electric field, this sheath will be effectively dragged by an electroosmotic force towards the electrode of opposite charge. Thus, in an uncoated capillary, the migration behaviour of a charged analyte will be determined both by its electrophoretic mobility and by the electroosmotic mobility, as total mobility is a result of vectorial addition of both parameters (Chiari *et al.* 1996). The importance of the pH of the BGE is also important in determining the effective ionization of the sample analytes themselves. Thus, the pH

of the BGE must be considered with both the extent of ionization, and hence mobility, of the analytes and the relative velocity of the EOF in mind.

In terms of the BGE composition, several factors need to be considered. In relation to the previous discussion, the BGE needs to provide pH stability and thus needs to provide good buffering capacity and be used within its buffering range (generally within 0.75 units of its pK_a) (Moring 1996). The ion concentration of the BGE is also of importance: greater concentrations generally impart a higher buffering capacity. Other factors to consider for BGE selection include electrical conductivity, running current, background UV (or other detection technique) absorbance, and compatibility with both the sample and other additives to the solution (Moring 1996).

Two methods are available for sample injection in CE: hydrodynamic and electrokinetic. Hydrodynamic injection types include pressure, siphoning and split-flow injection. By applying a pressure differential over the capillary, liquid can be pushed into the capillary at the site of higher pressure. This pressure can be achieved by applying pressure upon the sample inlet side of the capillary or by applying a vacuum upon the outlet side. As well, siphoning can be achieved by raising the height of the sample inlet side, whilst immersed in sample, to introduce liquid into the capillary. Most commercial units allow both of the former hydrodynamic injection methods. Hydrodynamic injections have the advantage of injection without quantitative bias and the ability to make very large injections (Olechno and Nolan 1996). Electrokinetic sample introduction consists of injecting charged analytes by applying a voltage across the capillary while the sample inlet is immersed in the sample liquid. Thus, the injection is

induced via the electrolytic mobility of the analyte. It is more difficult to quantify the volume of sample injected using this method, although various equations have been devised to serve this purpose (Olechno and Nolan 1996). Electrokinetic injections are subject to bias due to varying electrolytic mobilities of analytes, as well as to problems with ionic strength differences between the sample solution and the BGE (Olechno and Nolan 1996).

1.3.2 *CE for the Analysis of Humic Substances*

The analysis of HS (both HA and FA) has been performed using CE by several research groups over the past decade. One reason for this growth is the improvement in the reproducibility and sensitivity due to improved commercial apparatus, and the subsequent extrapolation of these methods to analyze complex chemical mixtures such as environmental samples (Craston and Saeed 1998). Certainly, a test of the capabilities of CE is in the analysis of HS. As both HA and FA contain UV-absorbing chromophores, CE with UV detection has been used to both separate and detect these samples. As the number of theoretical plates possible with CE is higher than with many other chromatographic methods, there was also an assumption that the greatest separation of the unique molecules of HS into relatively homogenous fractions may be achieved. Of course, resolution of the mixtures to single components is not possible, but analyses can provide characterization profiles (or fingerprints) as well as provide separation into relatively homogenous fractions based on charge and size, allowing an interpretation of environmental relevance (Craston and Saeed 1998).

Size exclusion chromatography (SEC) has been successfully used in the past to separate HS into fractions based on size for the subsequent analysis of interactions with various metal species (Zernichow and Lund 1995). Using SEC, however, the HS is separated solely in terms of its size. CE allows the concurrent separation of the HS into fractions based on both size and charge, allowing specific information regarding functionality of the separated fractions to be inferred.

Kopácek and coworkers (1991) were the first group to publish their observations of HS using CE. They realized that the ionic nature of HS made them candidates for separation using CE, and analyzed samples of HA and FA from both natural and commercial sources. Using UV absorbance at 405 nm, and various electrolytic buffers, they were able to conclude that some information on the degree of functionality of HS samples could be ascertained from electropherograms of the UV absorbance detection of the separation within the capillary. It should be noted that the mode of CE separation employed by Kopácek was isotachophoresis. This method is similar to isoelectric focusing, in that different leading and terminating electrolytes are used.

Rigol and coworkers (1994) hoped to establish a method to determine the HA content in soils. They tested several electrolytic solutions and both commercial and natural HA with similar trends in the resulting UV electropherograms for both. As they found a linear relationship between the UV signal and the concentration of injected sample, they concluded that CE provides a rough estimation of HA content in soils. Commercial HA (Fluka, Aldrich, and Janssen) in a concentration range of 20 to 400

mg L^{-1} were used. Papers published by this group in 1996 (Rigol *et al.* 1996) and 1998 (Rigol *et al.* 1998) used their prior work as a basis for a study of the associated radiocaesium to soil HS fractions and to quantify the amount of HS in ultrafiltrated samples, respectively. As they reported linear relationships between a "standard" HS (Fluka HA) and a defined and reproducible peak occurring in all electropherograms, they used this to quantify the amount of HS in environmental soil samples. This showed good correlation with other methods of quantification.

Publications of HS analyses using CE have been dominated by the Garrison/Schmitt-Kopplin group (e.g. Garrison *et al.* 1995; Schmitt *et al.* 1996; Schmitt *et al.* 1997a; Schmitt *et al.* 1997b; Schmitt-Kopplin *et al.* 1998a; Schmitt-Kopplin *et al.* 1998b). Initially, they set out to use CE to analyze HS of differing sources by developing characteristic "fingerprints", or the unique electropherograms that samples produce at specific UV wavelengths. They analyzed different electrolytic systems for optimum separation and both natural and commercial HA and FA. Specific contributions made by this group have included the recognition of the "humic hump" (a characteristic feature of HS electropherograms), the development of techniques to monitor the flocculation of HS with metal ions using CE, the use of capillary isoelectric focusing for the characterization of HS, and binding studies of s-triazines to HS. Most recently, analyses of the possible artifacts caused by the use of borate buffers in the analysis of HS have been published (Schmitt-Kopplin *et al.* 1998a; Schmitt-Kopplin *et al.* 1998b).

Another group that has made advancements in CE-HS techniques is that of Nordén and Dabek-Zlotorzynska (1996,1997). They have attempted to clarify the

detection and separation of HS using CE. Initially, this group used CE to analyze the complexation of metals (Sr, Pb, Cu, Hg and Al) with FA and they used various direct and indirect detection methods to determine the free metal concentrations in FA-metal solutions. They also analyzed the separation of FA and HA using a borate BGE with the addition of different organic solvents to invoke changes in the separation. They looked at the suitability of on-line laser induced fluorescence (LIF) and diode array detection (DAD) in comparison to single wavelength UV detection. Notable contributions from the work of Nordén and Dabek-Zlotorzynska is the verification of HS mobility changes upon the addition of metals due to changes in the net charge and mass of the HS (Nordén and Dabek-Zlotorzynska 1996), the increase in molar absorbtivity of FA with increasing FA-metal complexation (Nordén and Dabek-Zlotorzynska 1996), and the use of a denaturing agent such as urea to improve HS separation (Nordén and Dabek-Zlotorzynska 1997).

The work of Fetsch and coworkers (Fetsch and Havel 1998, Fetsch *et al.* 1998a, Fetsch *et al.* 1998b) is also worth noting, in particular for their development of BGE systems with better separation results than those reported elsewhere. Several BGEs were investigated in these works, including several of amino acid composition. The authors found little separation of HS using most BGEs, and the most fractions seen using high concentrations of borate and boric acid (Fetsch *et al.* 1998b). In fact, they believe that there is really no discernable separation of HS occurring in most BGEs, save borate, but the phenomenon being observed is the separation of HS oligomers (Fetsch and Havel 1998). One might see this as a difference in semantics, depending on the extent of

separation desired for an analysis. Fetsch and coworkers also propose the use of a BGE (rimantadine hydrochloride) with an additive (Mg(II) salts) that prevents the interaction of HS and the silanol groups of the capillary and present promising extensive separations of very low concentrations of HS (Fetsch *et al.* 1998a).

In chronological order, other publications regarding the use of CE to analyze HS are described in the following. Pompe and coworkers (1996) used CE to characterize HA and FA of different origins in hopes of developing a fingerprint database. They used a phosphate-borate BGE of pH 8.9 and analyzed samples of approximately 300 ppm, in terms of their HA or FA content. They saw definite differences in the electropherograms of the samples, and were able to infer some differences in aromatic content, the presence of different UV-active groups and variation in the concentration of individual fractions. Dunkelog and coworkers (1997) compared the use of CE to analyze environmental samples of HA and FA with capillary gel electrophoresis, isoelectric focusing, micellar electrokinetic chromatography, and SDS gradient-gel electrophoresis. They concluded that it was not possible to separate HA or FA with CE, at least under the conditions described, and that the most optimal separation and therefore the most informative electrophoretic method for their analysis is isoelectric focusing. Keuth and coworkers (1998) conducted a study using free-flow electrophoresis as a preparative technique for the analysis of HA by CE. They were able to see greater separation of the mixtures with the addition of hydroxycarboxylic acids, although they were unable to elucidate why this was observed. Another study looking at fractionated HAs was accomplished by De Nobili and coworkers (1998), although they employed

Amicon YM membranes to fractionate the HA into various size classes. This study shows limited success in determining any appreciable patterns using both polyacrylamide-coated and uncoated capillaries. Bragato and coworkers (1998) looked specifically at fractionated HS derived from peats. They found a linear relationship between migration time and the degree of decomposition of the peats. The BGE they use was a hydroxymethylaminomethane (Tris) BGE with high concentrations of polyethylene glycol, which presumably acts as a molecular sieve. They concluded that humification in mires results in an increase in the average size of HS molecules.

1.4 CE/ICP-MS

1.4.1 *ICP-MS and Sample Introduction*

In ICP-MS, a sample is introduced as an aerosol into plasma where it may be desolvated, vaporized, atomized, excited and ionized (Montaser *et al.* 1998a). The ions of the sample are then focused and transmitted to a mass analyzer (e.g. quadrupole mass filter). The main advantages of ICP-MS over other elemental analyzers (i.e. atomic absorption spectrometry) is its low detection limits, good precision, full-range of elemental detection, and broad dynamic concentration range (4 to 11 orders of magnitude) for many elements (Montaser *et al.* 1998a). Some of the basic concepts of ICP-MS, such as the principles of ICP generation, detection and sample introduction will be discussed in the following paragraphs.

Plasma is an ionized gas that is macroscopically neutral, such that it has the same number of positive particles (ions) and negative particles (electrons) (Mermet 1999). Ar is typically used to generate the plasma for ICP-MS due to its capability to excite and ionize most of the elements of the periodic table; as it is chemically inert, Ar will not form stable compounds with the analytes of the sample (Mermet 1999). Plasmas are classified according to the type of electric field used to create and sustain the plasma; inductively coupled plasma (ICP) results from a high frequency field [radio frequency (rf) energy] applied across a coil (Mermet 1999). In practice, plasmas are produced and maintained within a quartz torch that consists of three tubes of varying diameter; the inner tube carries the sample aerosol within a flow of Ar, and the intermediate and outer tubes carry Ar that both forms the plasma and cool the torch (O'Connor and Evans 1999). The intermediate Ar flow is seeded with electrons by initial excitation with a tesla coil, and the electrons are accelerated by the rf-induced magnetic field toward the coil that surrounds the torch. As the electrons are accelerated from the central area of the torch towards its perimeter, they collide with neutral Ar atoms and ionize them. Thus, there is a continual collision of ions and electrons within the torch as long as the radio frequency is maintained. This external energy allows the maintenance of the Ar as plasma, and the plasma can transfer part of its energy to atomize, ionize and excite sample introduced into it.

The ICP is, therefore, an ion source for mass spectrometry in the case of ICP-MS. The high temperatures of the plasma (5000 to 10000 K) serve to desolvate and atomize the sample, and the high energy of the plasma allows ionization (O'Connor and

Evans 1999). The main ionization processes within the plasma are charge transfer ionization, electron impact ionization and Penning ionization (Mermet 1999).

Mass analysis in ICP-MS is typically made using a quadrupole mass filter (QMF), although sector instruments, time of flight spectrometry and ion trap are also successfully employed detection methods. The QMF consists of four parallel electrically conducting rods that are able to allow the passage of selected ions. Ions are focused into the quadrupole, and the rf and dc voltage applied to opposite rods is changed such that an ion of specific mass-to-charge (*m/z*) can be successfully transferred through the rods and all others are not. This process can be repeated very quickly, allowing many such measurements to be made over a short period of time, and a range of up to 200 *m/z* can be scanned in less than 1 ms (O'Connor and Evans 1999).

Although ICP-MS has been widely used for about 30 years, the limiting factor in controlling analytical performance is still the sample introduction step (Greenfield and Montaser 1992, Gustavsson 1992). Gas, liquid and solid samples may be introduced to the plasma, but for the purposes of this discussion, only liquid sample introduction will be presented. Liquid samples must be introduced to the plasma as aerosols; the process by which a liquid sample is converted to an aerosol is referred to as nebulization (Boss and Fredeen 1997). The two main types of nebulizers used are pneumatic (high speed gas flows are used to create an aerosol) and ultrasonic (oscillations induced in a crystal that, in turn, induce systematic instabilities in a liquid surface that cause it to break up into a stream of aerosol) (Browner 1999). The governing axiom for aerosol production is to produce the smallest drops as possible, causing as little

changes as possible to the plasma and allowing for efficient atomization and ionization of the sample analytes. A discussion of the two nebulizers used for this research, the Meinhard® High Efficiency Nebulizer (HEN) (J.E. Meinhard Associates, Inc.) and the Meinhard® Direct Injection High Efficiency Nebulizer (DIHEN) follows.

Most pneumatic nebulizers used for ICP-MS are of the concentric type; the sample solution passes through a capillary surrounded by a high-velocity gas stream parallel to the capillary axis (Montaser *et al.* 1998b). A pressure differential across the sample capillary is created by the flow of gas, drawing the liquid sample through the capillary (self-aspiration). Meinhard® nebulizers are currently the most widely used nebulizers in ICP spectrometry (Montaser *et al.* 1998b, Browner 1999). This company offers several different nebulizers suited for different applications, but all have similar operating principles. The nebulizer itself is constructed of quartz glass, and the basic design can be seen in Figure 1.2 (a). Figure 1.2(b) is a cross-sectional view of the nebulizer's venturi end. The HEN is one of several nebulizers built according to these specifications, although the HEN operates at low solution uptake rates (as low as 10 $\mu L\ min^{-1}$ in comparison to 500 to 1000 $\mu L\ min^{-1}$ for other designs) (Montaser *et al.* 1998b). The HEN requires a very high gas pressure (~170 psi) for optimal nebulization, which, depending on the ICP-MS being used, must be supplied by an external gas regulator, as the mass flow regulator of most instruments can not supply this pressure. The HEN produces a very fine aerosol that is delivered into a spray chamber (e.g. Scott-type or conical) that removes the majority of large droplets as the gas flow delivers the sample to the plasma. The efficiency of sample transfer to the plasma using a spray

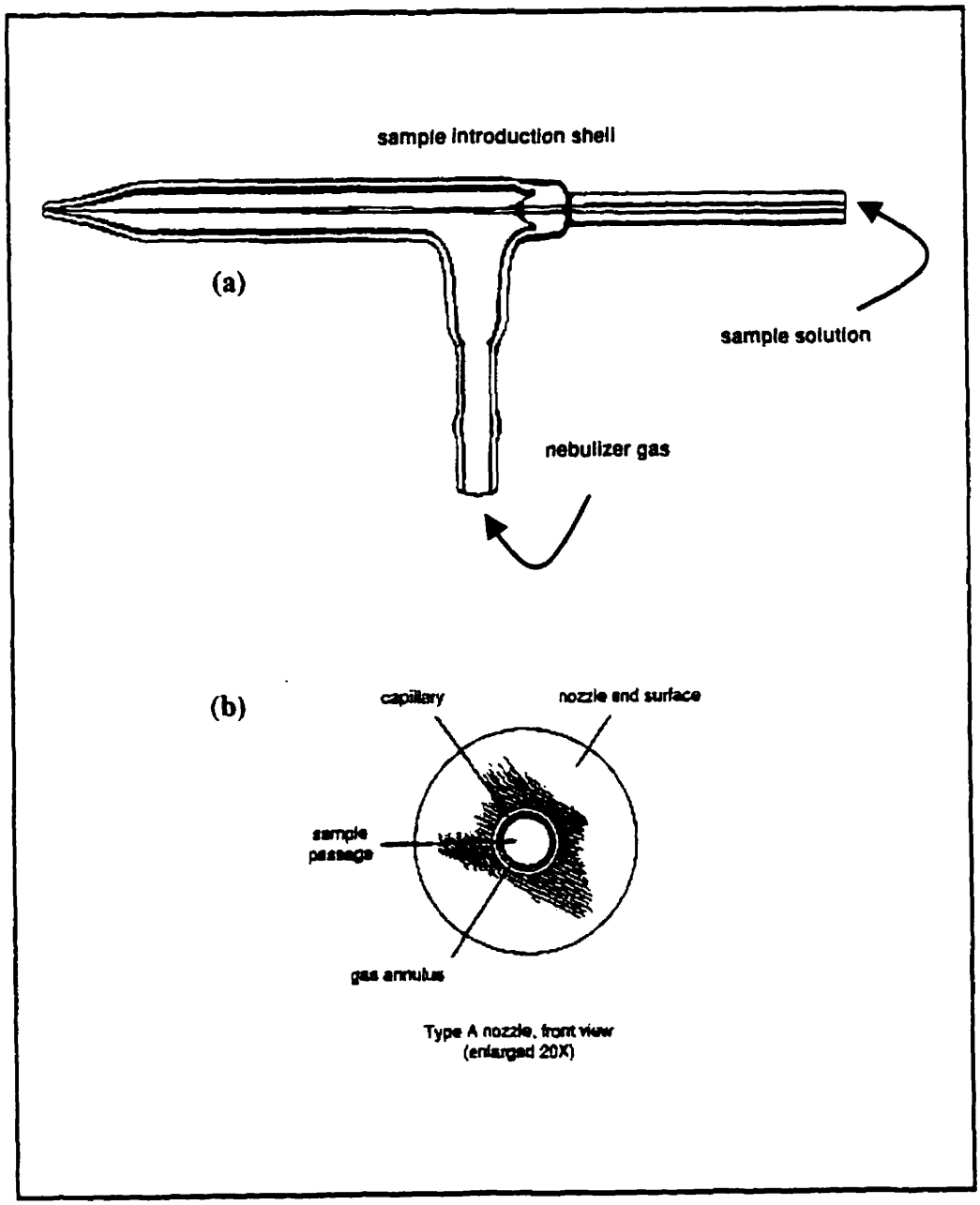

Figure 1.2: Basic design of the Meinhard® type pneumatic concentric Nebulizer. The important features of the nebulizer are indicated in (a), and a cross-sectional view of the nozzle is shown in (b).

chamber is typically in the range of 1 to 2% (McLean *et al.* 1998). An interesting characteristic of the HEN is that at sample flow rates less than 50 μL min^{-1}, the transport efficiency rises dramatically (as high as 70% at 10 μL min^{-1}) (Browner 1999). The HEN has been shown to be an effective interface for CE and other chromatographic techniques with ICP-MS, due to its simplicity, low cost, low dead volume, and high reproducibility (Montaser *et al.* 1998b).

Although the transport efficiency can be quite high for microconcentric nebulizers such as the HEN, there are still applications, especially in the environmental sciences, where very low detection limits are needed. In these cases, it would seem prudent to attempt to analyze the whole sample, allowing a greater bulk of analyte to be atomized and ionized. Various attempts have been made in direct injection nebulization (DIN) systems, such that the entire sample is nebulized and introduced to the plasma. The Meinhard® DIHEN is such an apparatus. The DIHEN looks conceptually very similar to the HEN (Figure 1.2). The need for a spray chamber is precluded by an elongated sample introduction shell that fits directly into the torchbox and torch of the ICP-MS, thus allowing sample aerosol to be introduced directly to the plasma. Initial experiments with the DIHEN showed detection limits in the ppt (part per trillion) range for many elements, and an overall 12-fold improvement in absolute detection limits in comparison to conventional pneumatic nebulizers (McLean *et al.* 1998). Recent work shows an even greater improvement over conventional techniques using the DIHEN for the analysis of long-lived radionuclides (14 to 38-fold improvement in detection) (Becker

et al. 1999). The DIHEN requires a very low gas flow rate for optimal aerosol production (~ 0.2 mL min^{-1}).

1.4.2 *CE/ICP-MS for Speciation Studies*

The unique character of this thesis as opposed to recent research in this area is to analyze HS-metal ion interactions using both CE and ICP-MS. ICP-MS is well recognized as a useful and powerful technique for the detection of trace elements in chromatographic separations (Tomlinson *et al.* 1995, Sutton *et al.* 1997). CE/ICP-MS has several advantages over predominant chromatographic and spectrometric hyphenation techniques: it combines the excellent resolution and separation efficiency of CE with the highly sensitive and selective elemental detection of ICP-MS. Difficulties arise in the coupling of CE and ICP-MS; in particular the low flow rate and sample volume of CE poses problems for ICP-MS as most nebulizers are designed to accommodate larger flow rates. As well, the completion of an electrical circuit is required for CE separation, and because one end must be coupled with the ICP-MS, problems with maintaining current ensue.

Since the publication of the first recorded coupling of CE and ICP-MS, several groups have presented viable coupling systems. Olesik and coworkers (1995) initially devised a system using a concentric pneumatic nebulizer. The capillary was placed into one end of the nebulizer, with a tight fit maintained by a thin layer of silver paint on the outside of the capillary. The silver paint also served to complete the electrical circuit to the flow leaving the terminus of the capillary. A small spray chamber

was built specifically for the system to accommodate the small flow rates from the capillary. Difficulties arose from silver contamination, and suction resulting from the nebulizer gas flow across the capillary. Detection limits were in the range of 0.06 to 2 $\mu g\ L^{-1}$ for the elements investigated (Cr, Fe, Ar, Sn and Sr).

In a paper discussing ICP-MS as a detector for chemical speciation studies, Tomlinson and coworkers (1995) presented their design of an interface for CE and ICP-MS. They completed the electrical circuit for the electrophoretic process by terminating the separation capillary within a grounded stainless steel tube, through which BGE was also pumped. The liquid flow was introduced to the plasma using a glass frit nebulizer. They found the performance of the glass frit was seriously affected by the BGE flow rate: slow rates caused a pulsing and a high background, and high rates would dilute the sensitivity of the response to the sample. They did, however, report excellent results for the separation of two Pb species.

Lui and coworkers (1995) attempted to bypass the inherent problems of CE/ICP-MS hyphenation by using a lab-built direct injection nebulizer (DIN) as an interface between the instruments. The separation capillary was placed concentrically within the DIN, with make-up solution pumped independently around it. The make-up solution and capillary flow were thus combined at the terminal end of the capillary, mixed, and placed such that this flow would be immediately and totally nebulized into the plasma torch of the ICP-MS. The make-up flow also served to complete the electrical circuit, as the grounding electrode was placed within this solution. The benefits of this system were the efficiency of the nebulization, resulting in excellent resolution of

analytes, and high sensitivity. Species separated using this method included a multi-element solution of Li, K, Cs, Cd, Co, Mn, Pb, Sr and Tl, and solutions of As and Se.

Another CE/ICP-MS interface was introduced in the literature in 1995 (Lu *et al.* 1995). As with the interface from Olesik and coworkers (1995), this group used a Meinhard® nebulizer for the aerosol production and introduction. Instead of completing the electrical circuit with silver paint, they instead devised a system that has seen much duplication in subsequent designs. A "tee" union was used to connect a concentric sheath flow of BGE around the capillary, which fits directly through the union. The solution was grounded via an electrode immersed in this flowing solution, thereby allowing the CE separation to be grounded by merit of the solution flowing over the terminal end of the capillary. It was also noted that the terminal position of the capillary was important in determining the sensitivity of the analyses. The sheath liquid, or make-up electrolyte, was allowed to be self-aspirated through the Meinhard® nebulizer (the self-aspiration due to the suction created by the Ar flow through the nebulizer as describes in section 1.5.1). This system was used to separate metal-binding proteins and quantify bound metal concentrations for ferritin and metallothionein isoforms. Using this system, an effective demonstration of the modeling of laminar flow was shown (Kinzer *et al.* 1996).

An ultrasonic nebulizer was used as an interface for CE and ICP-MS by Lu and Barnes (1996). As in the previous designs, the electrical circuit was completed by grounding in a concentric sheath flow. In direct comparison to work with a concentric glass nebulizer, improved detection limits (82 ng L^{-1} for ^{114}Cd and 1.18 μg L^{-1} for ^{64}Zn) were seen (Lu and Barnes 1996). Mei and coworkers (1997) used a microconcentric

nebulizer made by CETAC (CETAC Technologies Inc.) as their coupling device, and allowed the sheath liquid to be drawn concentrically over the separation capillary by self-aspiration of the nebulizer. They reported efficient and satisfactory sensitivity for both Cu and Cr species. Magnuson and coworkers (1997) reported As speciation studies using CE detected with hydride-generation ICP-MS. Because of the particular parameters used for analysis, sample was pushed hydrodynamically through the separation capillary during the electrophoretic process. Although this would presumably lead to odd peak shapes and poor resolution, efficient and sensitive separation and detection of As and Ge species was reported. As well, the authors claim that the use of pressure during the electrophoresis allows a greater volume of sample to be injected, as well as allowing for faster run times (Magnuson *et al.* 1997).

The work of the Michalke group shows much promise as indicated by their presence in the literature (e.g. Michalke *et al.* 1997, Michalke and Schramel 1997, Lustig *et al.* 1998, Michalke and Schramel 1998a, Michalke and Schramel 1998b, Michalke 1999). Initially, a modified Meinhard® nebulizer was used in combination with a "user assembled cartridge" (Bio-Rad, Munich). This cartridge is specially designed for CE-MS coupling and allows liquid coolant to be pumped around the capillary until entry into the nebulizer. A make-up liquid was again employed to increase the flow volume into the ICP-MS, and complete the electrical circuit for electrophoretic separation. A special feature of this set-up is a mechanism by which the capillary position within the nebulizer can be controlled during use. The authors conclude that this system is indeed viable and efficient, no detectable suction through the capillary is noted, and adequate

detection limits for both platinum and selenium species were seen (1 to 20 $\mu g\ L^{-1}$) (Michalke *et al.* 1997, Michalke and Schramel 1997). The separation and detection steps of these analyses were differentiated in the sense that after given amounts of time of applied voltage (the separation step), the contents of the capillary were pushed towards the ICP-MS (the detection step). This group has continued this work within the scope of studies of the speciation of platinum and selenium in body fluids such as human milk and serum.

Other contributions of note to the development of interfaces for, and applications of CE/ICP-MS include the work of Tangen and coworkers (1997, 1998) and Majidi and coworkers (Majidi and Miller-Ihli 1998a, 1998b, Majidi *et al.* 1999). Tangen and coworkers developed a direct injection nebulizer to couple the instruments, however, they had problems maintaining efficient aerosol production and they observed signal pulsing at low liquid flow rates (Tangen *et al.* 1998). Majidi and Miller-Ihli (1998b) presented two different interface designs. Both are very simple and robust designs, the first using a concentric nebulizer (similar to Lu *et al.* 1995) and the second using a standard cross-flow nebulizer fitted with a Scott-type spray chamber. Both interfaces are reported as allowing efficient and sensitive results for Cd, Zn and La speciation studies. In a more recent paper, Majidi and coworkers (1999) report the use of a number of capillaries in parallel (multicapillaries) to improve detection limits by increasing sample volume. For this work, a cross-flow nebulizer was used with the multicapillaries, and a comparison between a DIHEN and a cross-flow nebulizer are presented for a single capillary separation. The authors note that the DIHEN is advantageous over other

interfaces due to the elimination of residence time in the spray chamber for the analytes; sharper, more symmetrical peak shapes are seen, in particular for La (Majidi *et al.* 1999).

To date, there have been no literature references indicating the use of CE/ICP-MS for the analysis of HS and metal speciation, except for Ni speciation in the presence of HA presented as an example of the potential of CE/ICP-MS (Sharp *et al.* 1999). In this case, the separation of Ni and Ni-HA was shown as well resolved peaks, although the experimental conditions are not clearly presented. Many of the researchers using CE for the analysis of HS mention the utility of CE/ICP-MS or CE/MS in studying HS. It is my intention in the following sections, therefore, to describe the methods and results seen from the coupling of CE and ICP-MS as applied to the study of HS and their interactions with metal species.

1.5 Rationale for Study and Experimental Objectives

The objectives of this project were designed such that a greater understanding of HS and metal ion interactions may be achieved through the development of a novel method for such analyses. The objectives are as follows:

(i) to design and construct a viable and efficient coupling apparatus for CE and ICP-MS;

(ii) to optimize this method using simple speciation schemes and test the efficiency of various speciation schemes;

(iii) to compare these results with known detection limits for alternate CE/ICP-MS systems; and,

(iv) to apply this method to model HS systems to characterize and quantify metal ion interactions (i.e. free metal quantification and patterns in HS-fraction associations).

In performing this research, my initial goal was to develop a method whereby HS of environmental origin could be analyzed and characterized according to their metal-binding abilities. As I have outlined in the above introduction, it is known that HS play an important role in the bioavailability of metals through controlling their mobility and fate in environmental matrices (i.e. soil, water). There is no simple method, however, to look at these qualities. CE has shown promise in separating HS into somewhat homogeneous fractions (e.g. Fetsch and Havel 1998; Schmitt-Kopplin *et al.* 1998a), and its hyphenation to ICP-MS has been shown successfully in the literature several times (e.g. Olesik *et al.* 1995; Majidi and Miller-Ihli 1998b). The utility of the combination of CE and ICP-MS to look at metal interactions with HS seemed obvious. To realize this method, however, the separation of HS, and in particular, HS inoculated with metal, needed to be well characterized and understood during the CE process. To this end, the first section of this thesis will describe the attempts to optimize HS separation, and delineate the effects of metal addition to HS separation using UV absorbance to follow the changes in the organic matter in the electrophoretic process. Next, a simple and efficient CE/ICP-MS interface needed to be developed, and proven effective by comparison to results obtained from other interfaces for simple speciation schemes. Thus, a large portion of my work for this project was devoted to different interface designs and the verification of their efficiency. This is reflected in the results

section of this thesis. Finally, the separation and quantification of metals associated with the electrophoretic fractions of HS were analyzed using CE/ICP-MS. These data are in many ways preliminary results of what could be done using CE/ICP-MS for such analyses. The bulk of this work was involved in the development of the methods to allow such analyses. My hope is that this work will provide the framework for more detailed analyses using CE/ICP-MS to answer important questions regarding the nature of metal binding with HS.

2 EXPERIMENTAL

2.1 CE Separations of Humic Substances (*UV Detection*)

2.1.1 *Apparatus*

All separations were carried out using a Beckman P/ACE MDQ CE system equipped with a real-time UV-visible diode array detector (DAD, 190-600 nm) or a variable wavelength (λ) UV detector (UV, 214 nm or 254 nm as noted). When the DAD was used, only λ of 190 to 300 were collected, as this information was used to decide between the use of 214 and 254 nm for subsequent work. Absorbance data was collected at 4 Hz for 10 to 15 minutes and was measured via an on-line window approximately 57 cm along the length of the capillary. Separations were made at constant running voltage (15, 25 or 30 kV, in both normal and reverse modes). Current was monitored and varied according to running BGE and sample volume and matrix.

Uncoated fused-silica capillaries (50 μm ID, 65 cm length) were obtained from Polymicro Technologies. Capillaries were cleaned and conditioned daily by flushing with 100% methanol by pressure application (20 psi) for 10 minutes, 2 minutes with deionized distilled water (ddw), 5 minutes with 0.1 N NaOH, and finally 2 minutes with ddw. Before each sample injection the capillary was cleaned and reconditioned by flushing the column for 1 minute with 2% HNO_3, 2 minutes with 0.1 N NaOH, and 2 minutes with the running BGE. The capillaries were kept at a constant temperature of 25°C (except with rimantadine BGE, 40°C).

2.1.2 *Reagents*

When possible, all reagents used were of trace or HPLC-grade. Three BGEs of different concentrations and pH were used: borate, hydroxymethylamino-methane (Tris) and rimantadine hydrochloride. Borate BGEs were prepared using boric acid and sodium tetraborate obtained from Sigma. Reagents were dissolved to appropriate concentrations in ddw. Tris BGE solution was obtained from Fisher Scientific and used as directed (diluted with 100 % methanol and ddw). Rimantadine hydrochloride (Aldrich) and magnesium chloride (Fisher Scientific) solids were dissolved in ddw to appropriate concentrations and the pH of resulting solutions adjusted using 0.1 M NaOH (Fisher Scientific) or 0.1 M HCl (Fisher Scientific). All rinse solutions and BGEs were filtered (0.45 μm) and degassed before use.

2.1.3 *Samples*

Standard solutions of sulfanilamide (Fisher Scientific) and benzoic acid (Fisher Scientific) were prepared in ddw. These were filtered and degassed before analysis. The standard solution was run twice per day in triplicate to check CE reproducibility.

HAs (AHA) were obtained from Aldrich. Stock solutions of AHA were prepared by dissolving solid samples in a small volume of 0.1 M NaOH and diluting the solution to a total concentration of 1000 mg L^{-1} for AHA and 10^{-6} M NaOH (Fisher Scientific). An aliquot of this sample was set aside for preliminary method development, and to serve as a HA blank for the metal analyses. Aliquots of the stock solution were

diluted to 100 mg L^{-1} and 50 mg L^{-1} with additional NaOH added to maintain a total NaOH concentration of 10^{-6}M. Subsamples of each concentration of AHA were inoculated with various concentrations of Pb (in 2% HNO_3, Fisher Scientific) to achieve ratios of metal to humic content of 1:100, 1:1000, and 1:10000. For example, to achieve a 1:100 ratio of metal to humic content for the 100 mg L^{-1} AHA sample, 1 mg L^{-1} of Pb was added to the solution. Aliquots of each AHA concentration were set aside before Pb addition to serve as humic blanks. Blank solutions of 10^{-6} M NaOH and BGE were also prepared for simultaneous analysis. Approximate pH measurements were made for each sample. All samples were filtered (0.45 μm) and degassed before analysis. Samples were kept in darkness at room temperature for at least 24 hours before analysis.

2.1.4 *Experimental*

Various parameters were manipulated to achieve separations of the HAs. Initially, BGE composition was explored as the most important parameter that effects CE separations. Comparisons of results for the various concentrations of AHA using the borate, Tris and rimantadine BGEs were analyzed according to optimal separation, the criteria for which being short analysis time (<15 minutes), minimal background, and discernible and reproducible patterns in the "humic hump". Sample injection volumes and separation voltages were also manipulated to aid in achieving optimal separation, and these parameters used for analysis in subsequent experiments.

All BGEs were prepared daily from stock solutions (borate and Tris BGEs) or by dissolving the solids in ddw and diluting the solution to the appropriate

concentration (rimantadine hydrochloride), degassed and filtered through a 0.45 μm membrane. For the exploratory work, the DAD detector was used, gathering absorbance data from 190 nm to 300 nm at 10 nm intervals. Subsequent samples were analyzed using the UV absorbance detector at 214 nm or 254 nm as noted.

After the initial method development, samples were typically run on the CE using the following standard conditions (any deviations from these methods are noted). The separation capillary used was 65 cm length x 0.5 μm ID, with a UV window approximately 50 cm along the length to facilitate UV detection. The capillaries were treated as described in section 2.2.1 before and between each sample. Approximately 47 nL was injected onto the capillary, as calculated by CE Expert (Beckman) for an injection pressure of 1 psi for 15 seconds. For all BGEs, save the rimantadine hydrochloride, a positive voltage was applied at the injection end of the separation capillary (normal mode CE). The value of this voltage was typically 25 kV, resulting in a current of approximately 15 μA for borate BGE. Run times were usually 15 minutes, using either the UV or PDA detector. Data analysis was performed using both the Beckman P/ACE software package, with subsequent peak area and migration time analysis using ®PeakFit v.4 (SPSS Inc).

2.2 CE/ICP-MS Interfaces: Design and Optimization

2.2.1 *Apparatus*

The initial design for the interface for the CE system and the ICP-MS instrument is shown in Figure 2.1. To attach the CE to the direct injection high efficiency nebulizer (DIHEN, J.E. Meinhard & Associates), a PEEK cross was used within which the separation capillary from the CE system transverses 2 arms of the cross, allowing the make-up solution to be pumped concentrically around the separation capillary. As well, an electrode makes contact with the make-up electrolyte solution within the cross, allowing the current to be carried to the terminus of the separation capillary where the electrolyte solution and electrophoretic solution mix within the DIHEN before nebulization.

A second interface was designed, incorporating the use of a high efficiency nebulizer (HEN, J.E. Meinhard & Associates) and a cyclonic spray chamber (Precision Glassblowing). A picture of this interface is shown in Figure 2.2 (a schematic drawing of the HEN is shown in Figure 1.2, page 24). Again, a cross is used to attach the separation capillary, make-up electrolyte solution flow, and electrode to the nebulizer, as described for the DIHEN interface. The spray chamber fits directly into the normal injector for the PE Elan 6000 allowing aerosol to be delivered to the plasma, and large droplets to be pumped away via a drain on the bottom of the spray chamber.

The CE system used for these analyses is as described in section 2.2.1. Uncoated fused-silica capillaries (Polymicro Technologies) with an inner diameter of

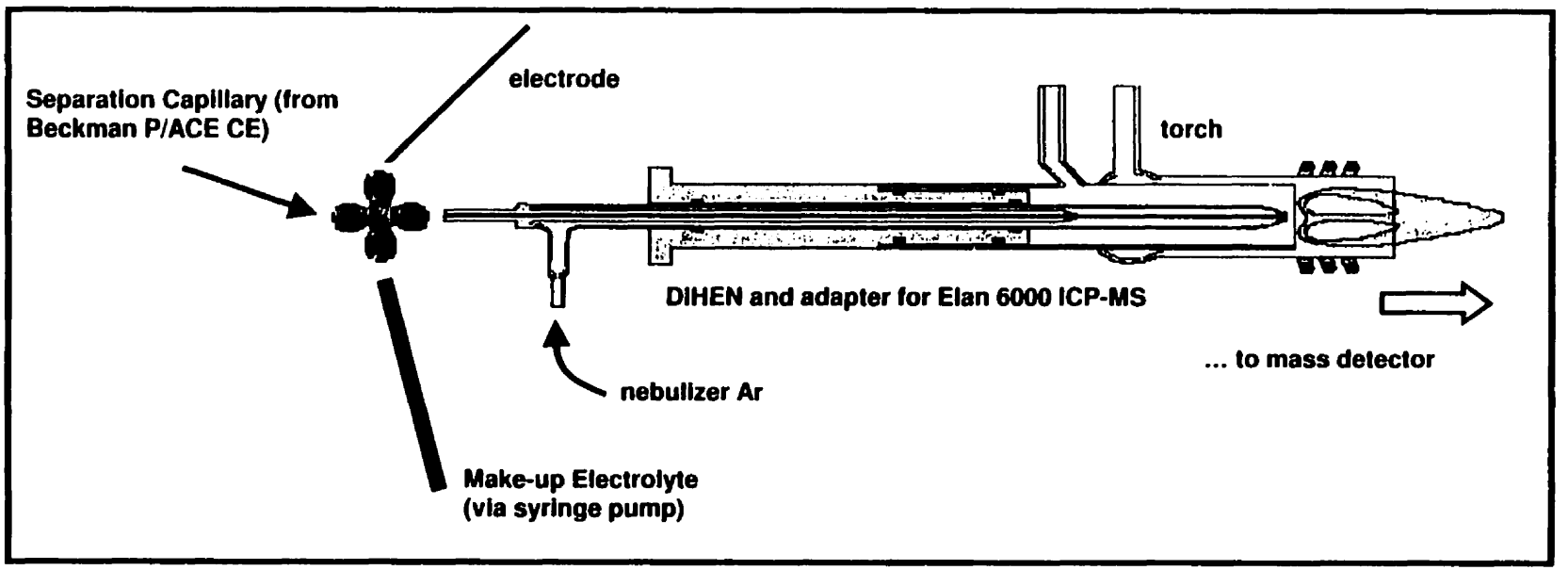

Figure 2.1: Schematic of DIHEN interface. The basic components of the CE/DIHEN/ICP-MS interface are shown. The DIHEN fits snugly in the adapter. The adapter replaces the normal injector allowing the DIHEN nozzle to be within a few mm of the plasma.

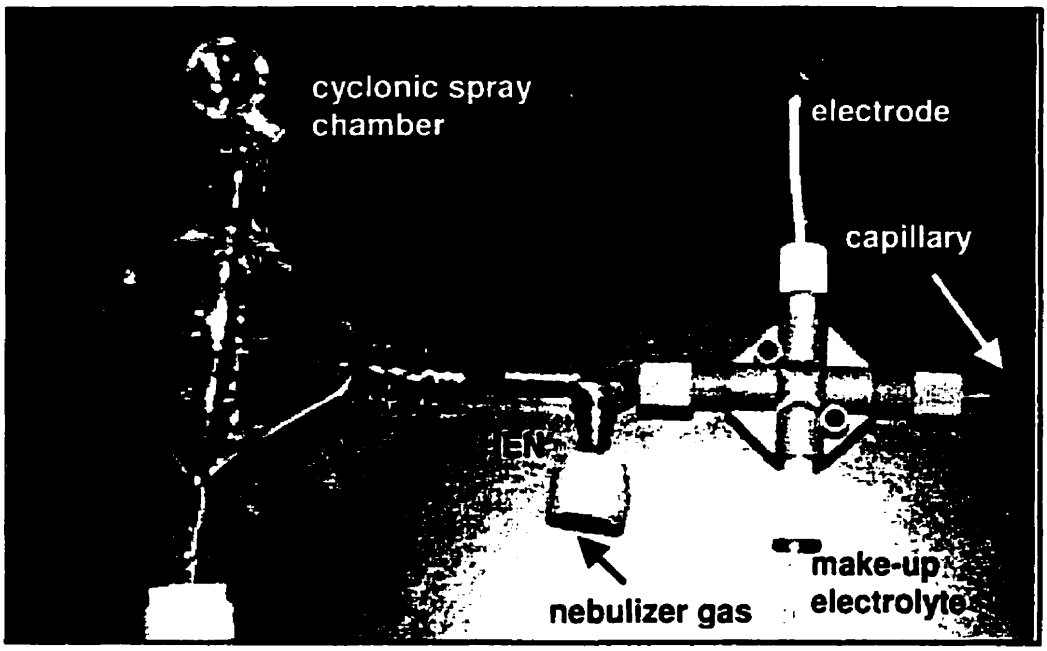

Figure 2.2: Details of the HEN/cyclonic spray chamber interface. All components of the interface can be seen in (a): the terminal end of the separation capillary can be seen in the right of the photo, and is attached to the HEN via the cross connector; extra electrolyte and an electrode are also connected to the HEN with the cross connector. Nebulizer Ar flows concentrically around the sample introduction of the capillary as solution flows out causing aerosol formation. Large droplets of sample collect on the walls of the spray chamber, and drain out at the bottom, and aerosols are introduced to the plasma via the Ar flow out the top. A schematic of the nebulizer can be seen in Figure 1.2.

50 μm were used. The column was housed in Beckman's specialized external detector adapter (EDA) allowing the terminus of the capillary to exit the side panel of the instrument. To accommodate the EDA and the distance needed to reach the interface, a 75 cm column was used for the HEN/conical interface, and a 65 cm capillary was sufficient for the DIHEN interface. Capillary conditioning and inter-sample cleaning were as described in section 2.1.1.

The ICP-MS instrument used for these analyses was a PE Sciex Elan 6000 (Perkin-Elmer). Adaptations to the normal sample introduction apparatus are described above. Plasma gas and intermediate gas flow rates were set at 15.0 L/min and 0.8 L/min respectively. Nebulizer gas rates for the DIHEN interface were optimized via the mass-flow controller of the ICP-MS nebulizer gas system. Nebulizer gas rates were optimized for the HEN/cyclonic interface using an external supply of Ar equipped with a high-pressure regulator. Nebulizer gas flows and RF power were optimized daily. RF power for the HEN/conical interface was typically about 650 W, as opposed to 1500 W for the DIHEN interface.

2.2.2 *Reagents*

The electrolytic solutions used for the validation of the CE/ICP-MS interfaces were phenanthroline and borate BGEs. In all cases, trace-grade or HPLC-grade reagents were used when possible. Phenanthroline BGEs were made by dissolving phenanthroline (Fisher Scientific) and ammonium nitrate (Fisher Scientific) in ddw to 10 mM and 5 mM, respectively, and adjusting the pH to 8.5 with 0.1 M ammonium

hydroxide (Fisher Scientific). Borate BGEs were made as described in section 2.1.2. All rinsing and cleaning agents are as described in section 2.2.2. All BGEs were filtered (0.45 μm) and degassed before use.

2.2.3 *Samples*

For the optimization of the DIHEN interface, a mixture of metals was used initially as a test of the resolution of the system. This pre-made metal mix of sample solution consisted of 1 mg L^{-1} for each of Ba, Cd, Co, Cs, Cu, Mg, Mn, Ni, Pb and Tl (CLMS-2, SPEC Certiprep, Inc.). Tuning solutions and mixed metal samples were made from stock solutions of Pb, Mg, Cu, Mn and Rh in 2 % nitric acid (Fisher Scientific). Stock solutions of Sr were obtained from Fisher Scientific and used as an addition to BGE solutions for electroosmotic flow (EOF) monitoring. In all cases, metals were diluted in ddw to the desired concentration.

Stock solution of EDTA (Fisher Scientific) was made in ddw. Blanks and samples spiked with Pb were made. Pb was added in small aliquots from stock solutions (Fisher Scientific). The concentrations of all samples are discussed in the results section. All samples were filtered (0.45 μm) and degassed prior to analysis.

2.2.4 *Experimental*

The DIHEN interface was optimized daily for RF and nebulizer gas flow rates using a tuning solution of 5 mg L^{-1} each of Cu, Mg and Rh, and 10 mg L^{-1} Pb. Optimization criteria were the settings for each at which the highest sensitivity was

observed. Daily checks for suction and backpressure were performed for the interface. In brief, these consisted of immersing the end of the capillary into stock solutions of Pb (1000 mg L^{-1}), waiting several minutes, then flushing the capillary with the BGE solution. The observance of Pb in the flushed solution would indicate that there was significant suction through the capillary. Alternately, the make-up solution could cause backpressure into the capillary. This backpressure was estimated in the following manner: the separation capillary was filled with BGE spiked with 200 μg L^{-1} Sr and allowed to sit for a few minutes. The capillary was then flushed at a reasonably low pressure (5 psi). If there is no appreciable backpressure, the BGE should be immediately seen by the detector as Sr. On the other hand, if the make-up is pushing back into the capillary, a substantial amount of time will pass upon the addition of pressure before the Sr signal is observed. In the development of these methods, it was found that there was typically a "sweet spot" where the backpressure and the suction seemingly cancelled each other. The height of the CE system relative to the ICP-MS injector at which this occurred, as well as the make-up solution flow rate were used for all analyses, and checked periodically to maintain the balance.

For all experiments requiring the separation of analytes via CE and detection using ICP-MS, the CE methods were as described in section 2.2.4, save the length of the separation capillary (65 cm for the DIHEN interface, 75 cm for the HEN/cyclonic). The pressure of the rinse steps was maintained at 10 psi to avoid creating excess pressure within the cross fitting and erratic nebulization due to excess liquid flow. All samples were run at least three times under the same conditions.

2.3 Analysis of AHA-Pb by CE/ICP-MS (*ICP-MS Detection*)

2.3.1 *Apparatus*

The CE/ICP-MS interface used is as described for the HEN/cyclonic interface in section 2.2.1.

2.3.2 *Reagents*

All reagents used pertaining to the CE-related portion of the AHA separation are as described in section 2.1.2. Borate BGEs were used for all analyses, including standard Pb samples. Borate BGE was used as the make-up solution as prepared for CE analysis. Sr was not added to aid the monitoring of EOF due to the suspicion that Sr ions may interfere with the interaction of Pb with the AHA molecules during separation. Data collection for ICP-MS electropherograms was started when the CE voltage was applied.

2.3.3 *Samples*

Solid samples of AHA were dissolved in a small volume of 0.1 M NaOH and diluted with ddw to a total AHA concentration of 500 mg L^{-1} and 10^{-6} M NaOH. An aliquot of this sample was set aside to serve as a HA blank for the metal analyses. Subsamples of AHA were inoculated with various concentrations of Pb (in 2% HNO_3) to achieve metal concentrations of 5, 25 and 50 mg L^{-1}. Solutions of 0.1 M NaOH and 0.1 M HCl were used to adjust the pH of subsamples of each metal concentration to an

acidic (pH < 5), neutral (pH 6 to 7) or alkaline (pH > 7) solution. Approximate pH measurements were made for each sample. All samples were filtered (0.45 μm) and degassed before analysis. Samples were kept in darkness at room temperature for at least 24 hours before analysis. Standard Pb solutions were analyzed as described in section 2.2.3.

2.3.4 *Experimental*

Daily optimization and instrumental tuning were performed as described in section 2.2.4. Standard solutions of sulfanilamide and benzoic acid were analyzed each morning using UV detection to provide an estimate of daily analytical error associated with the electrophoresis. Samples and standards were analyzed as described in section 2.2.4. Data analysis was performed using both the PE Elan 6000 software package, with subsequent peak area and migration time analysis using both ®MS Excel and ®PeakFit v.4 (SPSS Inc).

3 RESULTS AND DISCUSSION

The bulk of the work done towards this thesis involves the development of various methods before the final application of CE/ICP-MS to the study of HS-metal interactions. As such, a great deal of the following results/discussion section attempts to describe and clarify the procedures and outcome of these incremental steps in the development of the final methods. To begin, the separation of HS using CE is explored using Aldrich HA (AHA) as the model compound. The use of AHA will be carried throughout the experiment to allow for direct comparison of results. Initially, in section 3.1.1, the appropriate BGEs and wavelength for UV analysis are explored, with an emphasis on the descriptive differences seen with each parameter, and the criteria used to determine the optimal conditions. Then, in section 3.1.2, the CE method with UV detection was applied to an AHA-Pb mixture to explore the changes in mobility patterns, or fingerprints. This study allows for a better understanding of the changes metal addition makes upon the migration of the organic molecules, but analyses of the Pb binding patterns are not possible. To make the change from UV to ICP-MS detection, an analysis of the properties and efficacy of two interface designs (the DIHEN, and the HEN/Cyclonic) was undertaken. Section 3.2 describes this process in detail, including the optimization of both systems, and the quantification of simple speciation schemes. Finally, in section 3.3, the method in its entirety is described as the application of AHA inoculated with Pb. Samples are separated using CE and the associated Pb is detected using ICP-MS. Thus, the observations noted throughout the initial experiments can offer

insight for this final section, as the UV analysis of AHA will allow comparison of the organic data with the metal data. As well, the migration times and resolution of separation observed for simple speciation schemes allows an evaluation of the relative mobility of the metal species in the final experiment.

3.1 CE Separation of Humic Substances (*UV Detection*)

3.1.1 *Method Development: Choice of BGE and Wavelength*

One of the most important aspects of good electrophoretic separation is the choice of an appropriate BGE. As discussed in section 1.4.1, BGE pH and composition are important parameters for determining the separation potential of an application. Although several viable BGE systems have been presented in the literature for HS separation, none have been applied for use with ICP-MS as the detector. As well, Aldrich HA (AHA) is used as the model compounds for my analyses, necessitating the optimization of their separation for my purposes. The concentration of HS in natural waters is variable, but usually in the low (2 to 30) mg L^{-1} range. Thus, it would be preferable to use BGEs that allow sensitive quantification of very low concentrations of the model compounds to allow some reasonable assumptions regarding the behaviour of natural HS in CE.

In most cases, the study of HS using CE involves the use of very high concentrations of the analytes, generally in the range of 100 mg L^{-1} to 1000 mg L^{-1}. The results of Fetsch and coworkers (1998a) indicate that the need for high concentrations of

analytes is due, in part, to HS absorbance to the capillary walls. In tests where the sample was allowed to rest for increasing amounts of time after injection but before application of a voltage, the researchers found an inverse relationship between resting time and the magnitude of response seen. In fact, it was observed that no response would be seen if the plug of sample (~ 10 mg L^{-1} HA) was allowed to sit for over three minutes before pushing through the capillary (Fetsch *et al.* 1998a). This would indicate that there is a kinetic dependence on the absorption of HS to the capillary walls. The possibility of interactions between the silanol groups of the inner wall of the capillary and the many diverse functional groups of HS is great, particularly when the HS are highly deprotonated in an alkaline BGE. This is a fairly common problem in the separation of proteins and amino acids, and the problem has been rectified in many cases by the addition of a surfactant, the use of an organic solvent, or complexing agents (Fetsch *et al.* 1998a). In particular, the addition of metal ions to inhibit the interaction of the silanol groups with the analytes has been found to be a successful approach, and that which was used by Fetsch and coworkers (1998a). These researchers were able to enhance the UV response of low concentrations ($\geq$ 10 mg L^{-1}) of HS using BGEs consisting of rimantadine hydrochloride and magnesium (II) salts.

In determining the appropriate BGEs to use for this work, results obtained using rimantadine hydrochloride were compared to those of traditional HS separation BGEs. The more traditional (as they have been used the most) BGEs are borate (Dunkelog *et al.* 1997; Nordén and Dabek-Zlotorzynska 1997; Schmitt *et al.* 1998, Fetsch *et al.* 1998b) and Tris (Dunkelog *et al.* 1997). A comparison of these three BGEs

regarding the separation of a 50 mg L^{-1} sample of AHA can be seen in Figure 3.1. In all cases, the conditions are optimized for each BGE system in terms of the greatest separation possible that is above background noise. Parameters optimized include temperature of separation (20 to 60 °C), voltage (10 to 30 kV), concentration of BGE constituents, and pH of the BGE. Criteria for selection of parameters included reproducibility, sensitivity (measured as lowest concentration of AHA detectable above background and as function of response for various peaks), and the number of peaks detectable (taking into account the humic hump, peaks that emanate from the humic hump, and all other peaks). For Figures 3.1(b) and (c), electropherograms are representative results of three replicates, with RSD < 4 % for migration times, peak areas and peak heights of all apparent peaks. Figure 3.1 (a) does not represent a number of samples, but rather is the best results achieved for the 50 mg L^{-1} AHA sample according to the determined parameter selection criteria. This inconsistency in replication will be discussed presently.

These separations are comparable to those seen in other studies of AHA and model compounds. In particular, the humic hump is observed in all results; due to the heterogeneous nature of the HS, their separation cannot be finite, as each molecule of the mixture may be unique to the total composition. Instead, the separation results in broad bands representing a gradient of size and charge. In Figure 3.1 (a) the electropherogram for AHA separated in rimantadine hydrochloride shows some defined peaks and two distinct "hump" regions (migration times of 4 to 5.5 minutes and 5.5 minutes to 6.25 minutes, respectively). This shape is similar to that seen by Fetsch

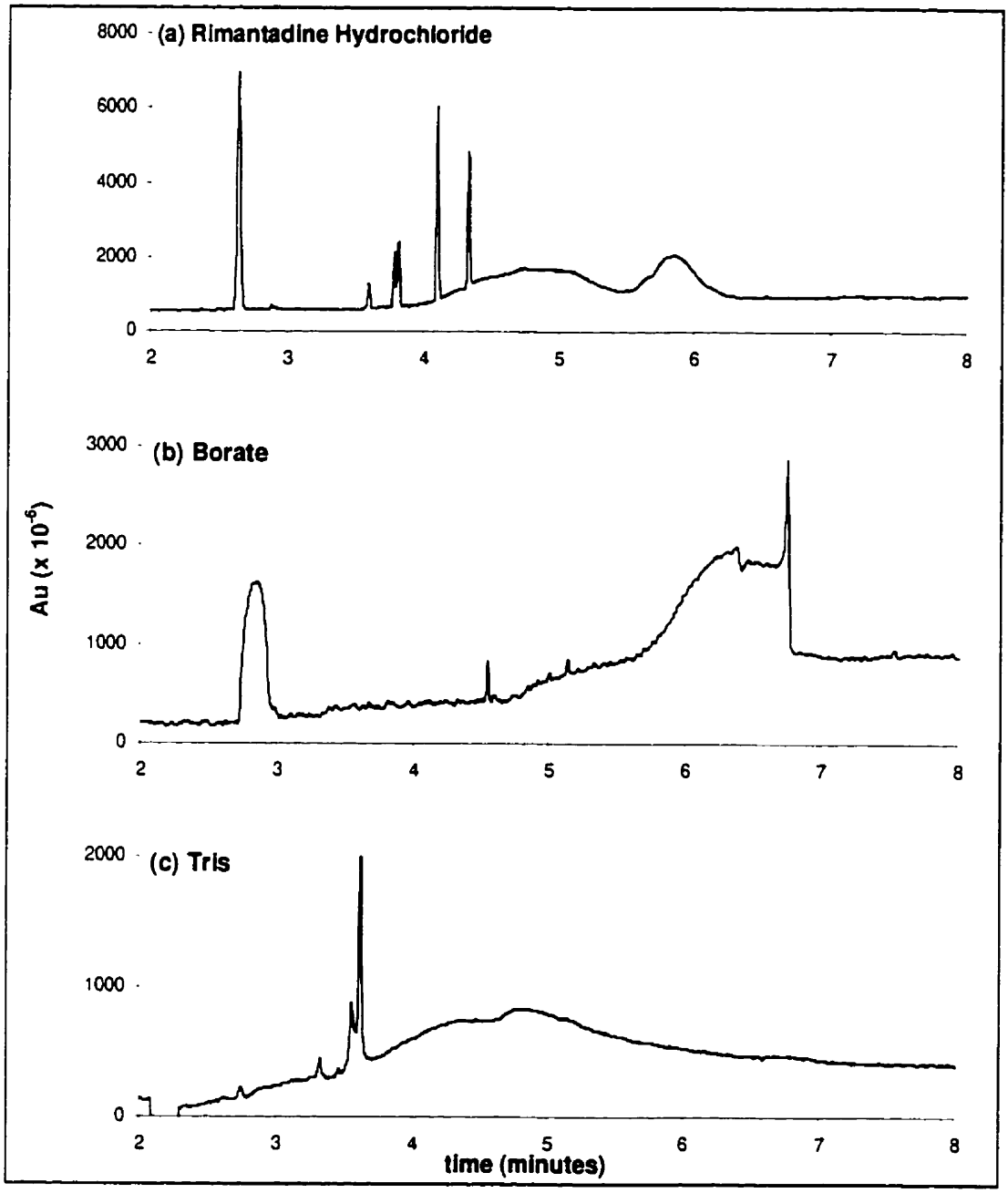

Figure 3.1: Comparison of BGE constituents. UV absorbance electropherograms (λ =214 nm) of 50 mg L^{-1} AHA separated in (a) 20 mM rimantadine hydrochloride, 25 mM $MgCl_2$ (pH 3.3), (b) 45 mM borate (pH 8.2), and (c) 20 mM Tris (pH 8.3). Separation conditions: 50 mM ID; -15 kV for (a), +25 kV for (b) and (c); 40°C for (a), 25°C for (b) and (c); pressure injection (15 seconds at 1 psi). Note the difference in scale for the y-axis of the figures.

et al. (1998a) for Fluka HA. The separation shown in Figure 3.1 (b) is, again, similar to typical separations of AHA seen in borate BGEs of various concentrations (Nordén and Dabek-Zlotorzynska 1997) and other model HAs in borate BGEs (Schmitt-Kopplin *et al.* 1998). The separation that is shown in 3.1 (c) is the least defined of the three, in terms of intensity of response and the number of apparent peaks. A large negative peak is seen at approximately two minutes due to NaOH in the sample solution. This observation was verified by the results of a blank solution containing only ddw and 10^{-6}M NaOH that exhibited a large negative peak with the same migration time. This is comparable to the large positive peak seen at 2.25 minutes in the borate BGE [Figure 3.1 (b)], which may also be attributable to NaOH in the sample matrix, as validated with a blank run in the same BGE solution. These early peaks can be used to determine the EOF under the different conditions (e.g. Schmitt-Kopplin *et al.* 1998b).

As the analyst is interested in obtaining the greatest separation of analytes while maintaining sensitivity above background and reproducible results, there may need to be a trade-off involved in the selection of BGEs. In the separation of AHA in rimantadine hydrochloride [Figure 3.1 (a)] there is the greatest number of individual peaks and the most definition (i.e. number of emanating peaks or resolution of those peaks) seen in the humic humps. As well, the response is the highest for the three BGEs tested (A_{max} = 7.5 mAu). The borate BGE is also promising as the humic hump shows a strong response (A_{max} = 2 to 3 mAu), yet the separation of HS components would seem to be limited to the approximately one minute wide peak area. The Tris BGE would appear to be the least desirable BGE for this application due to the low response (A_{max} = 0.85

mAu). There does appear to be, however, a very broad separation of the components, as the humic hump is very wide albeit of low UV absorbance.

An important consideration for this method development was the reproducibility of the electropherograms. The variability of the separations was estimated using the percentage RSD for the migration times, peak areas, and peak heights of the observed peaks for the separation in each BGE. As previously reported, the percentage RSD for all parameters was below 4 % for both the separation of three replicates of 50 mg L^{-1} AHA in borate and Tris BGEs [Figures 3.1 (b) and (c), respectively]. For three consecutive measurements of 50 mg L^{-1} AHA in rimantadine hydrochloride, RSDs for all measured parameters was greater than 15 %. For some replicates, the pattern observed in the results was so different from the others that they were not included in later calculations, as there were no reference points for comparison. This is contrary to the results of Fetsch *et al.* (1998a), who report very low percentage RSDs under the same conditions. This discrepancy may be due to differences in procedures (such as capillary conditioning before and during analysis) or to the quality of the HA analyzed. At this point, however, there is no clear explanation of why these differences were seen. Due to the lack of reproducibility observed using the rimantadine hydrochloride, this BGE was rejected for use, even though the results of some replicates indicated that its use may allow a greater separation of the HA components.

To obtain a better perspective of the differences in the separation between the two remaining BGEs (borate and Tris), samples were analyzed using the photodiode array (PDA) detector with the CE system. Electropherograms were recorded from 190

nm to 300 nm for the selection of a wavelength at which optimal absorbance occurs (i.e. 214 *vs.* 254 nm). The PDA is less sensitive than the UV detector, and was used only for my initial exploratory work.

Due to the ability of covalent organic bonds to absorb in the UV spectrum, there should be some continuity in absorbance throughout the wavelength range measured. At lower UV wavelengths such as 215 nm, carboxyl carbon-oxygen bonds dominate light absorbance, at 254 nm aromatic carbon-carbon bonds are the prevailing absorbents, and at 300 nm carbonyl carbon-oxygen bonds dominate (Perkampus 1992). All of these functional groups and molecular bonds are present in HS, so the response of the HS separations at different wavelengths could indicate the nature of the functionality of the separated fractions. Figure 3.2 presents the results of the separation of a 50 mg L^{-1} AHA sample in both (a) borate BGE and (b) Tris BGE. The absorbance response in absolute absorbance units is lower than seen in Figure 3.1 due to the lower sensitivity of the PDA detector. In the borate BGE, a peak is seen at approximately 2 minutes, which is constant throughout the spectrum. This is consistent with a NaOH peak. To verify the identity of this peak, a blank containing ddw and 10^{-6} M NaOH was analyzed and found to have a similar absorbance and migration time. The NaOH peak is very different in the Tris BGE; it appears as a negative peak at shorter wavelengths, and positive at longer wavelengths. This is consistent with results seen in other organic BGEs, such as alanine (Fetsch and Havel 1998).

To compare the results of the two separations to determine which BGE would be used for subsequent separations, criteria of peak separation, humic hump

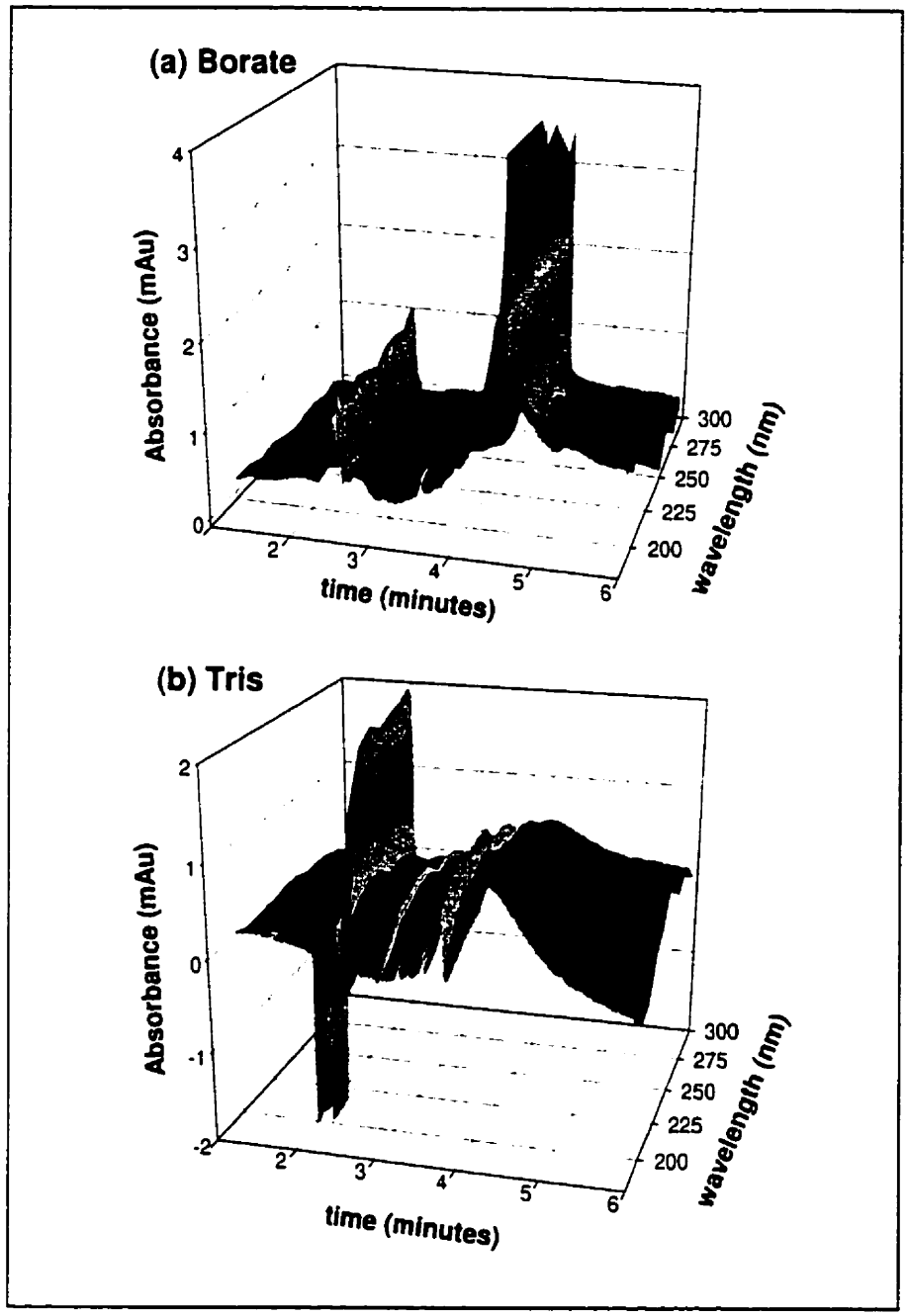

Figure 3.2: Comparison of BGE constituents: PDA results. Results of the separation of 50 mg L^{-1} AHA in (a) 45 mM borate BGE, and (b) 20 mM Tris BGE. Conditions are as described in Figure 3.1 (b) and (c), respectively for (a) and (b).

differentiation and sensitivity in response were used. Theoretical plates and resolution could not be directly calculated because two or more peaks, distinct from the humic hump, were not quantifiable. The separation in the Tris BGE shows a less sensitive response, save the initial water peak (not shown), than the borate separation. As well, there is a more defined humic hump fraction in the borate, although this may be due to the overall lower response seen with the Tris BGE. Finally, there are a greater number of individual peaks seen in the electropherogram for the borate BGE [Figure 3.2 (a)] than for the Tris BGE [Figure 3.2 (b)]. Thus, for all three defined criteria, the borate BGE provides the better BGE for AHA separation, and borate was consequently chosen as the BGE for subsequent experiments.

The use of borate BGEs for the characterization of HS has received criticism due to an understanding of the effect of HS-borate ion complexes on the separation of HS; the concentration of borate in the electrophoretic BGE can affect the separation of the HS particularly for the characterization of HS fingerprints (Schmitt-Kopplin *et al.* 1998a; Schmitt-Kopplin *et al.* 1998b). These authors propose that some differentiated peaks in electropherograms of HS may be caused by complexation of the hydroxy groups of boric acid or borate ions with *cis*-diol groups in the HA. They observed that a large, very reproducible peak could be seen emanating from the humic hump region for various soil-derived HA extracts. The migration time and amplitude of this peak was found to be dependent upon the concentration of borate or boric acid in the BGE, and not upon the concentration of HA in the sample. Figure 3.1 (b) shows a peak (migration time = 6.8 minutes) very similar to that described by Schmitt-Kopplin and

coworkers (1998a, 1998b). This peak, however, is not seen in subsequent analyses (see section 3.1.2), and thus it is assumed that possible artifacts due to the use of borate BGE are not a complicating factor for my studies. It is possible that the high concentrations of HA (50 to 1000 mg L^{1}) used in my subsequent work (section 3.1.2) may mask the interaction of borate ions and the HA. It is unclear what concentration of HS was used in the Schmitt-Kopplin *et al.* studies (1998a; 1998b), but it appears to be as low as 50 mg L^{-1}. As I did not observe these peaks for the lower concentration samples, my results may differ because the concentration of borate in the BGEs used for my experiments (45 mM) are not high enough to cause discernable problems with complexation. Schmitt-Kopplin *et al.* (1998b), however, observed the HS-borate complex for HS separations in borate BGEs with a concentration as low as 0.5 mM. The reasons for the differences between my results and the results of other researchers using borate BGEs are unclear. My goal, however, was to separate the HS to the extent to which metal complexes (both free metal and metal bound to the HS) could be analyzed, as well as to make some generalizations regarding the nature of metal binding to various size and charge classes of HS. Thus, the effect of HS-borate complexation was examined yet not considered a detriment to the present study.

In both plots shown in Figure 3.2, a greater response is seen at lower wavelengths; this is due to the increase in the types of chemical associations that are able to absorb the shorter wavelengths, and is typical for HS (Keuth *et al.* 1998). Thus, at higher λ-values there may be a more specific response for the various functional groups of AHA, yet the magnitude of the response, and therefore the sensitivity of the detector

will be lower. At the lower wavelengths, higher responses are seen yet this may not be due solely to the analytes of interest, but to a broader spectrum of organic and inorganic components. Two wavelengths were chosen for subsequent work: 214 nm and 254 nm. These values show substantial response for both the borate BGE and Tris BGE separations. As well, they are typical wavelengths used in the literature for this work, and thus will allow comparison to other works.

3.1.2 *Application to AHA-Pb Samples*

The ultimate goal of this work is to develop and evaluate a method for analyzing HA and its interaction with metals using CE/ICP-MS. The separation of HA using CE should be well characterized, especially upon addition of metal species that have the potential to change both the mass and charge of the molecules. As well, some observations may be made regarding the interaction of metal species and HA according to their migration patterns using UV detection. With these goals in mind, an analysis of AHA inoculated with varying amounts of Pb was analyzed using CE with on-line UV detection.

Like other separation processes, CE results can be slightly different from day to day, and are highly dependent upon the concentration of BGEs, capillary conditions, and sample matrices. Thus, for each analysis, standards were run to evaluate not only the day-to-day variability of the system, but also to estimate the reproducibility of the separation itself. For this work, a solution containing 20 mg L^{-1} sulfanilamide and 10 mg L^{-1} benzoic acid was used. These analytes can be resolved using a borate BGE,

and both show significant absorbance at the wavelengths analyzed (214 and 254 nm). Although these standards are not components of the HA mixtures, they are used to estimate the day-to-day variability that is due to instrumental and BGE differences. This does not reflect error due to analyte composition and interaction with the sample matrix. Thus, the variability in results estimated from the standard solutions represents the minimum variation for the separation of the AHA.

The standard solution results for the following AHA-Pb analysis are shown in Table 3.1. The migration times and peak areas for three replicates of the same solution are listed, as well as their average, standard deviation and percentage RSD. These peaks were highly reproducible in terms of both migration time and peak area (percentage RSD < 1 %). As this is a simplistic separation (only two analytes are

Table 3.1: Standard results for CE reproducibility. Migration times (MT) and peak areas (PA) for a solution containing 20 mg L^{-1} benzoic acid and 10 mg L^{-1} sulfanilamide are listed for three replicates. CE conditions are as in Figure 3.1 (b). Percentage RSD for both migration time and peak area are low for both standard compounds (< 1%).

	20 mg L^{-1} benzoic acid		**10 mg L^{-1} sulfanilamide**	
	MT (min)	*PA*	*MT (min)*	*PA*
replicate 1	2.94	259000	5.36	34100
replicate 2	2.95	255000	5.44	34300
replicate 3	2.95	255000	5.38	34500
average	*2.94*	*256000*	*5.39*	*34300*
% RSD	*0.07*	*0.86*	*0.74*	*0.63*

separated), the systematic error associated with this CE unit was considered to be approximately 1 %, although the error associated with the more complicated sample systems often proved higher than this value.

The samples of AHA inoculated with Pb were analyzed according to standard CE methods described in section 2.2. Briefly, they are as follows: 50 μm ID capillary; total length 65 cm (57 cm to UV window); 45 mM borate BGE; injection: 1 psi for 10 seconds, or approximately 47 nL; +25 kV. Samples were run in triplicate, and a representative electropherogram is shown in Figure 3.3 for each sample. The sample concentrations were chosen as three representative ratios of metal to AHA (mass per mass, metal:AHA): 1:100, 1:1000, and 1: 10000. Control samples consisted of AHA with no metal added, injections of BGE solution and injections of blanks. It was assumed that the lowest ratio of metal to AHA would guarantee the existence of free metal, as this may be above the complexation capacity of AHA, whereas the ratio of 1:10000 would allow the analysis of a sample with essentially all of the metal bound to the organic ligands. A similar study used 10 mg L^{-1} FA inoculated with 10 mg L^{-1} Pb; in neutral conditions less than 30 % of the metal was bound to the FA (Nordén and Dabek-Zlotorzynska 1996). Considering that HA are not considered as efficient in binding metal as FA, the concentration ratios used in my study should provide a range of metal speciation for analysis.

Three different concentrations of AHA were used for this work: 50, 100 and 1000 mg L^{-1}. The identification of the various peaks associated with these separations can be seen in Figure 3.4. Peak 1 was apparent in all samples, including the

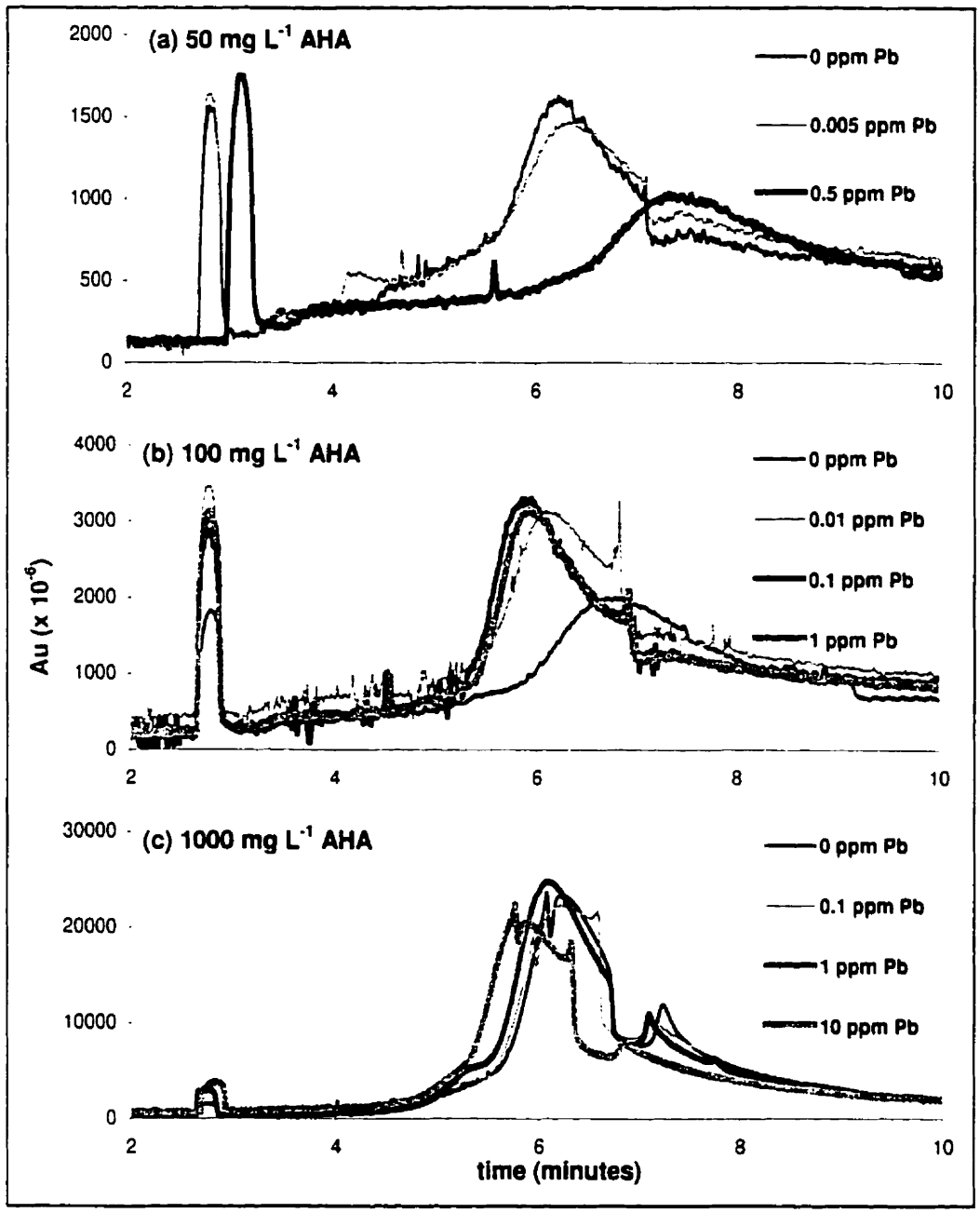

Figure 3.3: AHA-Pb UV analysis. Electropherograms of (a) 50 mg L^{-1}, (b) 100 mg L^{-1} and (c) 1000 mg L^{-1} AHA for samples inoculated with varying concentrations of Pb. For Figures (b) and (c) a decrease in migration is seen with increasing metal concentration. Separation conditions are as in Figure 3.1 (b). Note: 1 ppm = 1 mg L^{-1}.

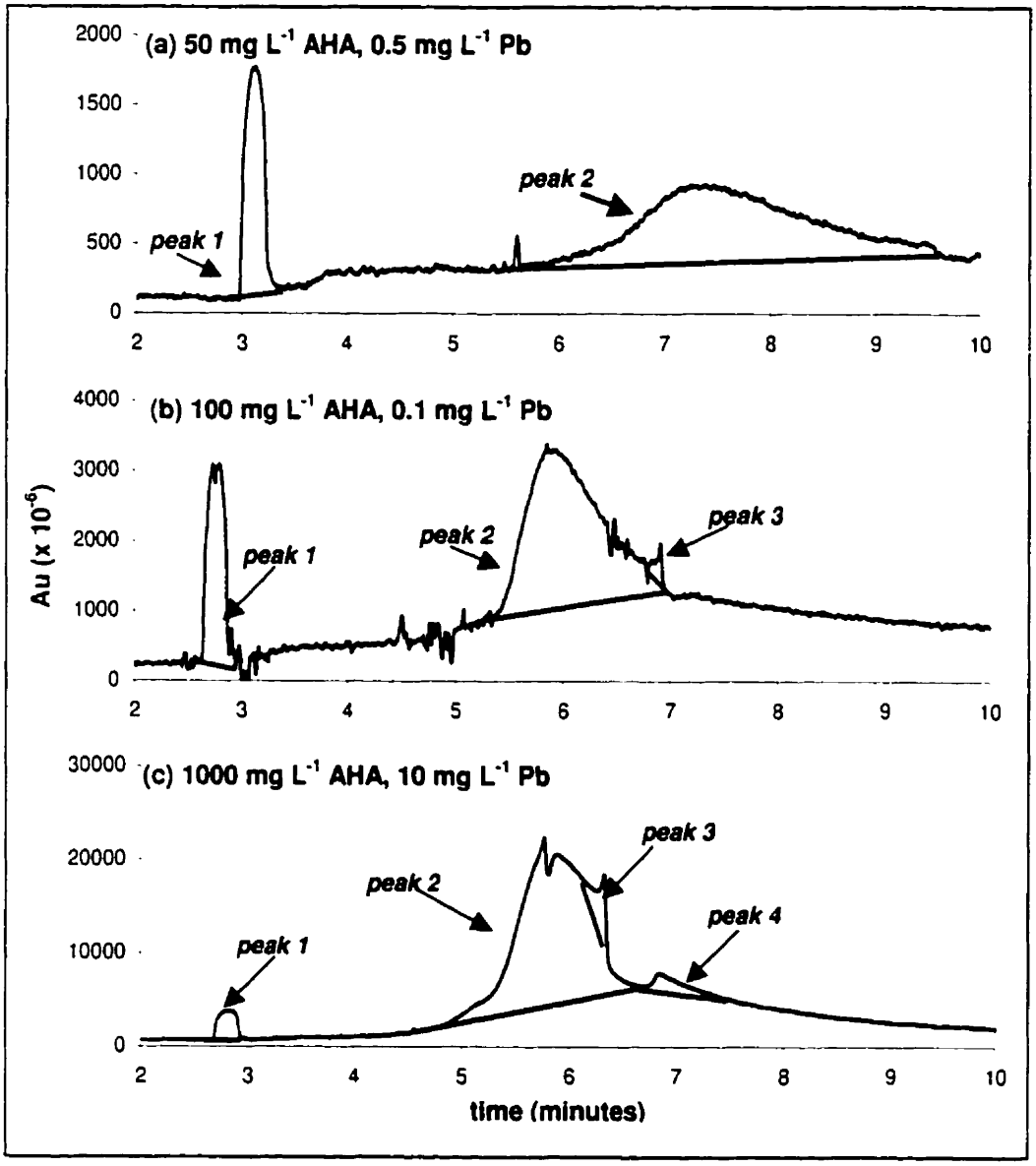

Figure 3.4: Peak identification for analysis of AHA peak areas. Peaks 1 and 2 could be identified in all samples, and are identified by the migration times as indicated in both (a) and (b) (water blanks have only peak 1). Peaks 3 and 4 were evident in some of the samples. All peak areas were determined from the baseline of the electropherogram, as indicated in for the peaks shown in both (a), (b) and (c). Separation conditions are as in Figure 3.1 (b).

blanks, but not in BGE blanks. This peak represents the NaOH associated with the sample matrix, and can be used to estimate the neutral migration (EOF) in the BGE under the conditions stated. All AHA samples exhibited peak 2, which is the main component of the migration of the humic material (i.e. the humic hump). Some samples also showed a somewhat reproducible peak (percentage RSD_{area} < 25 %) arising from peak 2 (peak 3). Peak 4 is only detected in the highest concentrations of AHA (1000 mg L^{-1}). The migration times of these peaks are listed for each sample in Table 3.2, and the peak areas

Table 3.2: AHA-Pb analysis: Migration times. Peak migration times (MT) for AHA samples inoculated with varying amounts of Pb. Peak identification is as shown in Figure 3.4. MTs are averages of replicates (n = 3). Percentage RSD for all peaks is < 12 %.

conc. AHA (mg L^{-1})	conc. Pb (mg L^{-1})	peak 1		peak 2		peak 3		peak 4	
		MT (min)	% *RSD*	MT (min)	% *RSD*	MT (min)	% *RSD*	MT (min)	% *RSD*
0	0	2.97	*7.18*						
50	0	2.83	*0.43*	6.26	*0.69*	6.75[a]			
	0.005	2.81	*0.13*	6.30	*1.11*				
	0.5[b]	2.97	*6.88*	6.65	*10.6*				
100	0	3.03	*7.20*	7.20	*11.6*				
	0.01	2.76	*0.15*	5.96	*6.72*	6.83	*0.24*		
	0.1	2.76	*0.26*	5.97	*0.74*	6.69	*6.36*		
	1	2.77	*0.17*	6.01	*0.55*	6.91	*0.38*		
1000	0	2.74	*1.14*	6.22	*0.47*			7.25	*0.07*
	0.1	2.74	*0.23*	6.26	*3.01*	6.56	*0.59*	7.11	*0.63*
	1	2.73	*0.09*	6.12	*0.42*			7.10	*0.26*
	10	2.81	*0.09*	5.82	*0.25*	6.32	*0.23*	6.86	*0.15*

[a] Peak seen in one replicate only. [b] Average and percentage RSD calculated from two replicates.

in Table 3.3. The data given are averages of three replicates, and their associated error is estimated as percentage RSD. For all migration times, percentage RSD is low (< 3.01 %), except for peaks seen in 50 mg L^{-1} AHA with 0.005 mg L^{-1} Pb and 100 mg L^{-1} AHA with no Pb added. Blanks of 10^{-6} M NaOH also show a higher variability (RSD = 7.18 %), which reflects that they were run at intervals throughout the analysis as a quick and simple measure of the variability between samples. Thus, the high variability of the blanks reflects gradual changes in the BGE system or in the electrophoretic system as a

Table 3.3: AHA-Pb analysis: Peak areas. Peak areas (PA) for samples as in Table 3.2. Peak areas are determined as indicated in Figure 3.4, and calculated using PeakFit v.4. Areas are averages of replicates (n = 3). Percentage RSD shows variation among sample subset; percentage RSD is greater for lower concentrations of AHA.

conc. AHA (mg L^{-1})	conc. Pb (mg L^{-1})	peak 1		peak 2		peak 3		peak 4	
		PA	% *RSD*	PA	% *RSD*	PA	% *RSD*	PA	% *RSD*
0	0	224	*16.5*						
50	0	250	*5.3*	849	*9.9*	77[a]			
	0.005	310	*8.3*	776	*8.9*				
	0.5[b]	343	*27.4*	1130	*3.2*				
100	0	326	*5.2*	2010	*7.4*				
	0.01	507	*10.3*	1870	*4.7*	29	*7.6*		
	0.1	557	*7.0*	1990	*12.1*	21	*12.1*		
	1	626	*7.9*	1920	*4.1*	26	*20.5*		
1000	0	273	*9.3*	13800	*6.1*			745	*14.2*
	0.1	622	*0.8*	12600	*6.3*	1610	*10.5*	674	*7.0*
	1	601	*9.4*	14000	*2.6*	555	*22.6*	610	*9.8*
	10	571	*4.1*	13200	*5.4*	462	*9.5*	382	*38.2*

[a] Peak seen in one replicate only. [b] Average and percentage RSD calculated from two replicates.

whole over the approximately 20 hours of this analysis. As the AHA samples were run consecutively, the estimation of error should not be greatly affected, although limitations in comparison between samples may be seen. There is large variability between the migration times of the different peaks for samples of the same concentration of AHA, but differing concentrations of Pb. This is most evident in the 1000 mg L^{-1} AHA set of samples, as there is a linear relationship between the migration time of peak 2 and the concentration of metal in the sample ($R^2 > 0.958$, n = 3). This indicates that the average size and charge is changing upon addition of metal. As well, as the migration time is decreasing with increasing metal concentration, the addition of metal is making the molecules both larger and of less negative net charge. The addition of mass (i.e. metal ions) and subsequent reduction in charge reduces the effective migration time of AHA.

In terms of a reduction in migration time with increasing metal concentration, my results are similar to those of Keuth *et al.* (1998) for 500 mg L^{-1} AHA inoculated with 125 to 250 mg L^{-1} "metals". These authors also analyzed a second peak seen after the humic hump that appeared to change with differences in metal concentration. The migration time of this peak increased and the peak area decreased with increasing metal concentration, presumably because the HA fraction with which the metal was binding is of higher mobility. This peak was observed in the 1000 mg L^{-1} AHA samples, and was identified as peak 4. Unlike the results of Keuth *et al.* (1998), the migration time of peak 4 decreases linearly with increasing Pb concentration ($R^2 > 0.863$, n = 3). As is also noted by Keuth and coworkers (1998), my results indicate that peak area of peak 4 decreases linearly with increasing metal concentration ($R^2 > 0.925$, n = 3).

Table 3.3 summarizes the areas of the peaks seen in the AHA-Pb analysis. Unlike the migration times for these peaks, the peak areas have a higher range of variability, in particular for the lower concentrations of AHA. For example, for peak 2, the percentage RSD of 100 mg L^{-1} AHA with 0 to 0.1 mg L^{-1} Pb ranges from 4 to 21 %. No reasonable explanation can be found for this variability. Most likely, it is due to insufficient sample to saturate certain sites on the capillary in the most dilute samples. Indeed, there could be some interaction between the silanol groups of the separation capillary and the functional groups of the AHA interfering with the separation. As described earlier, Fetsch *et al.* (1998a) found this to be a significant problem, and the leading reason why most analysts study HA at very high concentrations using CE. High concentrations (i.e. 1000 mg L^{-1}) serve to dilute these problems, allowing for reproducible results, but diminish the applicability of the method to environmentally realistic samples.

One simple conclusion that can be made from these data is that CE may be used to quantify HA in samples. A significant linear relationship is calculated ($R^2 > 0.999$, n = 33) between the area for peak 2 and AHA concentration. All data points were considered for this regression analysis, as it appears that metal concentration has little effect on the area of this peak. This idea has been proposed by others, and is of particular interest as a simple and fast method for HA content (Rigol *et al.* 1994, Rigol *et al.* 1996). The utility of this relationship may be limited to samples of known humic quality. In other words, one would need to run standards of the same humic characteristics as the unknown sample. Due to the complexity of the nature of HS, this is not practical for all

applications. On the other hand, this could be a very useful method for quantification if it were shown that the concentrations of different HS from many sources could be related to the area of the humic hump using model compounds as standards. A method using ultrafiltration to separate HS before CE analysis has been proposed that could possibly serve this purpose (Rigol *et al.* 1998).

Although some generalizations may be made regarding the effect of metal ions upon the electrophoretic migration of AHA, little else can be concluded from these results. Relationships can be seen for migration times of the humic hump with changing metal concentrations; these relationships are significant, and they are explained by the physical and chemical nature of the AHA. Changes in some minor features of the electropherograms of AHA can be seen upon the addition of a metal species, such as the peak area and migration time of peak 3. The change in migration time of this peak can be explained due to physical and chemical changes occurring upon addition of metal, yet the decrease in peak area with increasing metal concentration is more difficult to conceptualize. This may be due to precipitation of AHA complexes with the metal at higher metal concentrations, or coagulation and absorption to surfaces. Moreover, changes to the molar absorbtivity of the HS-Pb complex due to metal binding to chromophores will change the observed absorbance. These results do provide a framework for understanding of the mobility of AHA in electrophoresis, results that will be used to interpret the results of the analyses of AHA-Pb samples using CE/ICP-MS.

3.2 CE/ICP-MS Interfaces: Design and Optimization

3.2.1 *Introduction*

One obstacle for the improvement of modern capillary electrophoretic techniques is the ability to detect resolved analytes with the sensitivity needed for many trace compounds, such as the case in common environmental applications. The limiting factor for CE/ICP-MS is the ability to unite the two instruments such that effective and efficient measurements may be made. This work describes the design and optimization of two interfaces for CE/ICP-MS. The reader is directed to section 1.5 for an overview of the work done in this area over the past 5 years since its first appearance in the literature. Initially in this project, the direct injection high efficiency nebulizer (DIHEN) was used as an interface; figures of merit for the optimization of this apparatus are presented, as well as projected detection limits and relative suitability of this system. The second interface, and the interface used for subsequent analytical procedures regarding the analysis of HS, is the high efficiency nebulizer (HEN)/cyclonic spray chamber system. Figures of merit for the optimization and validation of this interface are also presented.

3.2.2 *The DIHEN Interface*

The DIHEN is a novel micronebulizer designed to accommodate the introduction of very low sample flow rates to ICP-MS or ICP-atomic emission spectroscopy (AES). These low flow rates are useful when the sample volume is limited (forensic or biological material), or the sample is toxic (limited exposure and production

of waste is desired). In many of these cases, the sample is limited, expensive or contains a large fraction of organic solvent (McLean *et al.* 1998). For environmental chemistry, these factors often apply, as the analyte of interest is present at very low concentrations, or the analyte is toxic and is therefore a health concern in the laboratory. For hyphenation of ICP-MS to CE, the DIHEN appears to be a logical source, as the EOF is typically very slow and of small volume.

The initial test of this interface included the calculation of the sensitivity of the interface for solutions injected for the typical use of the system (i.e. bulk solution flow). To do this, the CE system was attached but no voltage was applied, such that the capillary was filled with electrolyte solution and allowed to sit in the connecting cross while make-up electrolyte was pumped through the system. The make-up electrolyte was replaced with a tuning solution consisting of 5 mg L^{-1} each of Cu, Mg and Rh, and 10 mg L^{-1} Pb. The response of these analytes is reported as counts per second (cps) per mg L^{-1} metal in Figure 3.5 (a) and (b), for the optimization of RF power and nebulizer gas flow rate, respectively. Linear responses are seen for all metals as a function of increasing RF power. The highest response was seen for all metals at the instrumental power maximum (1500 W). This is indicative of the nebulization process using the DIHEN: the primary aerosol produced by this nebulizer is injected directly into the plasma, without time for desolvation as is typically seen in introduction systems using a spray chamber. Subsequently, the analytes requires higher power to be effectively ionized, and there is a greater risk of the production of oxides and polyatomic ions (McLean *et al.* 1998). Thus,

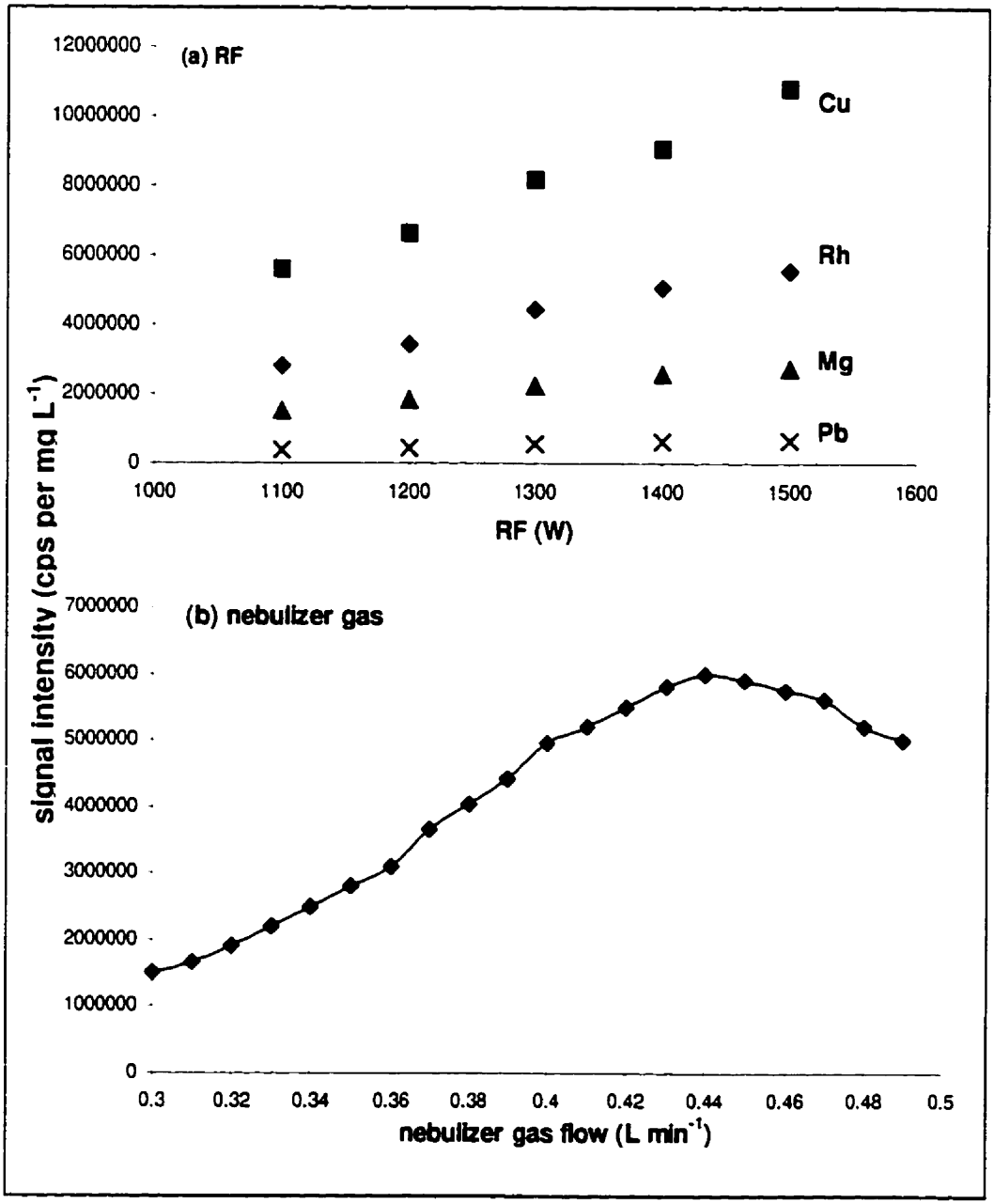

Figure 3.5: Optimization parameters for DIHEN. Response of Cu, Rh, Pb and Mg are shown in (a) as counts per mg L^{-1} of each metal. Response of Rh (cps per mg L^{-1}) with increasing nebulizer gas flow is shown in (b).

the higher RF power is needed to ensure adequate atomization and ionization of the metals.

The optimum nebulizer gas flow rate is very different than that typically seen for the normal Scott spray chamber (0.44 L min^{-1} as opposed to approximately 1 L min^{-1}) [Figure 3.5 (b)]. This optimal value is higher than that seen by McLean and coworkers (1998) and Becker and coworkers (1999). These groups found the optimal nebulizer gas flow rates to be 0.25 L min^{-1} and 0.16 L min^{-1}, respectively. The difference from the values observed in my work, and indeed the difference seen in the initial optimization of this parameter for the DIHEN used in this study is attributed to changes that occurred to the DIHEN during an accident involving the apparatus. The nozzle tip was exposed directly to the plasma when an excess of O_2 was added to the Ar flow for the plasma. The DIHEN was not significantly damaged and was used for subsequent experiments. This must be considered, however, when evaluating the DIHEN as a potential interface, as it was most probably not working as it was designed. The nebulization did not appear to be affected, and the DIHEN's performance was comparable to what it had been previously. The most obvious difference observed was the change in the optimal nebulizer gas flow rate. The DIHEN, therefore, cannot be evaluated for its potential performance, but rather is assessed for its post-accident performance.

The data in Figure 3.6 (a) show the response of several metals as a function of make-up electrolyte flow. Significant regressions ($R^2 > 0.970$) are seen for the response of all metals as functions of increasing flow rates. The significance of the linear response of the metal response with increasing flow rate is seen most distinctly

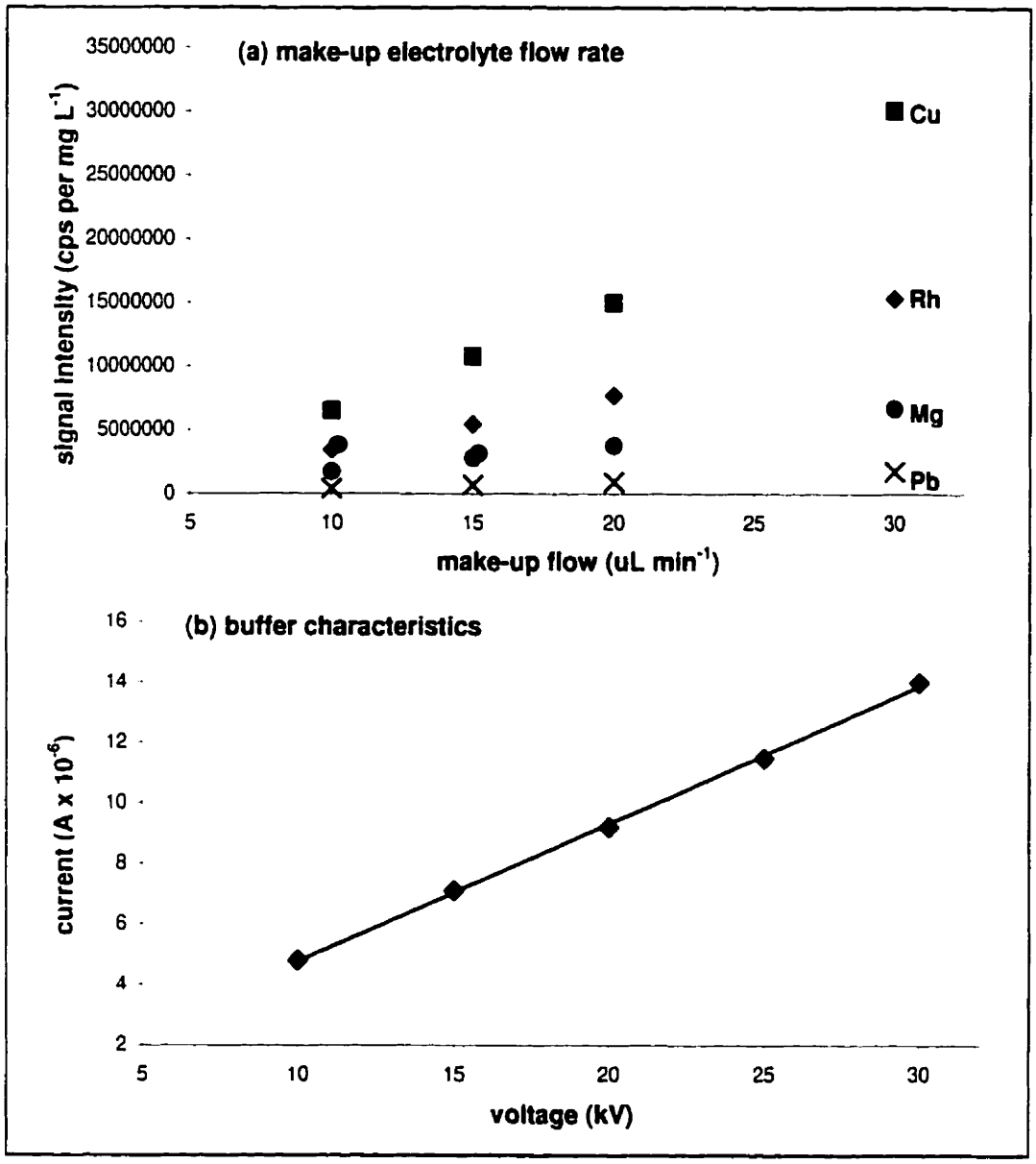

Figure 3.6: CE/DIHEN/ICP-MS optimization I. The response of Cu, Rh, Mg and Pb as counts per mg L^{-1} of metal present is shown in (a) as a function of make-up electrolyte flow rate. The current observed for the 45 mM borate BGE over a range of voltages is shown in (b). A linear response is noted for this relationship ($R^2 > 0.99$).

when compared to other introduction systems; systems including a spray chamber do not show a linear response. Instead, efficiency decreases with increasing flow rates. The purpose of the make-up electrolyte flow is to complete the electrical circuit for electrophoresis and to add to the EOF volume for effective nebulization. This final effect should be kept to a minimum, as the volume of the sample is so small that it could be dramatically diluted in a large volume. This is not a great concern when using the DIHEN, as the entire volume is introduced to the plasma, and therefore analyzed. Higher flow rates could cause backpressure into the capillary, and thus minimal electrolyte flow was preferred for the final set-up.

Improvements in detection limits as measured by direct comparison with a traditional introduction system were measured for the DIHEN at a flow rate of 85 $\mu L\ min^{-1}$ by McLean and coworkers (1998). Detection limits were further improved at lower flow rates (11 $\mu L\ min^{-1}$) (McLean *et al.* 1998). In my work, the optimal flow rate was found to be that rate at which no significant backpressure nor allowed suction was observed, while providing adequate sensitivity for analysis. This flow rate was determined through a series of checks. To test for backpressure, the separation capillary was filled with a solution containing a marker (i.e. Sr) present in high concentration. After a few minutes, during which the electrolyte solution flow rate was held at a constant flow, the capillary solution was flushed through with pressure. Backpressure would cause a lag time to appear between starting this flush and an increase in the Sr signal. On the other hand, the lack of backpressure was indicated by an almost immediate Sr response. To test for suction, the injection end of the separation capillary

was allowed to rest in a solution of high concentration of Pb. After a specified time, the capillary was flushed, and this solution analyzed. A peak of Pb in this flushing would indicate significant suction. Using these methods, the optimal flow rate for the DIHEN was found to be approximately 12 $\mu L\ min^{-1}$.

Figure 3.6 (b) shows the current as a function of voltage applied to the electrophoretic system as measured when the CE was attached to the ICP-MS using the DIHEN. A linear relationship between these parameters indicates that the BGE (45 mM borate) is being used within its buffering capabilities for the voltages measured. This is included as further evidence that there would appear to be no effect of the interfacing of the instruments upon the normal electrophoretic functioning of the CE.

A typical example of the time plots of Rh and Sr during electrophoretic separation is seen in Figure 3.7 (a). Rh (50 mg L^{-1}) was added to the make-up electrolyte and 200 mg L^{-1} Sr was added to the CE electrolyte. As indicated in the figure, when the CE voltage was applied, a rapid increase in the response of Sr can be seen. This shows the EOF in the capillary in response to the applied current. The decrease in response is very rapid, attesting to a fast washout time for the analyte within the introductory capillary of the DIHEN. The Rh signal is steady throughout this electropherogram. This indicates that the applied current or the addition of EOF to the total sample flow does not effect the make-up electrolyte.

The response of the Sr in the CE BGE was sufficiently sensitive that its presence was used as an indicator of sample run times. To clarify this statement, Figure 3.7 (b) shows a peak of Sr during sample injection. When analyzing data, time zero of

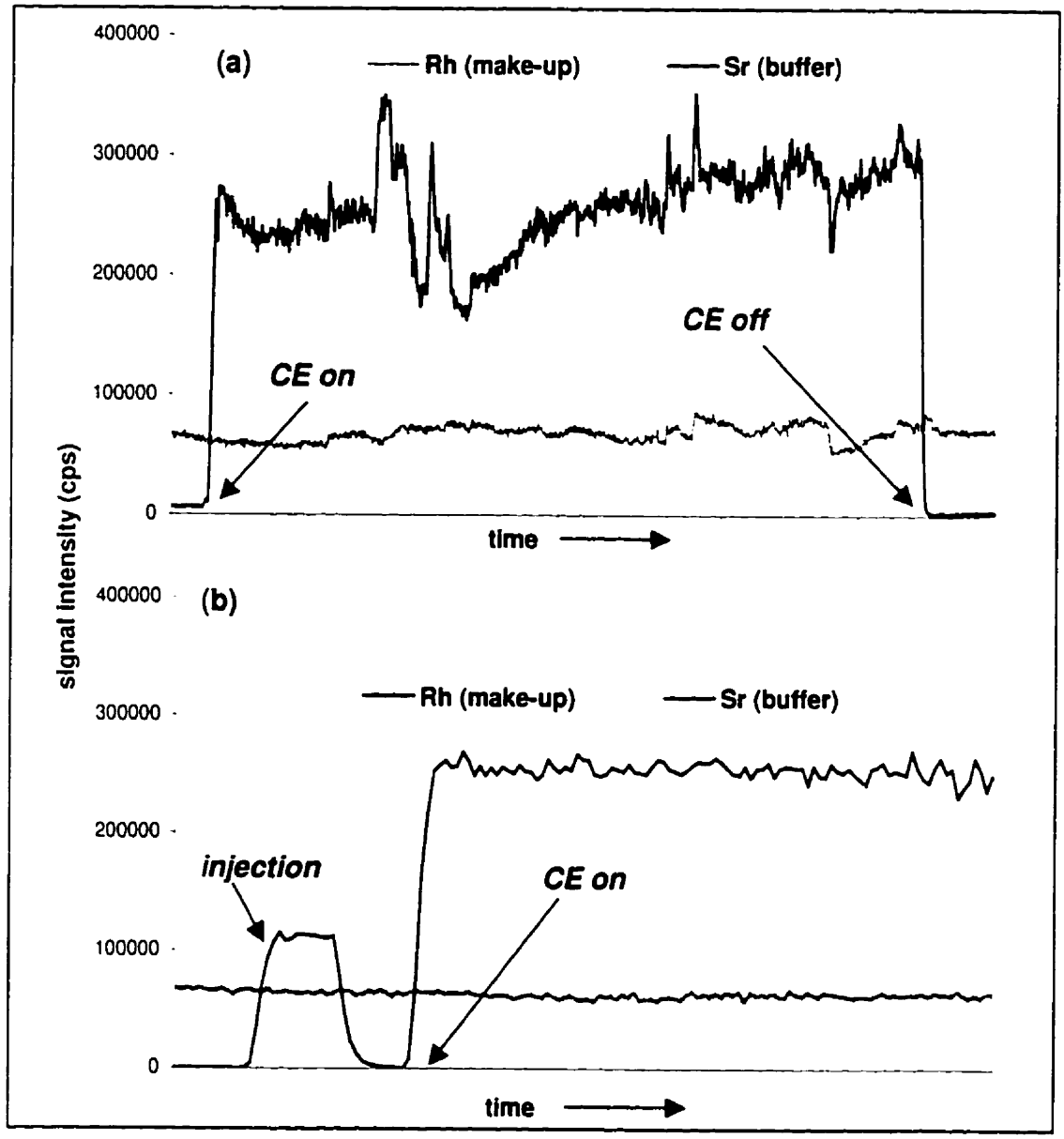

Figure 3.7: CE/DIHEN/ICP-MS optimization II. Figure (a) shows the typical response of both the make-up electrolyte (spiked with 50 mg L^{-1} Rh) and the electrolyte itself (spiked with 200 mg L^{-1} Sr). The presence of Sr in the electropherogram, therefore, indicates the EOF. Figure (b) describes the sensitivity of this system, as the injection of sample onto the capillary can be followed as an increase in Sr signal, due to the pressure injection itself. A very rapid increase in Sr signal is seen upon the application of the voltage (CE on).

the electrophoresis was adjusted to the observance of the tail end of this peak, and the beginning of the response due to the EOF. "CE on" indicates this point on the figure.

One notable feature of Figure 3.7 (a) is the pattern of the Sr signal observed within a few minutes of sample injection. There is an increase and subsequent decrease (although this is somewhat erratic) of the response. This is presumably due in part to an incomplete separation of Sr ions in the BGE solution. Thus, an increase is seen in the concentration of Sr ions at approximately five minutes, which indicates that a significant portion of these ions migrated in the electric field. The decrease soon following this peak is due to the loss of mass to migration.

In a paper by Liu and coworkers (1995), the separation of a mixture of metals was presented as a preliminary evaluation of their lab-built direct injection nebulizer (DIN) that was used as an interface for CE/ICP-MS. Figure 3.8 shows the results of a similar separation of metal species. The sample solution consisted of 1 mg L^{-1} for each of Ba, Cd, Co, Cs, Cu, Mg, Mn, Ni, Pb and Tl. All metals are shown separately for ease of interpretation, but were analyzed at the same time. The sample was run in triplicate, and a representative electropherogram is shown. The percentage RSDs for the migration time, peak area, and peak height were less than 10 %. The BGE used for this separation was 5 mM phenanthroline (pH 8.75). There is not a great range in migration time seen for the divalent metals (all metals but Cs and Tl), and as these can form complexes with phenanthroline, their separation is not well resolved due to low apparent mass and charge differences. The migration times of the monovalent cations (Cs and Tl) are lower (199 and 209 seconds, respectively). As Cs is lighter (*MW* = 199)

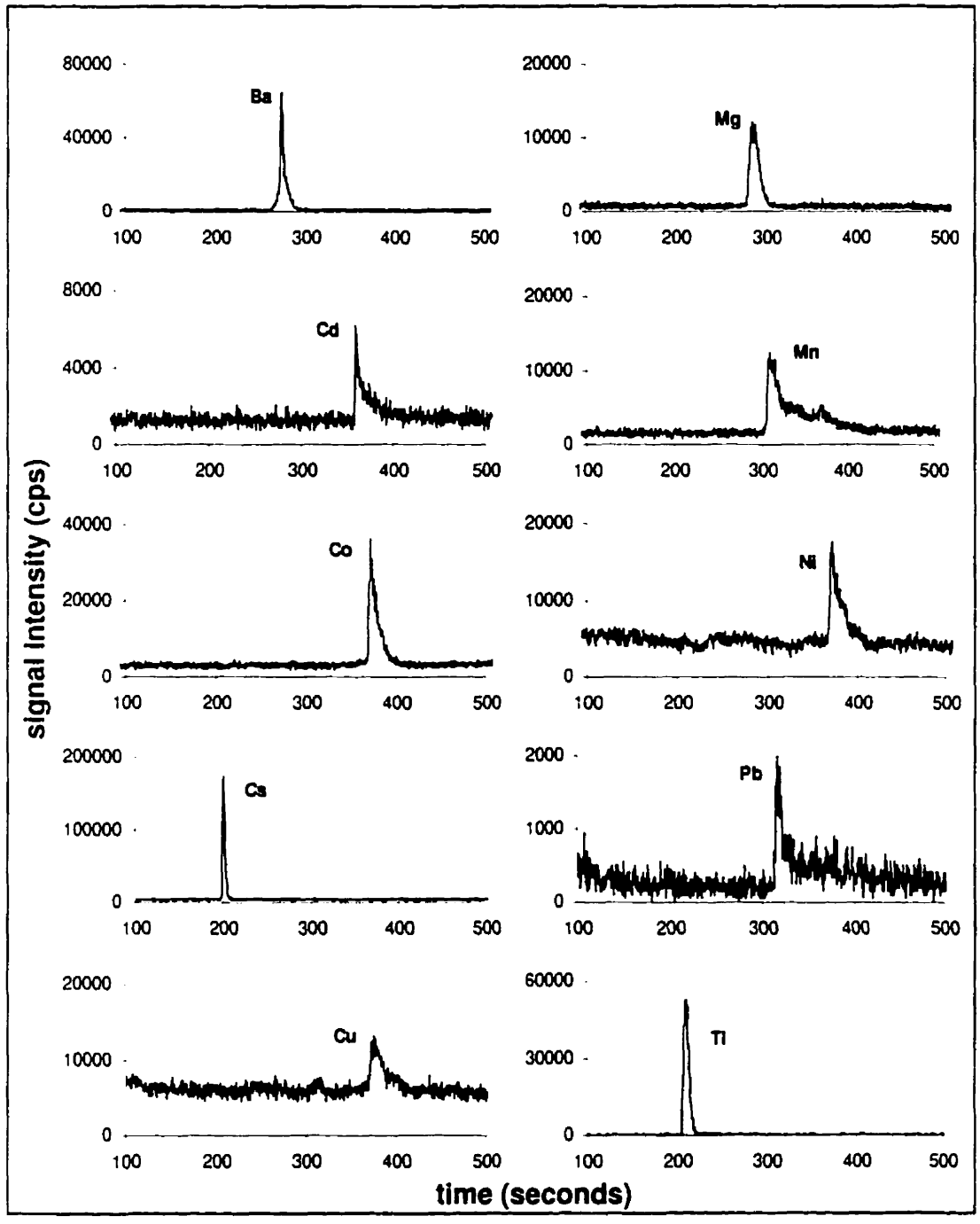

Figure 3.8: Separation of metal mixture using DIHEN interface. The signal intensity of each metal in a mixture is shown in the above figure. Most metals show baseline resolution. All metals are at a concentration of 1 mg L^{-1}. CE separation conditions are as in Figure 3.1 (b), except 5 mM phenanthroline is used as the BGE.

than Tl (*MW* = 204), the migration time is only slightly shorter. The majority of the metals would be expected to be in ionic form at pH 8.75 and be complexed phenanthroline, which will preferentially bind with hydroxyl species.

Further experiments were conducted to evaluate the utility of the interface using the DIHEN. Figure 3.9 shows the results of a separation of a mixture of divalent metals, at varying concentrations (0.2 mg L^{-1}, 1 mg L^{-1} and 10 mg L^{-1}). These data are used to calculate standard curves for the evaluation of detection limits. To ensure the applicability of this analysis to later work with AHA, the CE separation conditions were kept the same as those used for the analysis of AHA (i.e. 45 mM borate BGE, +25 kV, etc.).

Mg is well resolved from the other metals in this separation, although the migration times for Cu, Mn and Pb are similar. Table 3.4 summarizes the migration

Table 3.4: Statistics for migration times of metals. The migration times (MT) are listed below for the various metals separated using the DIHEN interface. Values are averages of three replicates of each concentration analyzed (n = 9).

	MT (seconds)	***% RSD***
Cu	560	*2.9*
Mg	331	*2.0*
Mn	574	*7.2*
Pb	524	*4.9*

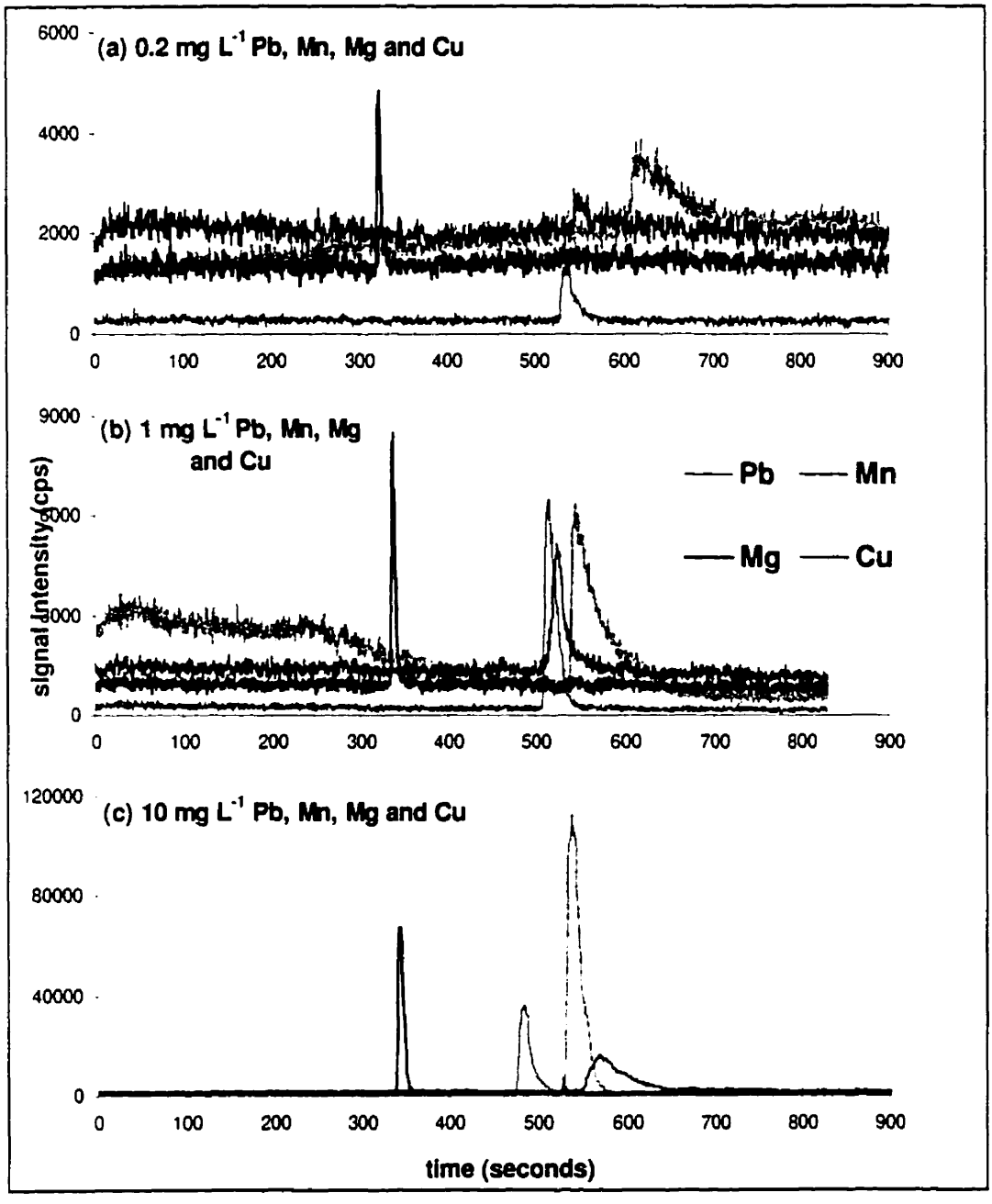

Figure 3.9: Sample electropherograms of metal mixture separation. CE separation of (a) 0.2 mg L^{-1}, (b) 1 mg L^{-1} and (c) 10 mg L^{-1} of each of Pb, Cu, Mn and Mg. Results are used to determine the detection limits for the DIHEN interface. CE separation conditions are as in Figure 3.1 (b) (i.e. 45 mM borate, + 25 kV).

times, and respective standard deviations and percentage RSD for each metal (n = 9). In general, the earlier the migration time, the lower the percentage RSD observed. This is a reasonable result considering the actual length of time of this separation (up to almost ten minutes for Pb), and the ensuing slight differences in separation conditions that may exist between runs. The longer the separation, the greater the chance of small differences in conditions causing a greater effect on the results.

Table 3.5 summarizes all statistics calculated for the analysis of the metal standards. Both peak areas and peak amplitudes are shown to illustrate the variability seen in this experiment. In general, the variability, as measured by percentage RSD was

Table 3.5: Statistics for the determination of detection limits for the DIHEN interface. All values are averages of three replicates. Total concentration refers to concentration of all isotopes of indicated metal; only one isotope of each metal is used for analysis purposes (i.e. ^{208}Pb is used for Pb).

	total conc. ($mg\ L^{-1}$)	**PA**		**amplitude**	
		mean	***%RSD***	***mean***	***%RSD***
Pb	*0.2*	15300	8.7	736	12.5
	1	97100	15.9	6190	9.3
	10	581000	15.1	65100	11.0
Mn	*0.2*	31600	19.9	925	18.1
	1	159000	0.1	4960	7.0
	10	1700000	5.6	118000	7.4
Mg	*0.2*	40600	9.0	3500	28.3
	1	57400	17.4	8070	8.8
	10	545000	8.2	68600	4.5
Cu	*0.2*	34900	24.5	1300	10.5
	1	56300	11.9	3970	1.7
	10	603000	6.4	14800	13.9

higher for samples of low concentration than for higher concentrations. This relationship with variability is noted for both the peak area and the peak amplitude. Calibration curves for these data are shown in Figure 3.10, and the corresponding regression equations and statistics are summarized in Table 3.6. Standard curves were analyzed for both peak area and peak amplitude. In both cases, linear relationships are calculated, with R^2 values greater than 0.990 for peak area, and greater than 0.970 for amplitude.

To determine the detection limits of this method, the linear regression for amplitude was used. The detection limit was assumed to be the concentration corresponding with 3 times the standard deviation of background noise. The detection limits calculated using this method are summarized in Table 3.7. Absolute detection limits are calculated assuming a sample injection of 47 nL, and were 9, 26, 3 and 4 pg for Pb, Mn, Mg and Cu respectively. These values are quite high in comparison to detection limits measured by others for the DIHEN (e.g. McLean *et al.* 1998). In fact, up to a factor of 10^5 difference is noted in the literature (McLean *et al.* 1998). This is most

Table 3.6: Regression statistics for limit of detection analysis (DIHEN). The result of the regression analyses for both peak area (PA) and amplitude for a mixture of metals separated using CE and detected with ICP-MS (n = 3). R^2 values indicate significant linear relationships for all metals and parameters.

	PA		**amplitude**	
	equation	***R^2***	***equation***	***R^2***
Pb	y = 107000x + 21800	0.996	y = 12200x – 2160	0.976
Mn	y = 170100x – 6820	0.999	y = 12200x – 4240	0.998
Mg	y = 66600x + 17900	0.998	y = 8460x + 1790	0.999
Cu	y = 85400x + 10700	0.998	y = 1890x + 1820	0.987

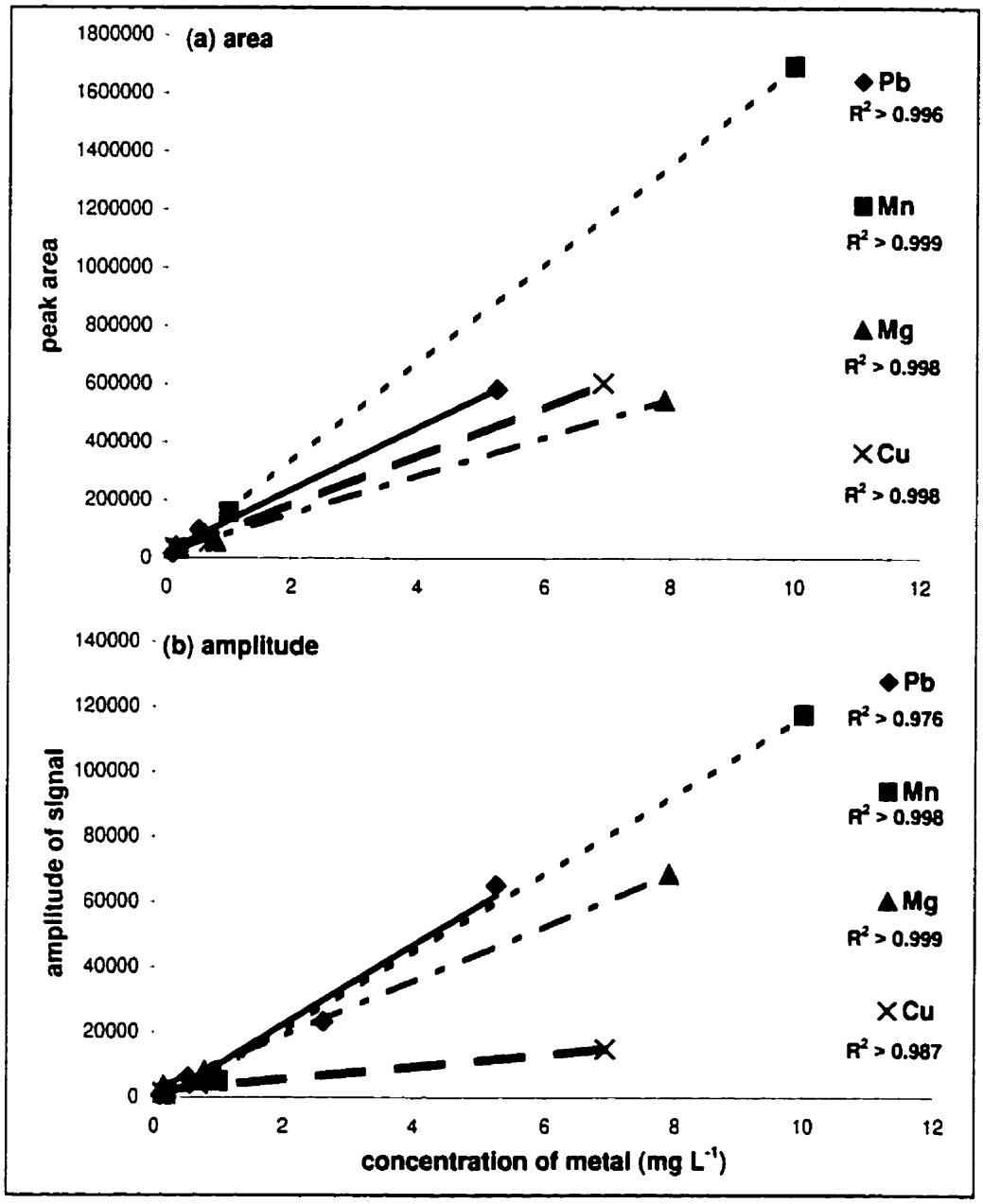

Figure 3.10: Calibration curves for metal separation analysis using the DIHEN interface. Regression analyses of (a) peak area, and (b) peak amplitude are shown above, with R^2 values indicated for each relationship.

Table 3.7: Detection limits for DIHEN interface. Limit of detection ($\mu g\ L^{-1}$) determined from calibration curves for amplitude of metal peaks separated using CE and detected with ICP-MS. Limit was calculated as concentration giving a signal equivalent to three times the background noise (from blank, n = 100). Absolute detection limit is based upon a 47 nL injection.

	detection limit ($ug\ L^{-1}$)	**absolute detection limit (pg)**
Pb	203	9
Mn	544	26
Mg	70	3
Cu	84	4

certainly due to the accidental modification of the sample nozzle. By changing the shape of the nozzle, there were probably changes in the ability of the nebulizer to produce a fine and constant aerosol. Another factor affecting the magnitude of the detection limits is the different applications for which the detection limits are derived. CE involves the injection of minute sample volumes, and hence concentration differences in detection limits will be great when comparing to normal liquid sample analysis.

This last issue raised is the main reason why the use of the DIHEN was abandoned, and a more traditional CE/ICP-MS interface (HEN/cyclonic spray chamber) was used instead. The DIHEN, despite the problems seen in this work, is gaining popularity for CE applications (Majidi *et al.*1999). The reasons for this are its relative ease of use, the ability to inject the entire capillary solution into the detector and the lack of band broadening when a spray chamber is used in some applications of CE/ICP-MS.

The analyte may interact to some extent with the spray chamber, causing a change in the observed migration time and peak shape. The results of my work do not indicate that any of these presumed merits of using the DIHEN are being realized, as the detection limits are high or comparable to detection limits measured using a traditional CE/ICP-MS interface (section 3.2.3). In is unclear if the results are indicative of the overall performance of the DIHEN as an interface for CE/ICP-MS or if my problems were due solely to the damage to the nebulizer tip. As I have no conclusive data from before the accident, I am unable to posit any judgement based on my results. In comparison to published data (McLean *et al.* 1998, Becker *et al.* 1999), however, it would seem that the problems seen with the DIHEN might be due to the modification of the nebulizer tip.

3.2.3 *The HEN/Cyclonic Spray Chamber Interface*

The HEN/cyclonic spray chamber interface is a traditional method for sample introduction, traditional in the sense that it has been used for many applications needing low sample introduction rates and reduced waste production. One very important aspect of the use of the HEN is the observation that efficiency of this system tends to increase with decreasing sample introduction rates (Lui and Montaser 1994, Olesik *et al.* 1994). This becomes an important consideration when applying this system to use with CE and ICP-MS. The objective is to achieve a sample introduction rate that is as low as possible, although the addition of a make-up electrolyte is still needed to complete the electrical circuit. The lower limit of sample introduction rates still allowing for effective nebulization is between 5 and 10 $\mu L\ min^{-1}$ for the HEN, and at these rates

near 100 % efficiency is observed for normal solution introduction (Lui and Montaser 1994).

The HEN/cyclonic spray chamber interface design can be seen in Figure 2.2 (section 2.3.1). The system was optimized in terms of sensitivity in a manner similar to the DIHEN interface. One exception to these methods was the optimization of nebulizer gas flow rates: an external source of Ar independent of the mass-flow controller of the ICP-MS was used due to the high pressure needed for optimal nebulization. The pressure of Ar that would provide the greatest sensitivity of a target analyte (Rh) was determined by manually increasing the Ar pressure. This pressure was typically about 180 psi. Optimization of the other parameters (i.e. RF power and make-up electrolyte flow rate) was determined automatically using the flow controls and power controls of the ICP-MS system.

Figure 3.11 describes these optimization steps. In Figure 3.11 (a), the signal intensity (cps per mg L^{-1}) is shown as a function of RF power. Unlike the DIHEN interface, this interface requires a much lower power input to the plasma for optimal sensitivity. In fact, the optimal RF power is very low, as the maximum signal intensity is seen for Cu, Rh and Pb between 650 and 700 W. This is essentially a "cool plasma", that has been used to change the background spectra from the ICP from one dominated by Ar^+ (m/z 40), ArH^+ (m/z 41) and O^+ (m/z 16) to one consisting mainly of NO^+ (m/z 30), O_2^+ (m/z 32) and H_3O^+ (m/z 19) (Hill *et al.* 1999). Depending on the application, it may be favourable to remove such interferences (i.e. ^{40}K, ^{41}K, ^{40}Ca determination). As the analyte of interest is Pb (as measured by ^{208}Pb), there is little chance of interference from

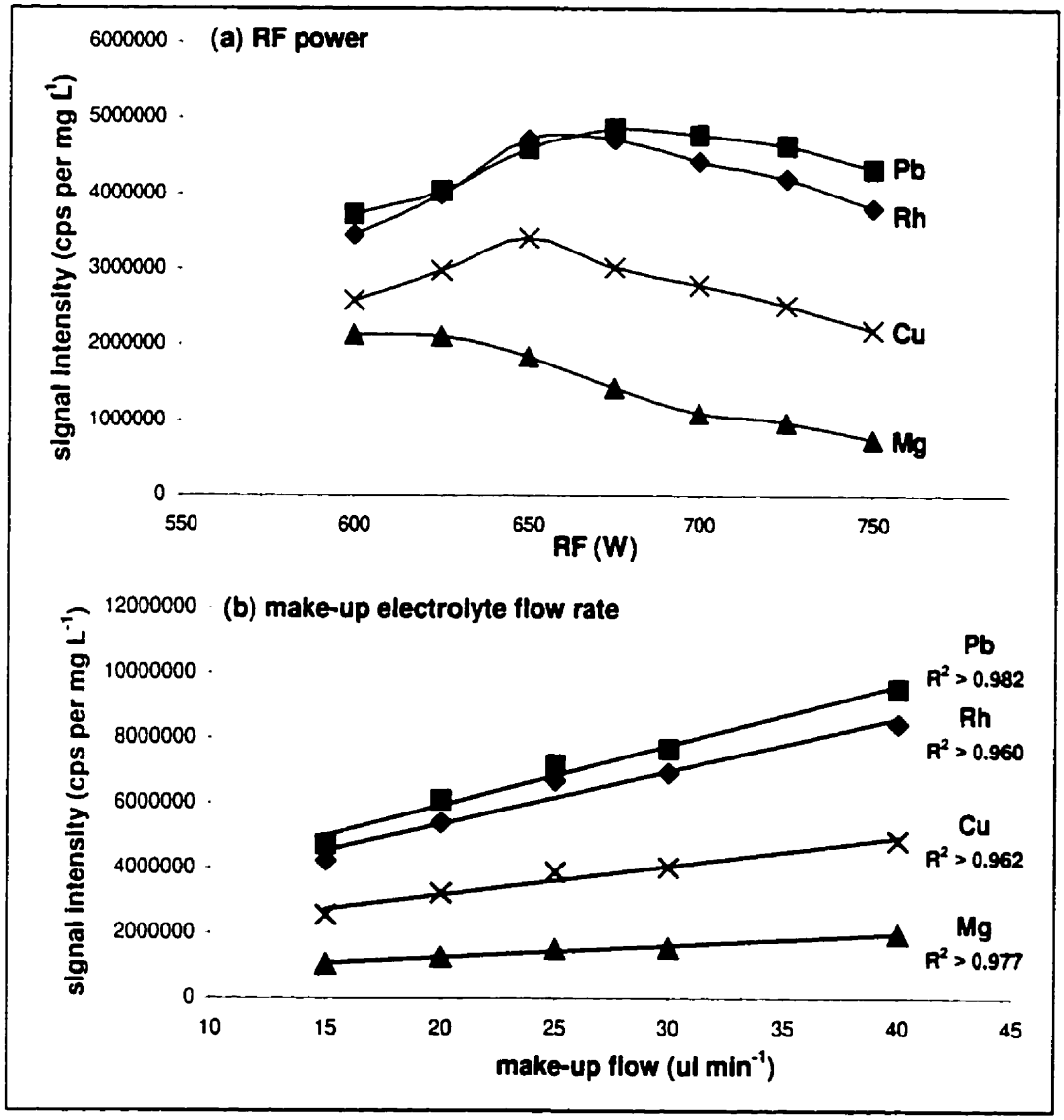

Figure 3.11: CE/HEN/Cyclonic/ICP-MS optimization I. The response of Pb, Rh, Cu and Mg (as cps per mg L^{-1} metal in solution) are shown as a function of operating RF power in (a). Non-linear relationships are noted for all analytes, with the highest response noted between 650 and 700 W for all metals except Mg. Figure 3.11 (b) shows the response of the analytes as linear functions of make-up flow. R^2 of all functions are indicated.

ions from either normal or cool plasmas. Lower power values were used, however, as the highest intensities of signals were obtained, hence the overall sensitivity of the system was assumed greater than at higher power. The need for cool plasmas in conjunction with the HEN has not been noted in the literature. Pending further investigation, I cannot explain why greater sensitivity was observed.

In Figure 3.11 (b) the signal intensity (cps per mg L^{-1}) of Cu, Mg, Rh and Pb are shown as a function of make-up electrolyte flow rate. All metals exhibit a significant linear response ($R^2 > 0.960$) with increasing make-up flow rate. In comparison to the similar optimization step for the DIHEN interface, seen in Figure 3.6,it was observed that the slopes of the equation were not as steep for the HEN/cyclonic spray chamber. This is due to the loss of efficiency with the HEN at higher flow rates. In fact, at flow rates above approximately 50 $\mu L\ min^{-1}$, the slope of this equation would decrease dramatically because of a loss in nebulization efficiency. A larger fraction of the sample would be lost as large droplets instead of being introduced to the plasma as an aerosol. It is also of importance to note that at the make-up electrolyte flow rates that are of interest for this application (i.e. < 15 $\mu L\ min^{-1}$) the two systems have comparable sensitivities for the analytes measured. In fact, the signal intensity of Pb is much higher at all flow rates using the HEN/cyclonic interface.

With the CE attached to the interface, the voltage was applied at incremental values, and the observed current was recorded. These results can be seen in Figure 3.12 (a). These data describe a linear relationship between current and voltage for this BGE ($R^2 > 0.999$). The same results were obtained for this BGE for normal CE with

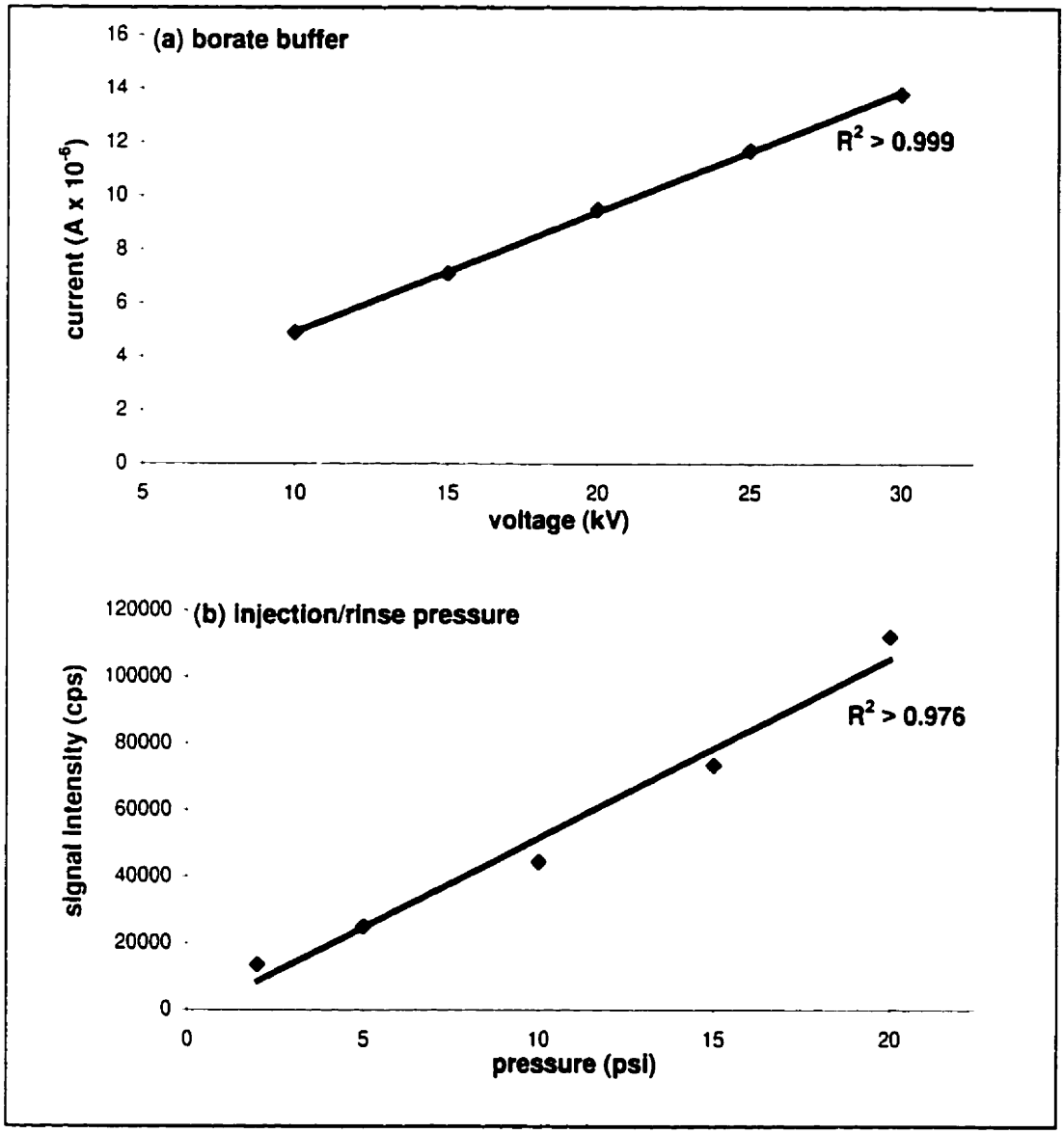

Figure 3.12: CE/HEN/Cyclonic/ICP-MS optimization II. Figures (a) and (b) describe the results of various tests designed to ensure the proper functioning of the CE while attached to the ICP-MS. Figure 3.12 (a) shows the change in current measured as a function of applied voltage. Figure 3.12 (b) shows the signal intensity of Sr (200 mg L^{-1}, added to separation BGE) as a function of the rinse pressure. R^2 for linear relationships are noted.

on-line UV detection, allowing the conclusion that the termination of the separation capillary within the flowing electrolyte system has no obvious effect on the electrophoretic abilities of this system. If problems were occurring, one may expect to see a deviation from this relationship.

The BGE used for the initial exploratory work with the CE/ICP-MS interfaces was spiked with Sr to allow for the visual analysis of EOF. Figure 3.12 (b) describes the response of Sr as a function of the pressure at which BGE was pushed through the capillary. Pressure pushes are used to both inject sample onto the capillary and to facilitate cleaning and surface preparation of the capillary for electrophoresis. The pressure at which the BGE was forced through the capillary shows a linear relationship ($R^2 > 0.976$) with the signal intensity (cps) observed for the Sr. This indicates that there are no significant problems in terms of transferring the solution to the plasma; the increase in pressure is seen clearly as an increase in sample reaching the detector.

A simple speciation scheme was used to validate the capability of the CE/ICP-MS system to measure different species of the same metal. The synthetic multidentate chelating agent EDTA (ethylenediaminetetraacetic acid) was mixed with Pb in concentrations calculated using MINEQL (Tipping) to allow for part of the Pb species to be bound with the EDTA, and part to be unbound, or free in solution. These concentrations are 241 μM for Pb and 50 μM EDTA (50 mg L^{-1} and 18.6 mg L^{-1}, respectively). This solution was injected into the CE using the same BGE system used with the AHA analysis. A representative electropherogram for this experiment is shown in Figure 3.13 (a). Figure 3.13 (b) shows the single peak observed for a 50 mg L^{-1} Pb

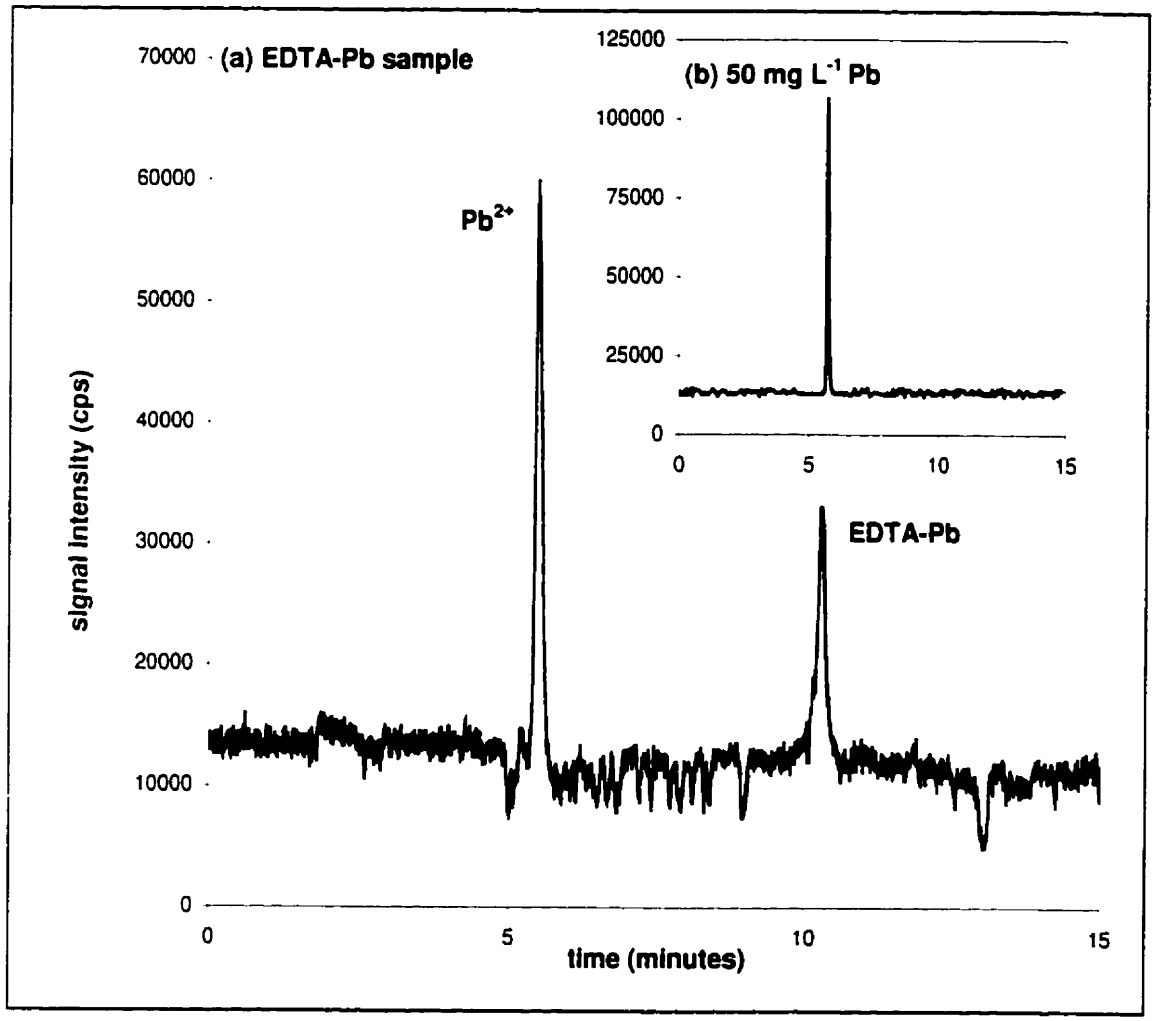

Figure 3.13: EDTA-Pb separation. An electropherogram showing the separation of "free" Pb and Pb bound to EDTA, measured as the Pb response. The inset graph (b) shows the peak observed for a 50 mg L^{-1} sample of Pb (i.e. no EDTA).

solution. Upon injection of the EDTA-Pb mixture [Figure 3.13 (a)], the two species of Pb are clearly resolved, and the peak shape is reasonably symmetrical, with no tailing in either direction. This indicates that there is neither suction nor backpressure effecting the EOF. Table 3.8 summarizes the results of this experiment. The percentage RSDs are very low (< 1 %) for migration times of the Pb-EDTA sample peaks, and slightly higher (< 5%) for the three replicates of the 50 mg L^{-1} solution. The variability is higher for the peak areas of both samples. This is most likely due to error associated with such small

Table 3.8: Results of EDTA-Pb analysis. Migration times (MT) and peak areas (PA) for peaks observed for 50 mg L^{-1} Pb solution and EDTA-Pb mixture (50 mg L^{-1} Pb, 19 mg L^{-1} EDTA).

	peak 1		peak 2	
sample	**MT (min)**	**PA**	**MT (min)**	**PA**
50 mg L^{-1} Pb				
replicate 1	5.40	956210	-	-
replicate 2	5.23	793690	-	-
replicate 3	5.12	853600	-	-
mean	*5.25*	*867833*	-	-
% RSD	*2.7*	*9.5*	-	-
EDTA-Pb				
replicate 1	5.51	528700	10.28	285800
replicate 2	5.48	593150	10.36	226458
replicate 3	5.55	621210	10.32	289295
mean	*5.51*	*581020*	*10.32*	*267184*
% RSD	*0.6*	*8.2*	*0.4*	*13.2*

injections, and to the relative length of the migration times. As was noted earlier, the error associated with peak parameters tends to increase with migration time, and could be due in part to the greater chance for differences in instrumental and sample conditions to show a greater effect in the results.

At the concentrations given for the analytes, the equilibrium concentrations of Pb^{2+} (unbound Pb) and Pb complexed with EDTA (EDTA-Pb) were calculated to be 73.8 % and 26.2 % respectively. My results indicate an average of 68.5 % of the total Pb associated with the peak at 5.51 minutes, and 31.5 % of the total Pb associated with the peak at 10.32 minutes. This would indicate that the first peak is the unbound Pb and the second is the EDTA-Pb complex. The identity of the first peak was confirmed by its similarity in migration times to the 50 mg L^{-1} Pb sample without EDTA. This order of migration is expected considering the relative size and charge of the species; the large EDTA-Pb molecule, with relatively neutralized charge due to the association of the Pb ion, would migrate more slowly towards the negative electrode than the small, highly charged Pb. These results also indicate that there is little change in the speciation of a sample as it is separated using this method. This is always a concern when developing methods for speciation analysis, as any changes in the conditions of the sample can compromise the original concentration of the various species. It would appear from these results that the speciation of the Pb in this case is maintained through to detection, and hence this can be assumed to be the case for the analysis of AHA in the following experiments, particularly as the same BGE is used for these experiments.

One important finding from this analysis is the observation that the migration time of the free Pb^{2+} peak (5.4 minutes) appears to coincide with the migration time observed for humic material as presented earlier. In other words, it would be difficult to distinguish the free Pb^{2+} from bound humic considering the migration times are similar. This issue will be addressed in the following section.

3.3 Analysis of AHA-Pb Samples by CE/ICP-MS (*ICP-MS Detection)*

3.3.1 *Introduction*

For the analysis of AHA samples using CE/ICP-MS, the HEN/cyclonic spray chamber interface was used. This system was shown to be effective for the separation of simple metal speciation systems (section 3.2.3). The separation of AHA into reproducible peaks of gradient molecular classes with moderate homogeneity has also been shown (section 3.1.2). As was previously discussed, a limitation to the analysis of associated metal with AHA using CE is the lack of an elemental detector. The combination of using CE to separate AHA, and ICP-MS to detect the associated metals is desirable in that the fraction of metal that is not associated with the organic matter (i.e. free) may be detectable using ICP-MS, as well as the relative amount of metal associated with the various separated fractions of the AHA. The latter analysis may be compromised, however, by the lack of resolvable peaks seen in the separation of AHA, but rather the characteristic humic hump, which represents a gradient of molecular classes.

For this analysis, samples of 500 mg L^{-1} AHA were inoculated with 5, 25 and 50 mg L^{-1} Pb. These solutions have concentrations of Pb varying from 10 to 100 mg Pb g^{-1} AHA. The lowest Pb concentration should show the metal as completely bound to the AHA, and the highest concentration should have some Pb free in solution, considering the typical Pb binding capacity of most HA (40 to 125 mg g^{-1}, Rashid 1985). By varying the concentration of NaOH used to dilute these samples, subsets representative of these concentrations under acidic, neutral and alkaline conditions were made. In general, the binding of metal to the AHA can be described with the following equilibrium equation:

$$M^{n+} + AHA \rightleftharpoons M\text{-}AHA,$$

where M^{n+} represents a metal in its ionic form, M-AHA represents some complexation between the metal and the HA, and at equilibrium the forward reaction would balance the reverse reaction. In acidic conditions, the Pb would be more likely to remain in solution as a cation, or in reference to the above equilibrium equation, the reverse reaction would dominate the equilibrium concentrations. In alkaline conditions, the hydroxy form of Pb would be predominant in solution. As well, increased stability of AHA-Pb complexes would be observed; the forward reaction would dominate.

The binding ability of the organic matter is also affected by the pH of the solution. The functional groups of the AHA have pK_a values between 3 and 5 (Schmitt-Kopplin *et al.* 1998b). Thus, at a pH between 3 and 5, some but not all of the functional groups would be deprotonated, and there would be significant competition between metal ions and protons for these binding sites. Under neutral conditions, the functional groups

would be deprotonated and available for binding with cations. Under alkaline conditions, the functional groups would most certainly be deprotonated, as would most other species, and there would be competition among these potential chelators for metal binding. By choosing to analyze AHA solutions of different metal concentrations over the range of pH, different binding patterns should be discernable, as well as the relative concentrations of free and bound metals.

The following discussion of my results of the analysis of AHA-Pb samples using CE/ICP-MS is divided into several sections. The first looks at the issue of reproducibility of sample electropherograms, followed by a discussion of a mass balance approach to the interpretation of the results. Then general trends observed for samples of increasing Pb concentration will be presented followed by a discussion of these trends as a function of solution pH. Finally, an overall interpretation of these trends and an evaluation of the analytical procedure will be presented.

3.3.2 *Pb Standard Results, HEN/Cyclonic LOD*

To determine the amount of Pb associated with AHA samples, Pb standards were first analyzed using CE/ICP-MS. Concentrations of 0.2, 0.5, 1 and 10 mg L^{-1} were injected into the capillary and separated in a 45 mM borate BGE (standard CE conditions as defined in section 2.2). The migration times, peak areas and peak amplitudes of the resulting Pb peaks were determined. The results of this analysis, as well as the statistics for the consequent standard curves are presented in Table 3.9. The mean migration time for the Pb peak is 4.77 minutes. Both peak area and peak amplitude

Table 3.9: Pb standard data. Migration times (MT), peak areas (PA) and amplitudes of Pb standards are listed. The regression analysis equations and percentage RSD are indicated for peak area and amplitude analyses (n = 3 for each standard).

conc. Pb (ppm)	MT		PA		amplitude	
	(min)	*% RSD*		*% RSD*		*% RSD*
0.2	4.94	*1.5*	345000	*4.8*	23200	*6.2*
0.5	4.78	*0.5*	595000	*2.0*	52100	*9.4*
1	4.69	*2.3*	852000	*13.7*	92300	*4.1*
10	4.67	*4.6*	6470000	*7.7*	894000	*3.6*
overall mean = 4.77			*equation:* $y = 623000x + 244000$		*equation:* $y = 88900x + 5540$	
overall % RSD = 2.6			($R^2 > 0.999$)		($R^2 > 0.999$)	

is positively correlated to standard concentration. The R^2 values for both equations are very high ($R^2 > 0.999$). For the analysis of the Pb concentrations seen in the AHA-Pb analysis, however, peak amplitudes could not be used, as some peaks were very broad, or consisted of several smaller peaks. Furthermore, it was found that the majority of peaks analyzed in the AHA analysis had peak areas less than the calculated intercept value of the calibration curve for peak area. Thus, the equation was modified such that it was forced through the origin. This is comparable to the assumption that a concentration of zero would have shown no peak area. While this may be intuitive, it does not account for the limits of quantification and detection inherent in a method, or for background concentration. This new calibration curve is shown in Figure 3.14. The resulting equation showed little difference in the slope, and the R^2 is still high ($R^2 > 0.999$). Due to the minimal effects on the significance of the regression, and the inability to analyze

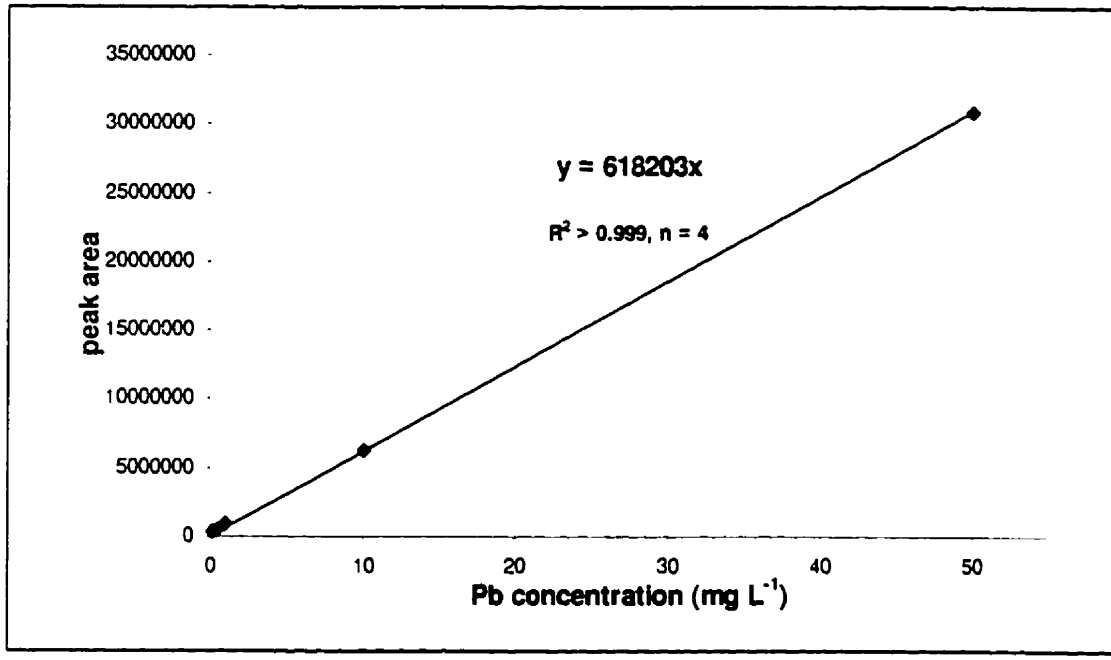

Figure 3.14: Calibration curve for determination of Pb concentrations. Peak areas for standard concentrations of 0.2, 0.5, 1, 10 and 50 mg L^{-1} Pb used to determine the concentration of Pb in the peak analysis of AHA samples. Separation conditions are as in Figure 3.3 (b). The standard curve was forced through the origin to allow for the analysis of peaks with low areas. This caused little difference in the statistical significance of the relationship (i.e. $R^2 > 0.9999$ when not forced through the origin).

peak areas without modifying the original equation, this second equation was used as the calibration curve for the AHA analysis.

The LOD for the HEN/cyclonic interface could also be calculated for Pb using the calibration curve. The LOD was estimated from the extrapolated concentration of metal that would correspond to a peak amplitude that is three times the standard deviation of typical background amplitude. The LOD is 9.9 $\mu g\ L^{-1}$, or in absolute mass terms, 0.5 pg (based on a 47 nL injection). This is more than ten times lower than the Pb LOD calculated for the DIHEN interface (see Table 3.7). The relative LOD for other elements were not measured, so no other comparisons between interfaces may be made according to LOD. A comparison of Figures 3.6 (a) and 3.11 (b), which show the respective signal intensities of several elements as a function of make-up solution flow rate for the DIHEN and HEN/cyclonic interfaces respectively, indicates that the HEN/cyclonic interface is more sensitive for Pb. This may not be the case for other elements. This, however, does indicate that the HEN/cyclonic interface may be more appropriate under the conditions used for the analysis of Pb interactions with AHA.

3.3.3 *Estimation of Variability*

The typical electropherograms observed for AHA samples inoculated with Pb are quite complex, and thus need a brief explanation of the process used to analyze them, as well as a description of the reproducibility seen for each sample. To illustrate a typical result, Figure 3.15 shows two replicates of the same sample separated in the same electrophoretic conditions used for the previous AHA-Pb UV analysis. Of course, the

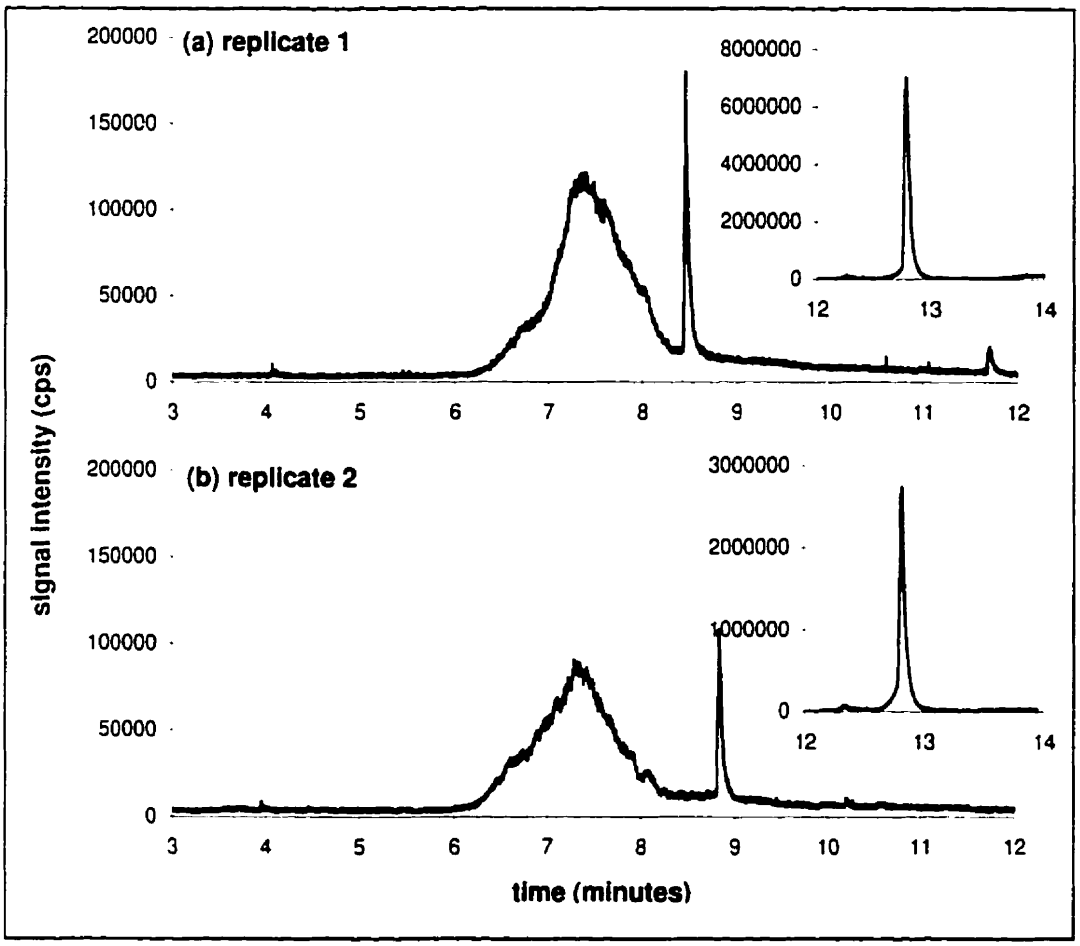

Figure 3.15: Reproducibility of AHA-Pb CE/ICP-MS analysis. Two replicates of one sample (500 mg L^{-1} AHA, 50 mg L^{-1} Pb, pH 6-7) are shown. The overall pattern of separation is similar, with the majority of Pb seen in a large peak from approximately 6 to 8minutes, and a more defined peak seen between 8.5 and 9 minutes. The inset plot on each figure shows the relative signal intensity for the push peak (see text for explanation).

main difference in this analysis is the use of ICP-MS to detect and record the sample's separation in terms of its Pb content, rather than the organic component of the sample. Similar patterns can be seen in the electropherograms from both the CE/ICP-MS analysis and in the UV analysis (for comparison, see Figure 3.3): the majority of the Pb is seen in a very wide peak from 6 minutes to approximately 8 minutes, and a smaller peak of a more narrow and defined shape is seen between 8.5 and 9 minutes. The results in Figure 3.15 indicate that the migration times for the first peaks of both Figures are essentially the same (percentage RSD < 1 %), but there is a 10 % difference in the migration time of the second peak. As well, the percentage RSD for area and amplitude of both peaks are quite high (< 25 %). This was generally the case for all samples analyzed, and it is unknown why the variability is so high.

The variability of the CE system was measured prior to all analyses using the standard mix, as described in section 3.1.2, and the variability as measured as percentage RSD for peak migration and area was at or below the levels described for the standards therein (see Table 3.1). As well, the simple speciation schemes described previously, such as the metal mixture and the EDTA-Pb sample, did not show such a disparity in reproducibility. Furthermore, the migration times, peak areas and amplitudes of the Pb standards used in this analysis (see section 3.3.2) are very reproducible. Accordingly, it appears that the variability in the AHA-Pb samples must be due to some effect of the sample, and not due to the CE/ICP-MS system. To continue the analysis, however, the variability of replicates was assumed to be approximately those values measured for the replicates shown in Figure 3.14 (i.e. ~ 10 % for migration time, ~ 25 %

for peak area and amplitude). A representative electropherogram of each sample was chosen for the bulk of the data analysis to allow concise comparisons to be made between samples. The replicates were chosen on the merits of their mass balance results. This is described in section 3.3.3.

The peak ranges are identified in Figures 3.16 to 3.18, which show the results of the AHA-Pb CE/ICP-MS analysis. The peaks are indicated on each electropherogram. As most samples show a number of peaks at various times and of differing size and shape, a standardized method for identification and quantification of the peaks was used to allow for a quantitative analysis of the data. Peaks were analyzed according to a general range of migration times and the total area for that range added together. For example, in Figure 3.16 (a), the areas of any peaks from zero to six minutes would be considered peak A. Peak B is the sum of the areas of peaks between six and nine minutes, peak C between nine and twelve minutes. These time ranges were chosen by observing all samples, and dividing the areas into sections that represent ranges that show change between samples. Also, the migration time of the Pb standard solution was considered; at approximately 5 minutes, the free Pb should be observed. Peak A will incorporate this peak, and will considered for the identification of all peaks. Additionally, comparison to the electropherograms seen in the AHA-Pb UV analysis (see Figure 3.3) allows some conjecture of peak identities to be made.

The peak A period represents a migration time zone in which generally the large humic hump is not observed, and also encompasses the times at which Pb standards are typically seen (see section 3.3.2). Peak A is where the unbound Pb is expected to

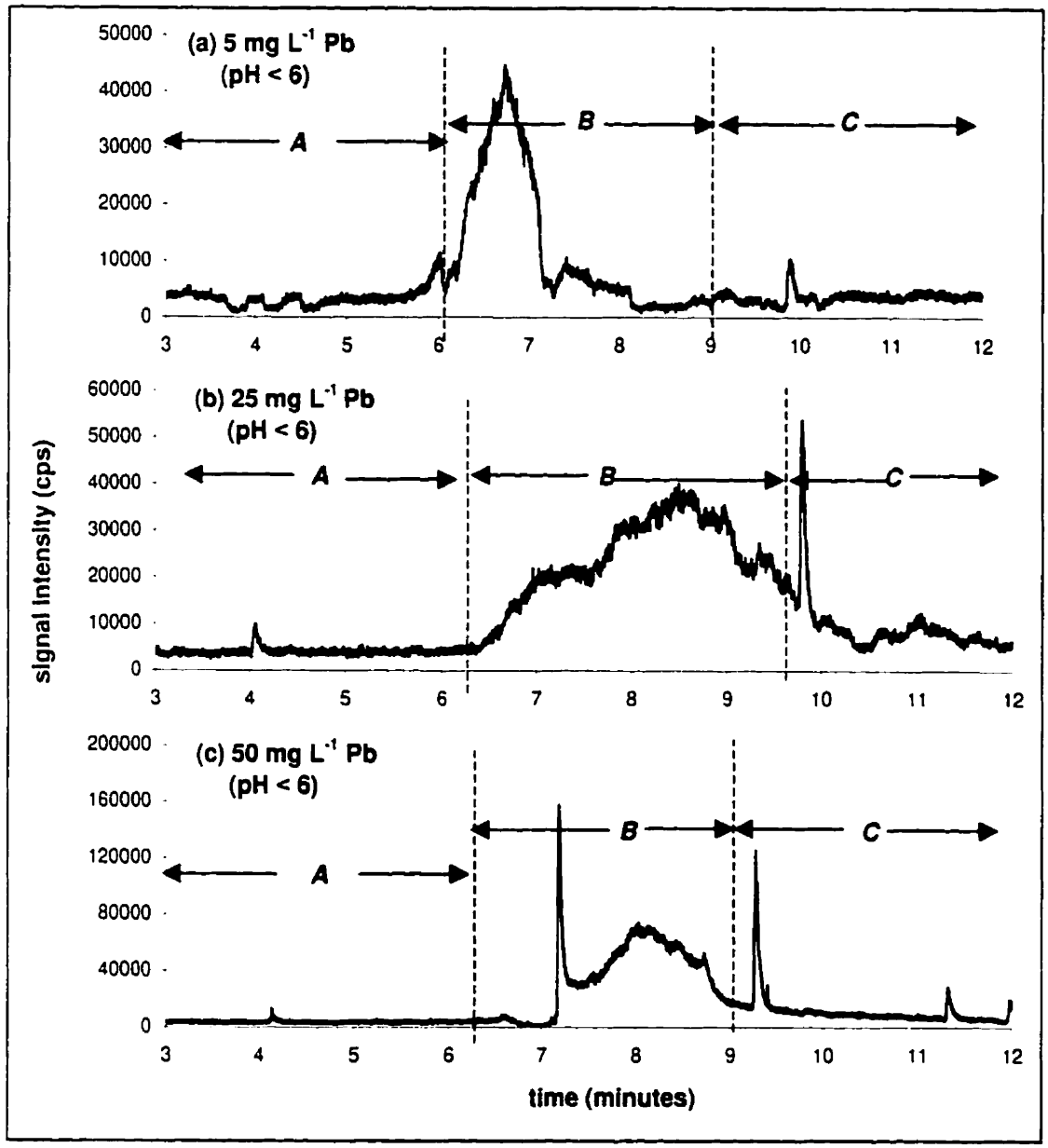

Figure 3.16: AHA-Pb CE/ICP-MS analysis: Acidic samples. 500 mg L^{-1} AHA solutions inoculated with (a) 5, (b) 25 and (c) 50 mg L^{-1} Pb are shown. Dotted lines indicate peak migration time ranges as defined in the text. For (b) the range of peak B is 6 to 9.5 minutes, and peak C is 9.5 to 12 minutes.

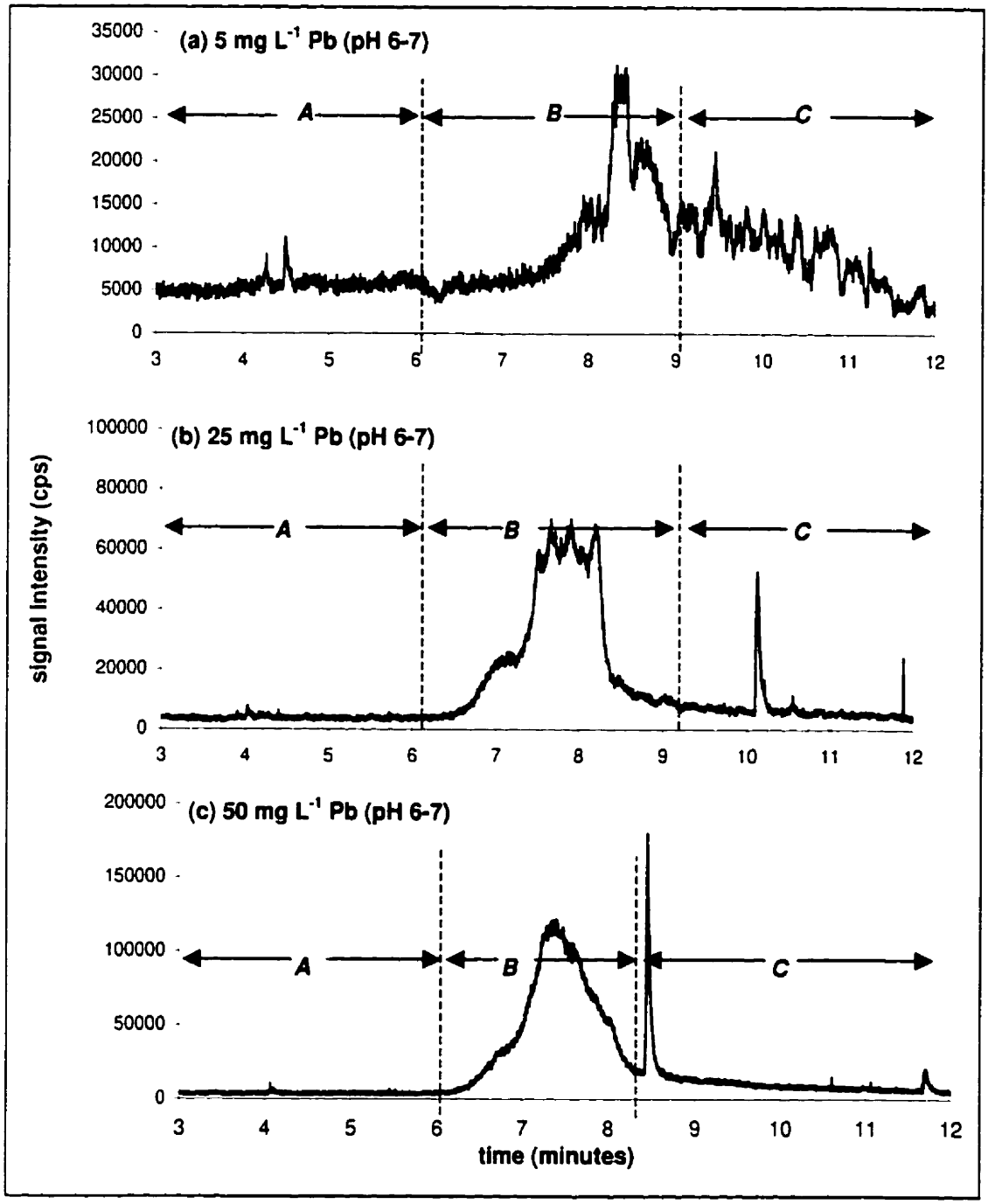

Figure 3.17: AHA-Pb CE/ICP-MS analysis: Neutral samples. 500 mg L^{-1} AHA solutions inoculated with (a) 5, (b) 25 and (c) 50 mg L^{-1} Pb are shown. Dotted lines indicate peak migration time ranges as defined in the text. For (c) the range of peak B is 6 to 8.3 minutes, and peak C is 8.3 to 12 minutes.

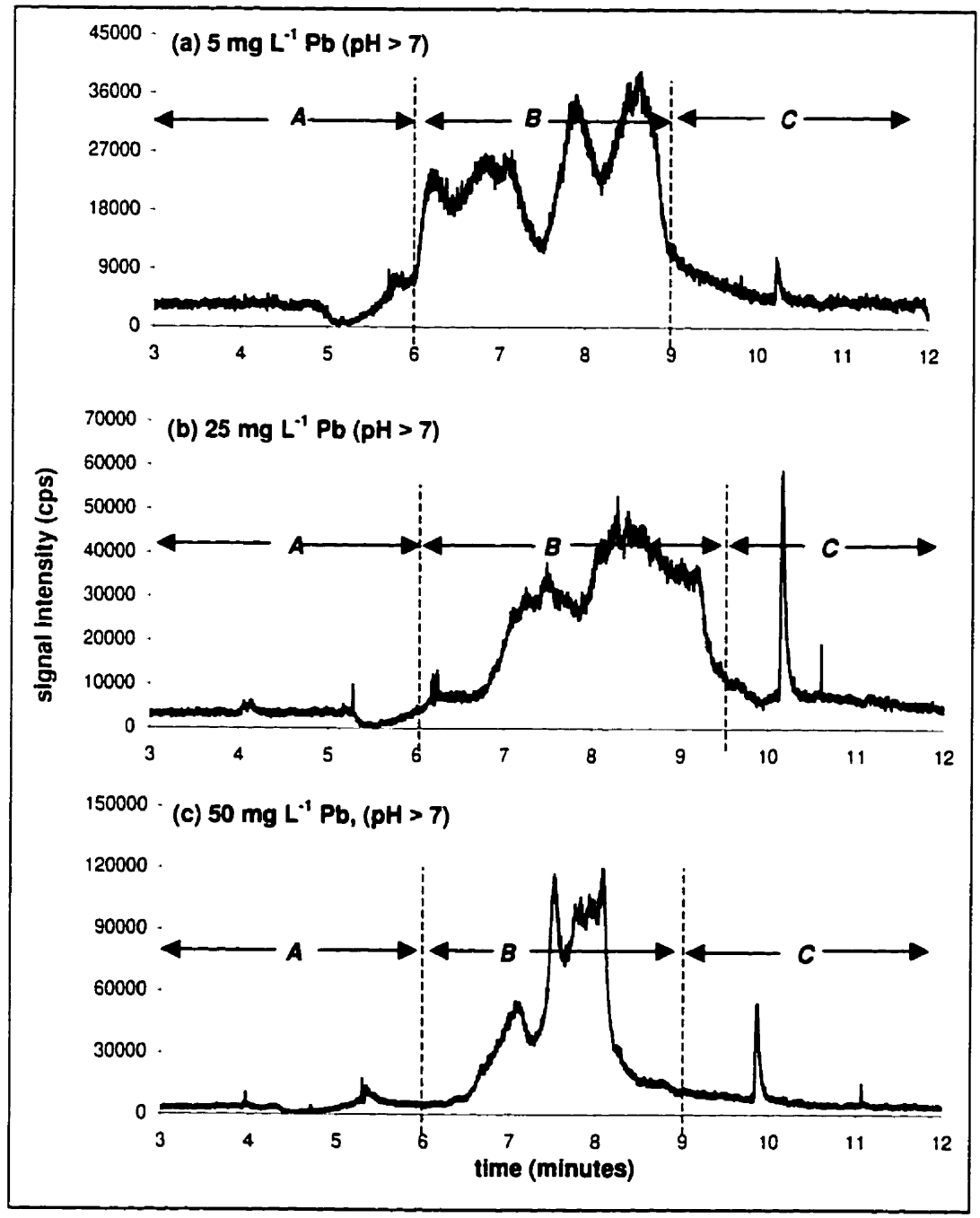

Figure 3.18: AHA-Pb CE/ICP-MS analysis: Alkaline samples. 500 mg L^{-1} AHA solutions inoculated with (a) 5, (b) 25 and (c) 50 mg L^{-1} Pb are shown. Dotted lines indicate peak migration time ranges as defined in the text. For (b) the range of peak B is 6 to 9.5 minutes, and peak C is 9.5 to 12 minutes.

appear. Peak B represents the times at which the majority of the humic hump is observed. Peak C represents a migration time range that is later than the humic hump. Finally, at 12 minutes, the contents of the capillary were flushed with nitric acid and pushed towards the detector, allowing the analysis of any residual sample. In all cases Pb is detected in this "push", hence the final peak analyzed is referred to as the push. The push can be seen as in the inset for both electropherograms in Figure 3.15. The possible identity of the push Pb will be discussed in detail in section 3.3.4.

Three exceptions to the peak migration times as defined above were made for the analysis. The exceptions were made due to the observance of a narrow defined peak that was generally seen in the peak C range, after the large Pb signal which was assumed to be associated with the humic hump (peak B). These exceptions are noted by changes in the division of peaks in Figure 3.16 (b), 3.17 (c) and 3.18 (b). For the electropherograms seen in Figures 3.16 (b) and 3.18 (b), peak B appeared to be longer, and therefore the migration time range for this peak was extended to 9.5 minutes. For Figure 3.17 (c), the humic hump of peak B appeared shorter and the narrow peak of peak C appeared earlier, and the migration time range of peak B was therefore shortened to end at 8.3 minutes, and the length of peak C extended accordingly.

3.3.4 *Mass Balance*

As discussed previously, the replicates of a given sample were evaluated using a mass balance approach. The samples were analyzed according to the total Pb observed in both the peaks of the defined migration time ranges of the electropherogram,

and in the push. The total Pb was determined as a concentration relative to the calibration curve calculated from the Pb standards and shown in Figure 3.14. Again, Figures 3.16 through Figure 3.18 are the representative results of the separation of samples for this AHA-Pb analysis (i.e. "average" electropherograms of complex separations are difficult to present). The results are grouped by the pH value of the sample, such that Figure 3.16 presents the electropherograms for the 500 mg L^{-1} AHA samples with pH < 6 (acidic) and (a) 5 mg L^{-1} Pb, (b) 25 mg L^{-1} Pb and (c) 50 mg L^{-1} Pb. The data is presented in the same manner for neutral samples (Figure 3.17) and alkaline samples (Figure 3.18). Ranges for migration times of peaks A, B, and C are indicated on all electropherograms.

A mass balance of the sample electropherogram was done in the following manner: peak areas were determined for all peaks and the approximate concentration of Pb associated with each peak calculated from the calibration curve for Pb standards (Figure 3.15). As the same volume of standard and sample were injected, the interpolated concentrations of the peak areas could be directly measured. Thus, the relative concentrations contributed by all peaks in each electropherogram were determined, including the push. The total Pb should be the same as the concentration of Pb added to the sample, assuming there is minimal loss of Pb during the electrophoretic process. In all cases, these values were similar within a wide range of variability; the 5 mg L^{-1} samples were up to 100 % higher in Pb than the added amount (e.g. total peak areas indicate that sample Pb concentration is 10 mg L^{-1}). The variability decreased with increasing Pb concentration (i.e. all 50 mg L^{-1} replicates were within 10 % of the actual mass). Representative electropherograms were chosen from this analysis; those replicates

that were closest to the actual value of Pb added were used for further analysis. The total Pb concentrations of the samples were not determined by any other analytical means, and thus the actual concentrations can only be predicted from the known volumes and concentrations added to the solutions.

Figure 3.19 shows the relative contribution of each peak range to the total concentration of Pb in each representative sample. The samples are grouped according to the concentration of Pb added (theoretical concentration) to the 500 mg L^{-1} solution of AHA. For example, Figure 3.19 (a) shows the neutral, acidic and alkaline AHA solutions with a Pb concentration of 5 mg L^{-1}. In all cases, the measured concentration of Pb is indicated at the top of the bar for each data set. The greatest difference between theoretical concentration and measured concentration is for the acidic 5 mg L^{-1} sample: the concentration measured differs by 32 %. The neutral and alkaline samples differ by 10 and 16 % respectively, from the theoretical Pb concentration of 5 mg L^{-1}. This is possibly due to experimental error in making the solutions. For the 25 mg L^{-1}samples, there is less than a 25 % difference between the measured values and the theoretical concentrations. The 50 mg L^{-1} samples show the greatest correspondence with their theoretical concentrations, showing a 4 % difference for both the acidic and neutral samples, and 2 % for the alkaline. Again, as the true values were not measured, it is difficult to assess how accurate these numbers are, but this analysis serves to allow a basis for discrimination of samples for further analysis.

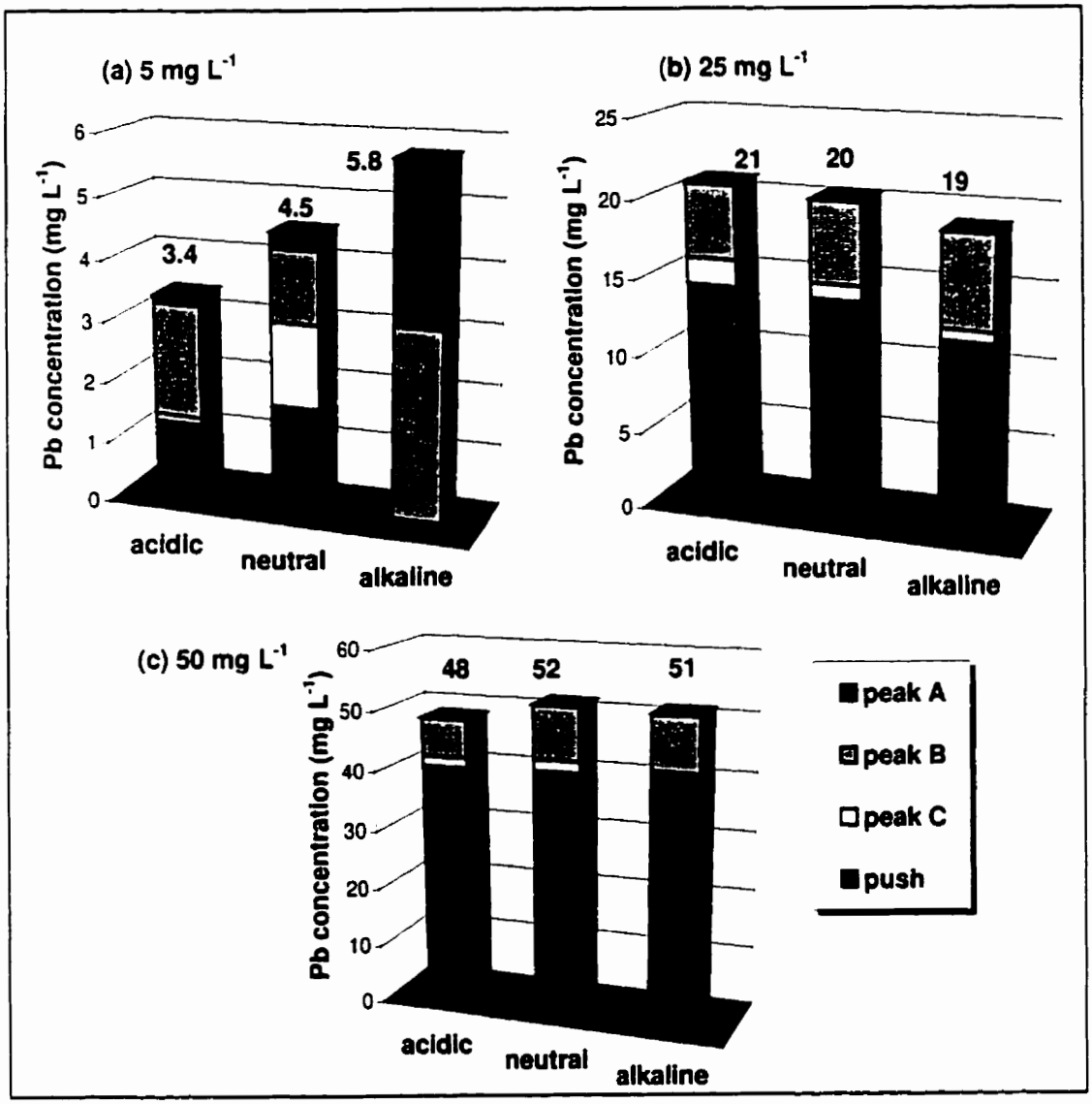

Figure 3.19: Mass balance results. The total Pb measured in each peak for all samples. Total concentration of Pb for each sample as calculated as the sum of all peaks is indicated at the top of each bar.

3.3.5 *General Trends*

One objective of this experiment was to develop a method to determine the free or unbound metal associated with a sample of HA. Moreover, this method was hypothesized to allow for the comparison of metal binding among separated fractions of HS. From the initial work done looking at the mobility of HA in CE with UV detection, the majority of organic matter was found to migrate as a humic hump representing a gradient of size and charge classes. This would initially appear to limit our ability to analyze "fractions" for metal interaction, as there is usually one discernable peak resulting from the separation.

Despite this seeming limitation, general trends can be observed for the samples, both in terms of concentration dependent trends, and changes in binding patterns according to pH of the solutions.

The results for the acidic samples of varying Pb concentration can be seen in Figure 3.16. The magnitude of the signal intensity increases with Pb concentration. A small peak can be seen in the peak A range for both the 25 and 50 mg L^{-1} samples. This peak does not have a linear relationship with Pb concentration, and has approximately the same area in both samples. For all electropherograms, there appears to be a large peak that corresponds to the humic hump seen in the UV analysis; this is defined as the peak B migration time range. There is a narrow peak in the peak C range that has a similar migration time for all samples (migration time = 9.7 minutes, percentage RSD = 2.7 %). The amplitude of this peak increases linearly with increasing Pb concentration ($R^2 >$ 0.996).

In Figure 3.17 the electropherograms of a neutral AHA solution according to their added Pb concentrations are shown. An obvious observation of these samples is the increase in Pb signal intensity measured for peak areas seen in the electropherograms as more Pb is added to the solution. Small peaks are observed in the peak A range, yet they remain relatively constant throughout the range of Pb concentrations analyzed. Assuming again that the large peaks seen in peak range B represents the metal bound to the humic hump, the average migration time of this fraction can be observed to be decreasing with increasing Pb concentration. As shown in the UV analysis of AHA-Pb samples, the binding of metal tends to increase the size of the AHA, leading to a shortened migration time under these electrophoretic conditions. As well, the narrow peak observed in the acidic samples is observed, although the migration times changes a great deal between the 25 mg L^{-1} sample and the 50 mg L^{-1} sample, and is not distinctly observed in the 5 mg L^{-1} sample. Again, a linear relationship is observed for the amplitude of this peak as a function of Pb concentration ($R^2 > 0.926$).

The alkaline sample results can be seen in Figure 3.18. Small peaks are observed in the peak A range, but there is no relationship between the amplitudes or areas of the peaks observed and the Pb concentration of the samples. The Pb associated with the humic hump can be observed in all concentrations; the magnitude of the signal intensity for these peaks increase with increasing Pb concentration. The pattern of these peaks changes with concentration as well. The presumed humic hump is wider for the 5 and 25 mg L^{-1} samples [Figure 3.18 (a) and (b), respectively] than for the 50 mg L^{-1} sample [Figure 3.18 (c)]. Again, a narrow peak is observed in the range of peak C but its

amplitude does not have a significant linear relationship with the concentration of Pb added to the solutions.

What is unclear from these electropherograms is the identity of a peak that is the free Pb, or unbound metal in solution. As well the push peak, the magnitudes of which can be seen in Figure 3.19 in comparison to the defined A, B and C peaks requires discussion. The push peak comprises more than half of the observed Pb in the electropherograms for both the 25 and 50 mg L^{-1} samples of all pH values. It also embodies a significant portion of the Pb for the 5 mg L^{-1} samples of acidic and neutral pH. Each peak will be discussed in turn, and tentative assumptions of the identity of each peak will be presented.

If unbound Pb is mostly cationic at the pH of the solutions analyzed, peaks seen in the peak A zone should represent this unbound Pb, as observed for the Pb solutions injected as standards (see Table 3.9). There are small peaks evident in almost all electropherograms in the migration time range of peak A. As well, one may expect these peaks to get larger with increasing metal concentration, as there should be more unbound Pb at higher concentrations. In Figure 3.20 (a), the concentrations of peak A for all samples analyzed can be seen. Converse to my prior assumption that the free Pb should be seen in peak A increasing linearly as a function of Pb concentration, an opposite trend is observed for all solutions. In fact, a linear decrease is observed in this peak for both the acidic and neutral solutions. From this evidence, if it is assumed that the free Pb is increasing with Pb concentration; it appears that the free metal peak is not seen in the migration time range of peak A for any of the solutions.

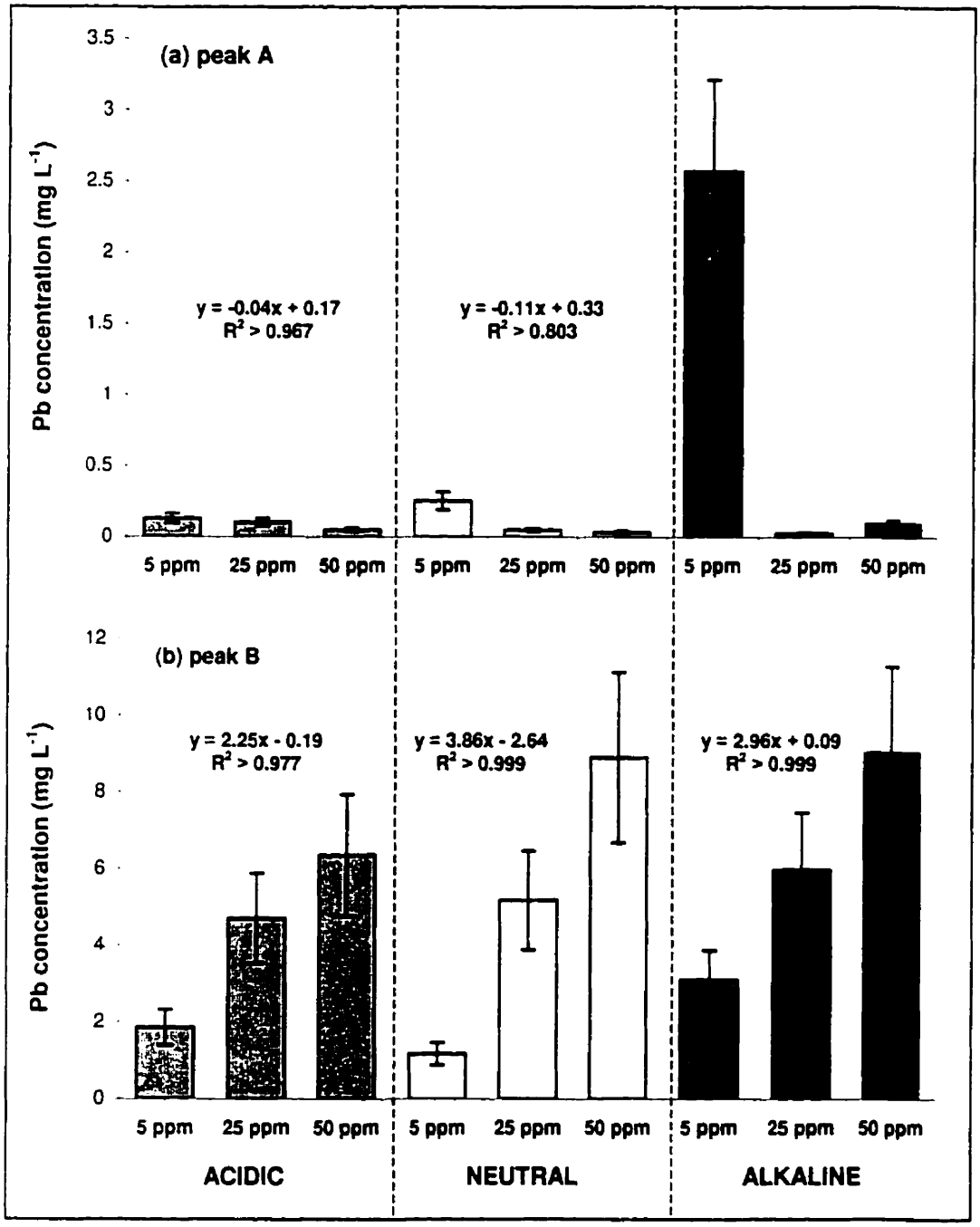

Figure 3.20: Relative concentration of peaks for all samples I. Pb concentrations of (a) peak A and (b) peak B are shown for acidic, neutral and alkaline samples for all concentrations of Pb analyzed. Significant relationships are noted. Error bars represent variability estimated as 25 % of peak area. Note: 1 ppm = 1 mg L^{-1}.

In Figure 3.20 (b), the Pb concentrations for peak B of all samples are shown. In all solutions, there is a significant linear relationship between the peak area and the Pb concentration of the sample. As I have previously defined this peak range to encompass the humic hump observed in the UV analysis, these relationships indicate that more metal is being bound to the AHA with increasing Pb concentration under all conditions of pH. This indicates that the range of Pb concentrations used for this analysis does not exceed the complexation capacity of the AHA. In other words, if the maximum amount of Pb that the AHA could bind were between 25 and 50 mg L^{-1}, a steady state should be reached in terms of Pb concentration for this peak. The relationship observed for the acidic samples, however, has a lower R^2 than for the neutral and alkaline samples. Under the conditions of high acidity, the complexation capacity of AHA should be reduced due to higher competition for binding sites with H^+, and the increased stability if the cationic Pb species. As well, the observed Pb concentrations between the 25 mg L^{-1} sample and the 50 mg L^{-1} sample are within the estimated percentage error for the measurement of peak B. This could indicate that complexation capacity for the acidic samples is between 25 and 50 mg L^{-1}.

As was indicated previously, there was a narrow peak observed in all electropherograms within the peak C period. The amplitude of this peak was found to have a significant linear relationship with Pb concentration. However, the area of this peak does not have this same relationship, as shown in Figure 3.21 (a) for all samples. The relationships observed for this peak in terms of amplitude and the overall magnitude of the areas observed, however, indicate that this peak could represent the free Pb, or at

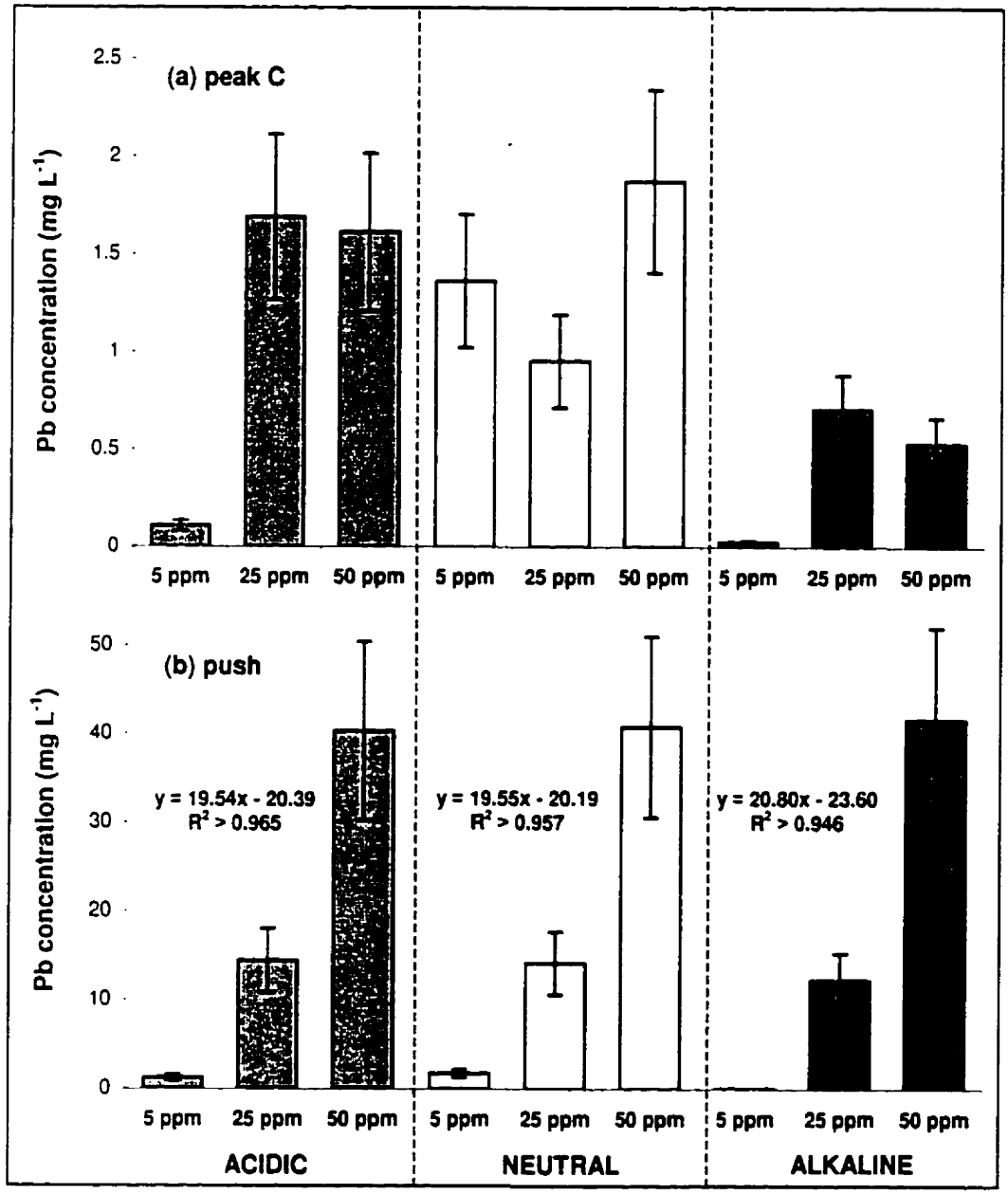

Figure 3.21: Relative concentration of peaks for all samples II. Pb concentrations of (a) peak C and (b) push are shown for acidic, neutral and alkaline samples for all concentrations of Pb analyzed. Significant linear relationships are noted. Error bars represent 25 % variability. Note: 1 ppm = 1 mg L^{-1}.

least a portion of this species in the samples. For example, from my assumption of the relative binding abilities of AHA under different pH conditions, I believe that the most unbound Pb would be observed in acidic samples, and the least in the alkaline. Save the large peak area observed for the neutral 50 mg L^{-1} sample, this trend can be seen in Figure 3.21 (a), indicating that under the different pH conditions, this peak is larger for the acidic and neutral samples than for the alkaline samples. As well, the linear relationships observed for the acidic and neutral samples in terms of peak amplitudesupport this hypothesis. Assuming the complexation capacity of AHA is greater under alkaline conditions, an increase in Pb concentration would not necessarily increase the unbound Pb at the concentrations analyzed, especially if all Pb was being bound to the AHA. If the complexation capacity were reached in the acidic and neutral samples, there would certainly be an increase in the relative concentrations of free Pb.

One consideration that needs to be made regarding peak C as being the free Pb is the migration time observed. The average migration time for the Pb standard, which was presumably in its cationic form was 4.77 minutes. The average migration time of peak C is 9.7 minutes (percentage RSD = 5.7 %). This is clearly very different than that observed for the Pb standards. The Pb standards, however, were very acidic (i.e. pH < 2) as they consist of Pb in nitric acid. Under these conditions, the Pb may maintain its cationic form in the alkaline BGE used (45 mM borate, pH 8.5). The acidic samples of this analysis ranged in pH values from 4 to 5. This may be enough of a difference to change the free Pb from its purely cationic form (i.e. Pb^{2+}) to complexes of negative charge when associated with the alkaline components of the separation BGE

(i.e. OH^-). This would change the migration of the "free" Pb in the electrophoresis, and could explain its late migration time. Standards of similar pH would need to be analyzed to confirm this conclusion.

Finally, the identity of the push peak must be addressed. For all samples analyzed, there is a significant linear relationship between the concentration of Pb added to the solution and the peak area observed for the push [Figure 3.21 (b)]. For all conditions of pH, there is a significant linear relationship between Pb concentration of the push peak and Pb concentration in the solution ($R^2 > 0.946$). It must be noted that no additional organic material was ever noted during the AHA-Pb UV analysis after 12 minutes of separation. It cannot be directly inferred from that data, therefore, that some Pb-bound organic material is left behind in the capillary. As well, there was no additional metal noted in any of the previous analyses (i.e. metal separation, EDTA-Pb, standard calibration curve analysis) using ICP-MS. Thus, it cannot be inferred from those data that this push peak is residual metal, either free or bound, left in the capillary solution after separation. The push is seen in all samples as a sharp peak around 12.5 to 13 minutes. As flushing by pressure is started during each sample analysis at 12 minutes, the lag time seen before the beginning of the push peak may allow some speculation on the source of this Pb. The migration time indicates that the Pb originates at the injection side of the capillary, as it would take roughly 30 seconds to flush the capillary at the low pressure used for rinses for CE/ICP-MS work (~ 5 psi).

The Pb could be at the injection side of the capillary for two reasons: it has remained there since injection, or it has migrated to the positive electrode in spite of the

EOF. There is a strong possibility that some AHA could bind with the silanol groups of the capillary, and thus maintain bound Pb with it. Fetsch and coworkers (1998a) claim that HA binding to capillary walls is the main reason why most low concentrations of organic matter are not detectable in CE applications. One would assume, however, that this would occur not only at the injection end of the capillary, but throughout the capillary. This could be the case, however, as the capillary is flushed with 2 % nitric acid for this push peak: the metal may only be removed from its association with the capillary wall by the acidic solution, and would therefore appear as a single peak regardless of its origin within the capillary.

Alternately, cationic Pb could associate with the silanol groups of the capillary. If this were the case I would have noted push peaks in the Pb standard solutions. If the Pb were migrating to the positive electrode, they would need to be in negatively charged complexes whose migration to the electrode was not overcome by the EOF. Such complexes could be possible in the alkaline BGE used for these analyses, but again, they would also have been observed for the Pb standards. This discrepancy has been previously discussed, and the differences in the pH of the standards and those of the AHA solutions analyzed may explain the observed differences in migration times. In particular, one would need to understand the difference in speciation of the Pb observed as peak C, and that which is not observed until the push. The push Pb could also be complexed with alkaline components of the BGE, but so small that its migration in an electric field toward the positive electrode is greater than the force of the EOF. Thus, it

would never be observed at the detector end of the capillary, and can only be analyzed during flushing of the capillary.

I can therefore conclude that there are two possible identities of the push Pb seen for all samples. First, it may consist of Pb that is bound to AHA that, in turn, has associated with the silanol groups of the capillary walls. AHA has been observed to do this in other studies, particularly at the high concentrations used in this experiment (Fetsch *et al.* 1998a). Thus, the push would represent Pb bound to AHA. The second alternative is that the push represents Pb that is not bound to AHA, but is not in the species-form consistent with the Pb standard analysis. In this case, we would be observing inorganic Pb species as may be seen in pH solutions higher than four, such as complexes with the hydroxide ion. Assuming this species is very small, of negative charge, or even easily associated with silanol groups if of positive charge, the push would represent the free Pb that is not associated with the AHA.

To distinguish these hypotheses, the relative concentrations of free and bound Pb have been shown in Figure 3.22 according to the assumptions of each hypothesis. Figure 3.22 (a) shows the push peak as Pb that is bound to AHA associated with the capillary wall, and hence did not migrate through the capillary during electrophoresis. In this case very little change in the free Pb is observed in solution for any of these samples, either when looking at them by pH subset, or by the concentration of Pb added to solution. The bound Pb concentration, on the other hand, is highly dependent upon the total Pb concentration, as indicated by the statistically significant relationships calculated ($R^2 > 0.979$). An ANOVA of the free concentrations reveals that

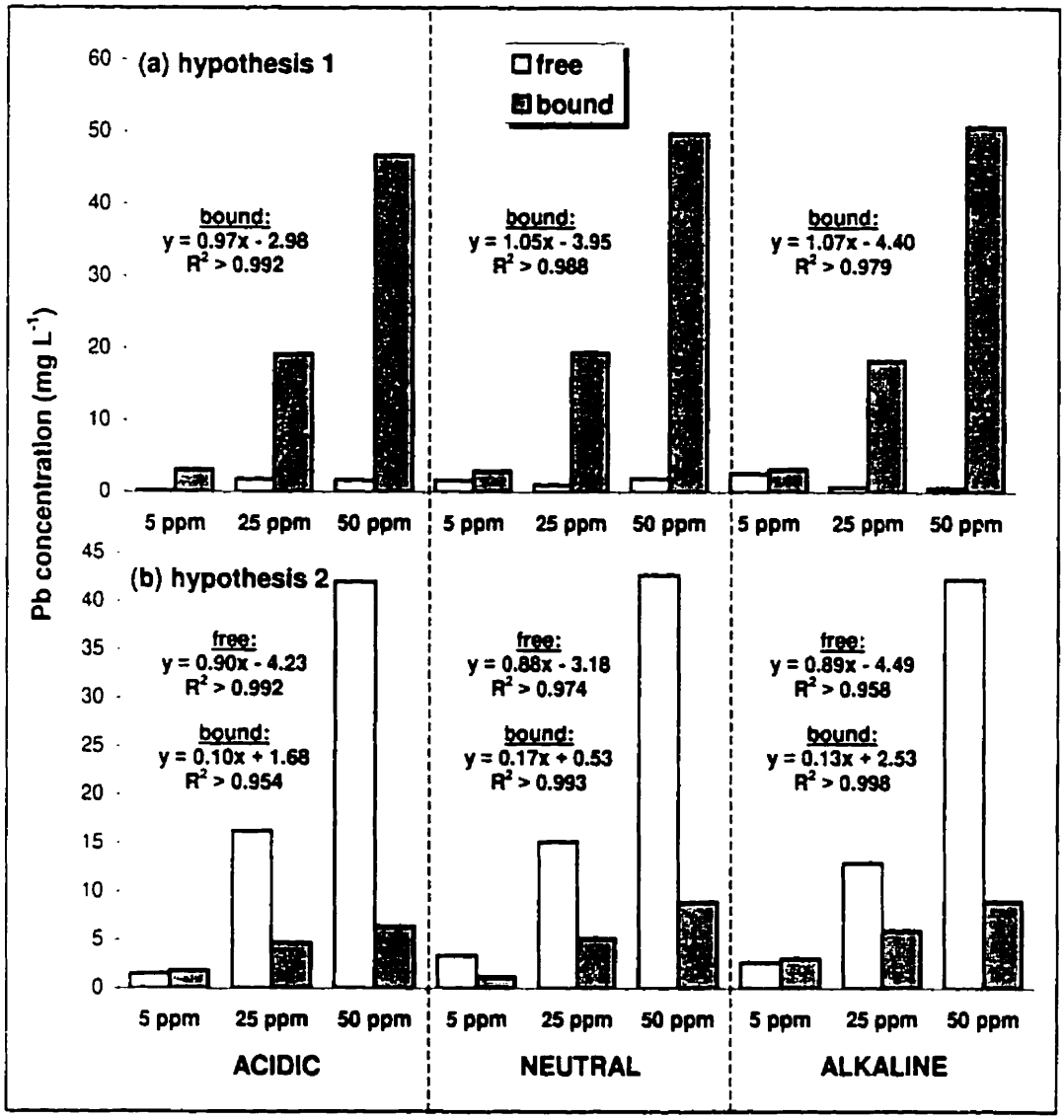

Figure 3.22: Relative concentrations of free and bound Pb. Results for (a) hypothesis 1 (push represents Pb bound to AHA) and (b) hypothesis 2 (push represents free Pb). All significant linear relationships between fraction concentration and Pb concentration are noted. No linear relationships are noted for hypothesis 1, free Pb. Note: 1 ppm = 1 mg L^{-1}.

there is no statistical difference between the concentrations of any of the free peaks. This would indicate that the amount of free Pb in all solutions, regardless of pH or total Pb concentrations has the same amount of free Pb. Consequently, the bound concentration is simply the total concentration of Pb less the average free Pb concentration (1.7 ± 0.7 mg L^{-1}).

The calculations for hypothesis 1 would indicate that the complexation capacity of the AHA has not been reached using the concentrations of both Pb and AHA used for these experiments. This is indicated by the negligible change in free Pb concentration, and the high dependence of the bound concentration upon the Pb concentration of the solution. These data support this hypothesis for several reasons: the range of complexation capacity for most HA is between 40 and 125 mg Pb per g HA (Rashid 1985). My highest concentration has 100 mg Pb per g HA. AHA are commercial soil-derived HA, and have been shown in many studies to be a reasonable analog of aquatic HA, but may have a higher complexation capacity due to increased functional group density. Thus, my highest concentration of Pb may not represent a fully saturated AHA-Pb, and it would stand to reason that the complexation capacity has not been reached in these samples. In this situation, one would expect to see the free metal concentrations be negligible or at least very low, as is the case as depicted in Figure 3.22 (a). Alternately, one may expect to see an effect due to the pH conditions of the sample than is indicated by these samples. Slight differences are noted qualitatively (e.g. overall there appears to be a greater concentration of free Pb in the acidic samples than the alkaline), but these differences are not statistically significant.

The alternate hypothesis is shown in Figure 3.22 (b): the push peak represents metal that is not bound to AHA but is associated in other inorganic species that are not detectable using my CE methods. In this scenario, the concentrations of both the free and bound Pb are linearly related to the concentration of Pb added to solution. In other words, as the concentration of Pb is increased for each solution type, both the amount of free Pb and the amount of bound Pb increase, and are thus dependent on the total Pb concentrations. An ANOVA reveals that there is a significant difference between the concentrations of Pb associated with the free and bound peaks according to the concentration of Pb added ($P < 0.005$, n = 9). The ANOVA, however, also reveals that there is no significant difference between the results seen for the acidic, neutral and alkaline samples. In other words, there appears to be no effect on the relative concentrations of free or bound Pb according to the relative acidity of the sample solutions.

Hypothesis 2 also represents a viable explanation of the data seen in this study; considering literature values for the complexation capacity of AHA, my experimental conditions may well represent samples within that range. This is manifested in the small changes in the bound concentrations that are seen as a function of Pb concentration in relation to the large increase in the free concentrations observed. As indicated in Figure 3.22 (b), the concentration of bound Pb is shown to be dependent upon the concentration of Pb added to solution as a linear function. A closer examination of these data is shown in Figure 3.23. The data are shown as a function of pH of the sample solution with each series representing the concentration of Pb added to the sample

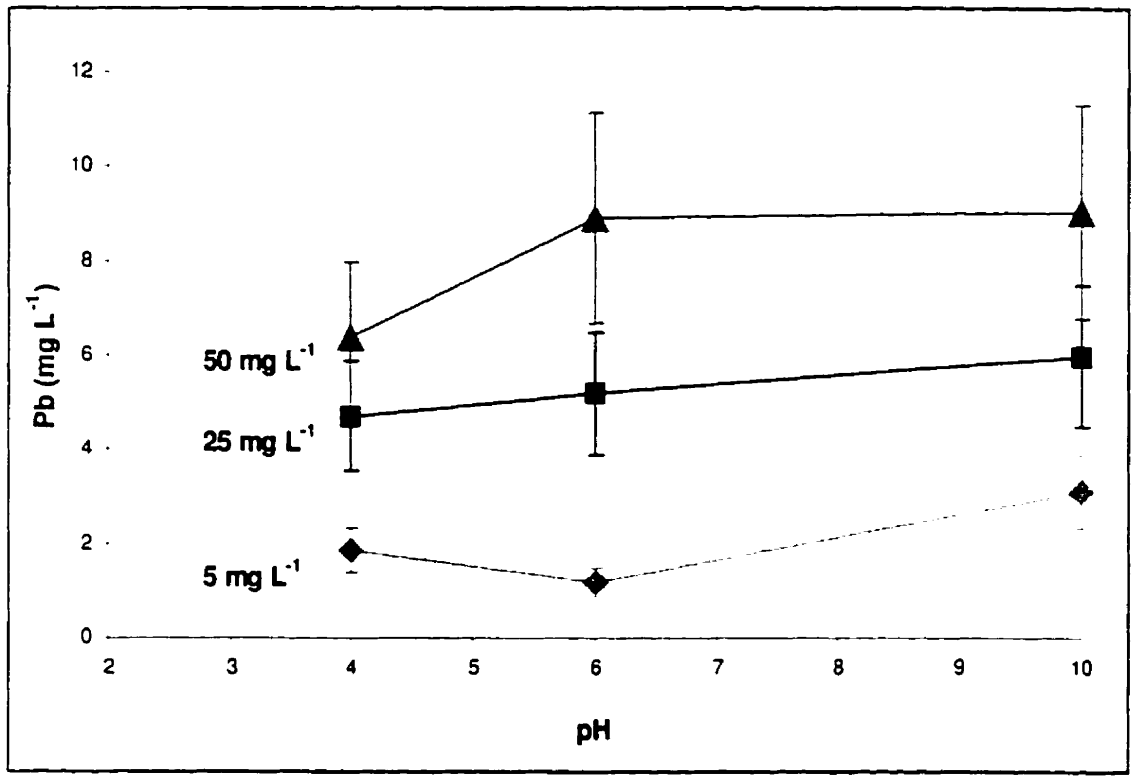

Figure 3.23: Bound Pb concentrations for AHA-Pb as a function of sample pH conditions: Hypothesis 2. The concentration of the bound Pb assuming the push represents free Pb that is not detectable using the applied CE methods is shown for all samples. The series represent samples of the same theoretical Pb concentration and the trend indicates the relationship between that concentration and the pH of the sample solution. Error in pH is not indicated, but is +/- 0.5 units. Error bars represent 25 % variability as described in text.

solution. The error bars indicate the 25 % variability observed in the initial replicates. With this variability in mind, the bound concentrations of Pb may not be statistically significant for the 25 and 50 mg L^{-1} samples. This would indicate that the bound concentration has not changed for these samples, and the complexation capacity of the AHA is between these two concentrations. As well, this relationship indicates that the complexation capacity of the AHA increases with the pH of the solution. This conclusion is well founded; the stability of the metal-AHA complex would be higher at higher pH.

In the discussion of the two hypotheses for the identity of the push, I have shown that both are possible. With the data available from this work, it is impossible to determine which of these is correct. It is my belief that indeed the push peak represents a portion of each hypothesis; it is most likely comprised of some Pb that is bound to AHA associated with the silanol groups of the capillary, and perhaps also some inorganic species of Pb that are not detectable with these CE methods. Again, it is impossible to discern or prove this conclusion with the data, but this explanation serves to explain the observed phenomenon and is scientifically plausible. Further study is warranted.

Although I am unable to clearly distinguish between the overall free and bound concentration of Pb seen in these analyses, there are some other general trends observed that are informative about the nature of the binding of Pb to AHA. Looking specifically at the peaks observed in the migration time range of peak B, some important trends can be seen. For example, for the neutral and alkaline samples (Figures 3.17 and 3.18, respectively), the average migration time appears to decrease with increasing Pb concentration. This change could be due to changes in the electrophoretic mobility of

smaller, more highly charged moieties becoming larger and less charged, hence the change in the migration time. Conversely, this could be due to binding of Pb to sites previously unfilled on larger molecules. It was observed in the AHA-Pb UV (section 3.1.2) analysis that there was a significant linear relationship between the migration time of peak 2 and the concentration of metal added for the 1000 mg L^{-1} AHA solutions. The equation describing this relationship is,

$$y = -0.0404x + 6.22 \quad (R^2 > 0.958, n = 4).$$

The slope of this relationship indicates that for every additional mg L^{-1} of Pb added to the solution, the migration time of the peak decreases by approximately 0.04 minutes (or 2.4 seconds). Assuming a comparable relationship for the 500 mg L^{-1} AHA, one may expect the migration time of a peak to be decreased up to 2 minutes when comparing a solution with 50 mg L^{-1} Pb to a solution with a 5 mg L^{-1} solution. Thus, it is difficult to discern the pattern of binding from these results due to changes caused in the electrophoretic mobility due to the addition of the Pb.

Finally, the changes in the Pb signals for the various electropherograms shown in Figures 3.16 through 3.18 indicate that the addition of Pb to AHA leads to a reduction in the separation of the species. Specifically, the migration time range of the various peaks become narrower and even sharper upon the addition of Pb, regardless of the pH of the solution. For example, in Figure 3.18 (a) the Pb can be seen as a very wide peak extending fully from 6 to 9 minutes. As well, many wide peaks are seen emanating from this greater peak. The same general shape can be observed for the Pb in Figure 3.18 (b). This sample has 25 mg L^{-1} of Pb added to an alkaline 500 mg L^{-1} AHA solution as

opposed to 5 mg L^{-1} of Pb as in Figure 3.18 (a). The migration time range for the Pb has decreased by approximately 30 seconds (7 to 9.5 minutes), and the wide peaks emanating from the presumed humic hump is less differentiated. The migration time range of the humic hump in the 50 mg L^{-1} sample [Figure 3.18 (c)] is even shorter (6.5 minutes to 8 minutes) and the average migration time is significantly reduced. As Pb is incorporated into the AHA molecule, the average mass of the molecule is increased, and the charge reduced. This is seen as a decrease in the average migration time of the peaks. The molecules also become less differentiated in their migration patterns; their charge differences are reduced, and they are separated mostly by merit of their mass differences. Considering the vast range of mass possible for a sample of HA molecules, this could lead to less differentiation for CE analysis. This may be important for the use of CE for fingerprinting various HA, as there may be a loss of discrimination power between samples of high metal content.

Overall, the analysis of AHA using CE/ICP-MS has raised many questions, while allowing an observation of HS in a manner previously unexplored. The results proved to be quite complex, showing reproducible patterns of Pb of high variability from sample to sample. Trends were observed in the samples, however, particularly for those of similar pH conditions. In particular, an attempt was made to identify the nature of the various peaks observed. A comparison to the UV analysis of similar samples allowed the correlation of a large, erratic Pb peak with the humic hump of the AHA. This Pb was assumed to be bound to the AHA, and the average migration time of this peak decreased with increasing metal concentration, due to binding of sites

with lower affinity for Pb, or due to the overall change in the mobility of AHA due to the additional mass and charge of the Pb. As well, a narrow, well-resolved peak was observed in most results around 10 minutes. This peak is not thought to represent bound Pb, as no organic matter had previously been observed in the UV spectra at this time. As well, the area of this peak is highly dependent upon the concentration of Pb in the sample. It was concluded that this peak most likely represents a Pb species that is not bound to the AHA, but is not necessarily cationic in solution. Finally, the nature of the push peak was investigated. Two hypothetical identities were proposed and the tentative conclusion is that the push represents both Pb bound to AHA, and Pb of other speciation. Some overall conclusions can therefore be made regarding the relative binding of Pb to AHA under different pH conditions, although more investigations would need to be made before more decisive conclusions may be made.

4 Conclusions and Recommendations for Future Work

4.1 Summary and Conclusions

To reiterate the objectives, the goals of this work were to develop a viable coupling apparatus for CE and ICP-MS and optimize this method using a simple speciation scheme, to compare the efficiency and sensitivity of this apparatus to alternate CE/ICP-MS systems, and finally to use this method for the analysis of HS-metal ion interactions. To reach these goals, it was first noted that the separation of HS using CE needed to be explored, which is demonstrated in section 3.1. The first three objectives were then attempted, as described in section 3.2. Section 3.3 incorporated the knowledge gained in the first two sections, that is the manner in which HS separate in CE and the development of an efficient CE/ICP-MS interface, to investigate the HS-metal interactions of a model HS, Aldrich humic acids (AHA), and Pb.

Borate buffers were used to separate AHA into relatively homogenous mass and charge molecular classes. As HS are structurally complex by nature, separation into broad molecular classes representing a gradient of size and charge is achieved rather than separation into easily definable and homogenous molecular classes. Borate buffers have been criticized for these analyses as they tend to form complexes with HS (Schmitt-Kopplin *et al.* 1998a; Schmitt-Kopplin *et al.* 1998b), but as my goal was to look initially at the relative amount of free and bound Pb, it was determined that the possibility of borate-HS interaction would not necessarily affect this analysis.

Using borate buffer, a reproducible pattern of AHA separation was achieved using UV absorbance analysis. These results indicate that the majority of the humic material migrated in the electrophoretic process as a large humic hump with a broad migration time of up to 2 to 3 minutes in length. Smaller, resolved peaks were also observed emanating from the humic hump. The peak area of the humic hump was found to have a linear relationship with the concentration of AHA, indicating that quantification of humic matter could be accomplished using CE (see also Rigol *et al.* 1994; Rigol *et al.* 1996). It was also determined that the migration time of the humic hump decreased with increasing metal concentration. In particular, a small peak seen in 1000 mg L^{-1} samples was also noted by another study (Keuth *et al.* 1998), and this peak showed a very significant dependence upon Pb concentration ($R^2 > 0.925$).

The development of the CE/ICP-MS interface proved to be a challenging undertaking. The original design used a Meinhard direct injection high efficiency nebulizer (DIHEN) as the main link between the instruments. The DIHEN was chosen because it would allow the entire sample to be analyzed and it allows the use of very low flow rates. Both features are of utmost importance for CE/ICP-MS hyphenation, as the EOF of the electrophoretic process is very low (~ nL min^{-1}) therefore requiring very sensitive detectors as the mass of analyte will be necessarily small in comparison. Unfortunately, the nebulizer was damaged in an accident, and it was unclear if its performance was effected. In comparison to a more traditional interface design using the Meinhard high efficiency nebulizer (HEN), it had comparable detection limits for some elements, and lower for others (in particular Pb). Ultimately, it was decided to use the

HEN for the final analysis, as Pb was the metal of interest for this study. The results of the work leading to the development of the DIHEN interface are included in this thesis, however, as may show much promise for future work, and allowed for a thorough investigation for comparison to the interface that was used in the end.

The CE/ICP-MS interface appeared to be a very efficient tool for metal speciation studies as indicated by the results for various metal separation experiments, and in particular for a Pb speciation study using EDTA. Three replicates of an EDTA-Pb mixture were shown to have reproducible separation using the HEN/cyclonic interface and a borate buffer. Furthermore, the relative amount speciation of Pb as an EDTA-Pb complex and Pb^{2+} were within 5 % of the equilibrium concentrations as calculated by MINEQL (Tipping).

Finally, AHA samples inoculated with Pb were analyzed using CE/ICP-MS. Unlike the CE analyses, where the separations could be followed using UV absorbance of the organic material through the column, the ICP-MS detector allows us to follow the movement of metal species through the column. Due to the physical configuration of the apparatus necessary for hyphenation, it was not possible to acquire both UV absorbance data and ICP-MS element-specific data simultaneously. When interpreting these results, one must remember that an understanding of the mobility of the humic material can only be inferred from relative Pb response as well as from the prior analysis of AHA using CE. As my initial goal was to endeavor to quantify both free and bound Pb, such comparisons needed to be made to allow a distinction between Pb peaks to be made.

The results of the AHA-Pb CE/ICP-MS analysis proved to be quite complex; the reproducibility of the samples was low (~ 25 %), and therefore it was difficult to discern what a representative electropherogram would look like for each sample. To deal with this problem, a mass balance approach was used to determine the sample for subsequent analysis. Using this method, it was found that most samples had a total Pb content comparable to the mass that had been added to the solution.

Many general conclusions were determined from this analysis. These include the basic observation that the response of Pb closely resembles the UV absorbance electropherograms obtained in the earlier analyses. This is because of the chelating nature of the HS; it binds metals very efficiently. Therefore, the response of Pb will generally indicate the separation of the organic humic material. As the HA does not separate into well-resolved and definable fractions, the pattern of broad and variable Pb response is also seen in this analysis.

The determination of the free metal in these samples also proved difficult. As the migration time of Pb was within the time of the migration time of the humic material itself, it was troublesome to decipher the free Pb from that which is bound to humic material. Many of the existing peaks were explored as possible free Pb, taking into consideration changes in the sample matrix that may be involved in changing from the acidic standards to the samples of different pH regimes. In particular, the possibility of residual Pb left in the capillary after separation was explored in terms of it representing the free Pb component of the sample. It was concluded that this residual Pb most probably represents Pb bound to AHA that has complexed with the capillary wall. The

identity of a peak representing free metal, or that Pb which was not bound to HS, was not clearly identified in this analysis, but general trends in metal binding with AHA were determined.

4.2 Recommendations for Future Study

Research involving HS can be quite complex due to the heterogeneous nature of the humic material itself. Studies looking specifically at the structural properties of HS are difficult, particularly if one hopes to elucidate a defined structure. However, it is possible to use generalized approaches to these questions to observe trends and commonalties for these substances. Using CE for the separation of HS into broad size and charge classes is one such approach. Assuming that the fractions separated in CE form some broad molecular classes, observing the relative metal associations with these fractions could illuminate some general metal binding trends for HS. As well, the metal associated with the humic material may be distinguishable from that which is free in solution.

In practice, however, the use of CE to separate HS confounded by several factors, most importantly the complexation of humic material with the capillary column itself. A goal that would most certainly improve upon the results of this study would be the investigation of procedures that would preclude interaction of the HS functional groups with the silanol groups of the capillary. Fetsch and coworkers (1998a) claim to have produced such results, yet their methods were not reproducible in my experiments.

Certainly, the use of borate buffers are not the ideal for HS separation studies (Schmitt-Kopplin *et al.* 1998a; Schmitt-Kopplin *et al.* 1998b), yet they were found to be the most viable buffer systems available at the time of these studies. An in-depth investigation of the buffers for these analyses would be warranted, with particular attention to developing a buffer system in which the migration time of free Pb is very different than that observed for humic material.

An important feature of this thesis that must be presented in a discussion of recommendations for future work is the method of CE/ICP-MS itself. These results show that this instrumental hyphenation could prove very useful for studies of metal speciation including and beyond those involving HS. Many speciation studies have exploited the high resolution of CE combined with the elemental sensitivity of ICP-MS (e.g. Michalke and Schramel 1998a; Taylor *et al.* 1998; Majidi *et al.* 1999). Certainly the speciation of As and Se have shown promise for their detection using CE/ICP-MS. I would encourage the use of these results to be used as a guide for the hyphenation of the instruments in this regard.

5 REFERENCES

Aiken, G.R., D.M. McKnight, R.L. Wershaw, P. MacCarthy. An introduction to humic substances in soil, sediment and water. In: *Humic Substances in Soil, Sediment and Water*. G.R. Aiken, P. MacCarthy, R.L. Malcolm, R.S. Swift (eds.). Wiley, New York: 1985 (pages 1-9).

Allen, H.E., R.H. Hall, T.D. Brisbin. 1980. Metal speciation: Effects on aquatic toxicity. *Environmental Science and Technology*, 14: 441-443.

Allen, H.E., A.W. Garrison, G.W. Luther. Preface. In: *Metals in Surface Waters*. Sleeping Bear Press, Inc, USA: 1998 (pages v-vii).

Batley, G.E., G.K.C. Low. Applications of high-performance liquid chromatography to trace element speciation studies. In: *Trace Element Speciation: Analytical Methods and Problems*. G.E. Batley (ed.). CRC Press, Boca Raton: 1989 (pages 185-217).

Becker, J.S., H. Dietze, J.A. McLean, A. Montaser. 1999. Ultratrace and isotope analysis of long-lived radionuclides by inductively coupled plasma quadrupole mass spectrometry using a direct injection high-efficiency nebulizer. *Analytical Chemistry*, 71: 3077-3084.

Boss, C.B., K.J. Fredeen. *Concepts, Instrumentation, and Techniques in Inductively Coupled Plasma Optical Emission Spectrometry, Second Edition*. The Perkin-Elmer Corporation, USA: 1997.

Bragato, G., A. Mori, M. De Nobili. 1998. Capillary electrophoretic behaviour of humic substances from *Sphagnum* peats of various geographical origin: relation with the degree of decomposition. *European Journal of Soil Science*, 49: 589-596.

Browner, R.F. Aerosol generation and sample transport in plasma spectrometry. In: *Inductively Coupled Plasma Spectrometry and its Applications*. S.J. Hill (ed.). Sheffield Academic Press, Sheffield: 1999 (pages 99-118).

Bunce, N. *Environmental Chemistry, 2nd Edition*. Wuerz Publishing Ltd, Winnipeg: 1994 (pages 333-364).

Campbell, P.G.C. Interactions between trace metals and aquatic organisms: A critique of the free-ion activity model. In: *Metal Speciation and Bioavailability in Aquatic Systems*. A. Tessier, R.D. Turner (eds.). John Wiley & Sons, New York: 1995.

Chau, Y.K., P.T.S. Wong. Applications of gas chromatography to trace element speciation. In: *Trace Element Speciation: Analytical Methods and Problems*. G.E. Batley (ed.). CRC Press, Boca Raton: 1989 (pages 219-244).

Chiari, M., M. Nesi, P.G. Righetti. Surface modification of silica walls: A review of different methodologies. In: *Capillary Electrophoresis in Analytical Biotechnology*. P.G. Righetti (ed.). CRC Press, Boca Raton: 1996 (pages 1-36).

Craston, D.H., M. Saeed. 1998. Analysis of carboxylic and related acids in the environment by capillary electrophoretic techniques. *Journal of Chromatography A*, 827: 1-12.

Dabek-Zlotorzynska, E., E.P.C. Lai, A.R. Timerbaev. 1998. Capillary electrophoresis: the state-of-the-art in metal speciation studies. *Analytica Chimica Acta*, 359: 1-26.

Decho AW, SN Luoma. 1994. Humic and fulvic acids: sink or source in the availability of metals to the marine bivalves *Macoma bathica* and *Potacorbula amurensis*? *Marine Ecology Progress Series*, 108: 133-145.

De Nobili, M., G. Bragato, A. Mori. 1998. Combined effects of molecular size and electroendosmotic flow on the capillary electrophoretic behaviour of humic substances. *Acta Hydrochimica Hydrobiologica*, 26: 183-190.

Dunkelog, R., H.H. Rüttinger, K. Peisker. 1997. Comparative study for the separation of aquatic humic substances by electrophoresis. *Journal of Chromatography A*, 777: 355-362.

Ebbing, D.D. *General Chemistry, 3rd Edition.* Houghton Mifflin Company, Boston: 1990.

Fetsch, D., J. Havel. 1998. Capillary zone electrophoresis for the separation and characterization of humic acids. *Journal of Chromatography A*, 802: 189-202.

Fetsch, D., M. Fetsch, E.M. Pena Méndez, J Havel. 1998a. Humic acid capillary zone electrophoresis adsorption on capillary walls, separation in metal ion supplemented buffer and the fingerprints. *Electrophoresis*, 19: 2465-2473.

Fetsch, D., M. Hradilová, E.M. Pena Méndez, J Havel. 1998b. Capillary zone electrophoresis study of aggregation of humic substances. *Journal of Chromatography A*, 817: 313-323.

Garrison, A.W., P. Schmitt, A. Kettrup. 1995. Capillary electrophoresis for the characterization of humic substances. *Water Research*, 29: 2149-2159.

Grassi, M., E. Oldani, G. Gatti. 1996. Metal-humus interaction: NMR study of model compounds. *Annali di Chimica*, 86: 353-357.

Greenfield, S., A. Montaser. Common RF generator, torches, and sample introduction systems. In: *Inductively Coupled Plasmas in Analytical Atomic Spectrometry, Second Edition*. A. Montaser, D.W. Golightly (eds.). VCH Publishers, New York: 1992 (pages 187-248).

Gustavsson, G. T. Liquid sample introduction into plasmas. In: *Inductively Coupled Plasmas in Analytical Atomic Spectrometry, Second Edition*. A. Montaser, D.W. Golightly (eds.). VCH Publishers, New York: 1992 (pages 679-720).

Hayes, M.H.B. Emerging concepts of the composition and structures of humic substances. In: *Humic Substances in Soils, Peats and Waters: Health and Environmental Aspects*. M.H.B. Hayes and W.S. Wilson (eds.). The Royal Society of Chemistry, Cambridge: 1997 (pages 1-30).

Hayes, M.H.B., P. MacCarthy, R.L. Malcolm, R.S. Swift. The search for structure: Setting the scene. In: *Humic Substances II: In Search of Structure*. M.H.B. Hayes, P. MacCarthy, R.L Malcolm, R.S. Swift (eds.). John Wiley & Sons, Chichester: 1989 (pages 3-31).

Hill, S.J., A. Fisher, G. O'Connor, E.H. Evans. Alternative plasmas and sample introduction systems. In: *Inductively Coupled Plasma Spectrometry and its Applications*. S.J. Hill (ed.). Sheffield Academic Press, Sheffield: 1999 (pages 208-244).

Hjerten, S. 1967. High performance electrophoresis. *Chromatographic Reviews*, 9: 122.

Jorgenson, J.W., K.D. Lukacs. 1981. Zone Electrophoresis in Open-Tubular Glass Capillaries. *Analytical Chemistry*, 53: 1298-1302.

Keuth, U., A. Leinenbach, H.P. Beck, H. Wagner. 1998. Separation and characterization of humic acids and metal humates by electrophoretic methods. *Electrophoresis*, 19: 1091-1096.

Kinzer, J.A., J.W. Olesik, S.V. Olesik. 1996. Effect of laminar flow in capillary electrophoresis: model and experimental results on controlling analysis time and resolution with inductively coupled plasma mass spectrometry detection. *Analytical Chemistry*, 68: 3250-3257.

Kopácek, P., D. Kániansky, J. Hejzlar. 1991. Characterization of humic substances by capillary isotachophoresis. *Journal of Chromatography*, 545: 461-470.

Leenheer, J.A., G.K. Brown, P. MacCarthy, S.E. Cabaniss. 1998. Models of metal binding structures in fulvic acid from the Suwannee River, Georgia. *Environmental Science and Technology*, 32: 2410-2416.

Lehninger, A.L., D.L. Nelson, M.M. Cox. *Principles of Biochemistry, 2nd Edition.* Worth Publishers, USA: 1993.

Liu, Y., V. Lopez-Avila, J.J. Zhu, D.R. Wiederin, W.F. Beckert. 1995. Capillary electrophoresis coupled on-line with inductively coupled plasma mass spectrometry for elemental speciation. *Analytical Chemistry*, 67: 2020-2025.

Lu, Q., R. M. Barnes. 1996. Evaluation of an ultrasonic nebulizer for capillary electrophoresis and inductively coupled plasma mass spectrometry. *Microchemical Journal*, 54: 129-143.

Lu, Q., S. M. Bird, R. M. Barnes. 1995. Interface for capillary electrophoresis and inductively coupled plasma mass spectrometry. *Analytical Chemistry*, 67: 2949-2956.

Lund W. The complexation of metal ions by humic substances in natural waters. In: *Metal Speciation in the Environment.* JAC Broekaert, S Gucer, F Adams (eds.). Springer-Verlag, Berlin: 1989.

Lustig, S., B. Michalke, W. Beck, P. Schramel. 1998. Platinum speciation with hyphenated techniques: high performance liquid chromatography and capillary

electrophoresis on-line coupled to an inductively coupled plasma mass spectrometer – application to aqueous extracts from a platinum treated soil. *Fresenius Journal of Analytical Chemistry*, 360: 18-25.

Magnuson, M.L., J.T. Creed, C.A. Brockhoff. 1997. Speciation of arsenic compounds in drinking water by capillary electrophoresis with hydrodynamically modified electroosmotic flow detected through hydride generation inductively coupled plasma mass spectrometry with a membrane gas-liquid separator. *Journal of Analytical Atomic Spectrometry*, 12: 689-695.

Majidi, V., N. J. Miller-Ihli. 1998a. Potential sources of error in capillary electrophoresis-inductively coupled plasma mass spectrometry for chemical speciation. *Analyst*, 123: 809-813.

Majidi, V., N. J. Miller-Ihli. 1998b. Two simple interface designs for capillary electrophoresis-inductively coupled plasma mass spectrometry. *Analyst*, 123: 803-808.

Majidi, V., J. Qvarnström, Q. Tu, W. Frech, Y. Thomassen. 1999. Improving sensitivity for CE-ICP-MS using multicapillary parallel separation. *Journal of Analytical Atomic Spectrometry*, 14: 1933-1935.

McLean, J.A., H. Zhang, A. Montaser. 1998. A direct injection high-efficiency nebulizer for inductively coupled plasma mass spectrometry. *Analytical Chemistry*, 70: 1012-1020.

Mei, E., H. Ichihashi, W. Gu, S. Yamasaki. 1997. Interface for coupling capillary electrophoresis to inductively coupled plasma and on-column concentration technique. *Analytical Chemistry*, 69: 2187-2192.

Mermet, J.M. Fundamental principles of inductively coupled plasmas. In: *Inductively Coupled Plasma Spectrometry and its Applications*. S.J. Hill (ed.). Sheffield Academic Press, Sheffield: 1999 (pages 35-70).

Michalke, B. 1999. Potential and limitations of capillary electrophoresis inductively coupled plasma mass spectrometry. *Journal of Analytical Atomic Spectrometry*, 14: 1297-1302.

Michalke, B., S. Lustig, P. Schramel. 1997. Analysis for the stability of platinum-containing species in soil samples using capillary electrophoresis interfaced on-

line with inductively coupled plasma mass spectrometry. *Electrophoresis*, 18: 196-201.

Michalke, B., P. Schramel. 1997. Coupling of capillary electrophoresis with ICP-MS for speciation investigations. *Fresenius Journal of Analytical Chemistry*, 357: 594-599.

Michalke, B., P. Schramel. 1998a. Application of capillary zone electrophoresis – inductively coupled plasma mass spectrometry and capillary isoelectric focusing – inductively coupled plasma mass spectrometry for selenium speciation. *Journal of Chromatography A*, 807: 71-80.

Michalke, B., P. Schramel. 1998b. Selenium speciation by interfacing capillary electrophoresis with inductively coupled plasma-mass spectrometry. *Electrophoresis*, 19: 270-275.

Montaser, A., J.A. McLean, H. Liu, J. Mermet. An introduction to ICP spectrometries for elemental analysis. In: *Inductively Coupled Plasma Mass Spectrometry*. A. Montaser (ed.). Wiley-VCH, Inc., USA: 1998a (pages 1-32).

Montaser, A., M.G. Minnich, J.A. McLean, H. Liu, J.A. Caruso, C.W. McLeod. Sample introduction in ICPMS. In: *Inductively Coupled Plasma Mass Spectrometry*. A. Montaser (ed.). Wiley-VCH, Inc., USA: 1998b (pages 83-264).

Moring, S.E. Buffers, electrolytes, and additives for capillary electrophoresis. In: *Capillary Electrophoresis in Analytical Biotechnology*. P.G. Righetti (ed.). CRC Press, Boca Raton: 1996 (pages 37-60).

Nordén, M., E. Dabek-Zlotorzynska. 1996. Study of metal-fulvic acid interactions by capillary electrophoresis. *Journal of Chromatography A*: 421-429.

Nordén, M., E. Dabek-Zlotorzynska. 1997. Characterization of humic substances using capillary electrophoresis with photodiode array and laser-induced fluorescence detection. *Electrophoresis*, 18: 292-299.

O'Connor, G., E.H. Evans. Fundamental aspects of ICP-MS. In: *Inductively Coupled Plasma Spectrometry and its Applications*. S.J. Hill (ed.). Sheffield Academic Press, Sheffield: 1999 (pages 119-144).

Oda, R.P., J.P. Landers. Introduction to Capillary Electrophoresis. In: *Handbook of Capillary Electrophoresis, 2nd Edition.* J.P. Landers (ed.). CRC Press, Boca Raton: 1997 (pages 1-48).

Olechno, J.D., J.A. Nolan. Injection methods in capillary electrophoresis. In: *Capillary Electrophoresis in Analytical Biotechnology.* P.G. Righetti (ed.). CRC Press, Boca Raton: 1996 (pages 61-100).

Olesik, J.W., J.A. Kinzer, E.J. Grunwald, K.K. Thaxton, S.V. Olesik. 1998. The potential and challenges of elemental speciation by capillary electrophoresis-inductively coupled plasma mass spectrometry or ion spray mass spectrometry. *Spectrochimica Acta Part B*, 53: 239-251.

Olesik, J.W., J.A. Kinzer, S.V. Olesik. 1995. Capillary electrophoresis inductively coupled plasma spectrometry for rapid elemental speciation. *Analytical Chemistry*, 67: 1-12.

Perdue, E.M. Chemical composition, structure, and metal binding properties. In: *Aquatic Humic Substances: Ecology and Biogeochemistry.* D.O. Hessen, L.J. Tranvik (eds.). Springer, Berlin: 1998a (pages 41-61).

Perdue, E.M. Metal binding by humic substances in surface waters – experimental and modeling constraints. In: *Metals in Surface Waters.* H.E. Allen, A.W. Garrison, G.W. Luther (eds.). Sleeping Bear Press, Ltd., USA: 1998b (pages 169-190).

Perkampus, H. *UV-VIS Spectroscopy and Its Applications.* Springer-Verlag, Berlin: 1992.

Piccolo, A. 1989. Reactivity of added humic substances towards plant available heavy metals in soils. *The Science of the Total Environment*, 81/82: 607-614.

Pickering, W.F. General strategies for speciation. In: *Chemical Speciation in the Environment.* A.M. Ure, C.M. Davidson (eds.). Chapman & Hall, Great Britain: 1995 (pages 9-32).

Pinheiro, J.P, A.M. Mota, H.P. van Leeuwen. 1999. On lability of chemically heterogeneous systems: Complexes between trace metals and humic matter. *Colloids and Surfaces A: Physicochemical and Engineering Aspects*, 151: 181-187.

Pompe, S., K. Heise, H. Nitsche. 1996. Capillary electrophoresis for a "finger-print" characterization of fulvic and humic acids. *Journal of Chromatography A*, 723: 215-218.

Rashid, M.A. *The Geochemistry of Marine Humic Substances*, Springer-Verlag, New York: 1985.

Rigol, A., J.F. López-Sánchez, G. Rauret. 1994. Capillary zone electrophoresis of humic acids. *Journal of Chromatography A*, 664: 301-305.

Rigol, A., M. Vidal, G. Rauret. 1996. Capillary zone electrophoresis to study the humic fraction in inorganic soils and its relationship with radiocaesium mobility. *Journal of Radioanalytical and Nuclear Chemistry*, 208: 617-630.

Rigol, A., M. Vidal, G. Rauret. 1998. Ultrafiltration-capillary zone electrophoresis for the determination of humic acid fractions. *Journal of Chromatography A*, 807: 275-284.

Schmitt, P., D. Freitag, I. Trapp, A.W. Garrison, M. Schiavon, A. Kettrup. 1997a. Binding of s-triazines to dissolved humic substances: electrophoretic approaches using affinity capillary electrophoresis (ACE) and micellar electrokinetic chromatography (MEKC). *Chemosphere*, 35: 55-75.

Schmitt, P., A.W. Garrison, D. Freitag, A. Kettrup. 1997b. Capillary isoelectric focussing (CIEF) for the characterization of humic substances. *Water Research*, 31: 2037-2049.

Schmitt, P., A. Kettrup, D. Freitag, A.W. Garrison. 1996. Flocculation of humic substances with metal ions as followed by capillary zone electrophoresis. *Fresenius Journal of Analytical Chemistry*, 354: 915-920.

Schmitt-Kopplin, P., A.W. Garrison, E.M. Perdue, D. Freitag, A. Kettrup. 1998a. Capillary electrophoresis in the analysis of humic substances: Facts and artifacts. *Journal of Chromatography A*, 807: 101-109.

Schmitt-Kopplin, P., N. Hertkorn, A.W. Garrison, D. Freitag, A. Kettrup. 1998b. Influence of borate buffers on the electrophoretic behavior of humic substances in capillary zone electrophoresis. *Analytical Chemistry*, 70: 3798-3808.

Schulten, H. A new approach to the structural analysis of humic substances in water and soils: Humic acid oligomers. In: Humic and Fulvic Acids: Isolation, Structure, and Environmental Role. J.S. Gaffney, N.A. Marley, S.B. Clark (eds.). American Chemical Society, USA: 1996 (pages 42-56).

Sharp, B.L., J. Batey, I.S. Begley, D. Gregson, J. Skilling, A.B. Sulaiman, G. Verbogt. 1999. Information retrieval from the inductively coupled plasma. *Journal of Analytical Atomic Spectroscopy*, 14: 99-108.

Spark, K.M., J.D. Wells, B.B. Johnson. 1997. The interaction of a humic acid with heavy metals. *Australian Journal of Soil Research*, 35: 89-101.

Sutton, K., R.M.C. Sutton, J.A. Caruso (1997) Inductively coupled plasma mass capillary electrophoresis. *Journal of Chromatography A*, 789: 85-126.

Tangen, A., W. Lund, B. Josefsson, H. Borg. 1998. Interface for the coupling of capillary electrophoresis and inductively coupled plasma mass spectrometry. *Journal of Chromatography A*, 826: 87-94.

Tangen, A., R. Trones, T. Greibrokk, W. Lund. 1997. Microconcentric nebulizer for the coupling of micro-liquid chromatography and capillary zone electrophoresis with inductively coupled plasma mass spectrometry. *Journal of Analytical Atomic Spectrometry*, 12: 667-670.

Taylor, K.A., B.L. Sharp, D.J. Lewis, H.M. Crews. 1998. Design and characterisation of a microconcentric nebuliser for capillary-electrophoresis-inductively coupled plasma mass spectrometry. *Journal of Analytical Atomic Spectrometry*, 13: 1095-1100.

Tomlinson, M. J., L. Lin, J. A. Caruso. 1995. Plasma mass spectrometry as a detector for chemical speciation studies. *Analyst*, 120: 583-589.

Tranvik, L.J. Degradation of dissolved organic matter in humic waters by bacteria. In: *Aquatic Humic Substances: Ecology and Biochemistry.* D.O. Hessen, L.J. Tranvik (eds.). Springer, New York: 1998 (pages 259-283).

Ure, A.M., C.M. Davidson. Introduction to speciation. In: *Chemical Speciation in the Environment.* A.M. Ure, C.M. Davidson (eds.). Chapman & Hall, Great Britain.: 1995.

van den Berg, C.M.G. Determination of metal speciation in seawater using cathodic stripping voltammetry. In: M*etals in Surface Waters*. H.E. Allen, A.W. Garrison, G.W. Luther (eds.). Sleeping Bear Press, Ltd., USA: 1998 (pages 133-153).

van den Hoop, M.A.G.T., H.P. van Leeuwen. 1997. Influence of molar mass distribution on the complexation of heavy metals by humic material. *Colloids and Surfaces A: Physicochemical and Engineering Aspects*, 120: 235-242.

Weber, J.H. Binding and transport of metals by humic materials. In: *Humic Substances and Their Role in the Environment.* F.H. Frimmel, R.F. Christman (eds.). Wiley, New York: 1988 (pages 165-178).

Zernichow, L., W. Lund. 1995. Size exclusion chromatography of aluminium species in natural waters. *Analytical Chimica Acta*, 300: 167-171.

Zhang, Y., N.D. Nicholas, D. Bryan, F.R. Livens, M.N. Jones. Complexing of metal ions by humic substances. In: *Humic and Fulvic Acids: Isolation, Structure, and Environmental Role.* J.S. Gaffney, N.A. Marley, S.B. Clark (eds.). American Chemical Society, USA: 1996 (pages 194-206).

Ziechmann, W. Evolution of structural models from consideration of physical and chemical properties. In: *Humic Substances and their Role in the Environment.* F.H. Frimmel and R.F. Christman (eds.). Wiley, New York: 1988 (pages 113-132).

Zoorob, G.K., J.W. McKiernan, J.A. Caruso. 1998. ICP-MS for elemental speciation studies. *Mikrochimica Acta*, 128: 145-168.